Sources of Business Cycle Fluctuations and Financial Spillovers

Srečko Zimic

Thesis submitted for assessment with a view to obtaining the degree of Doctor of Economics of the European University Institute

Florence, 22 May 2015

European University Institute
Department of Economics

Sources of Business Cycle Fluctuations and Financial Spillovers

Srečko Zimic

Thesis submitted for assessment with a view to obtaining the degree of
Doctor of Economics of the European University Institute

Examining Board

Prof. Fabio Canova, EUI, Supervisor
Prof. Luca Benati, University of Bern
Prof. Luca Gambetti, Universitat Autonoma de Barcelona
Prof. Evi Pappa, EUI

Abstract

This thesis studies the importance of non-fundamental factors in economic and financial fluctuations. In particular, it studies how the economy responds to changes in expectations about economic fundamentals, independently of actual changes in those fundamentals, and to what extent financial fluctuations in one country spillover to other countries.

The first chapter investigates how the economy reacts to the arrival of news about future technological progress. I find that the economy expands following a so-called news shock, but the bulk of the effect is delayed until technology starts to actually improve. News shocks explain around 30 percent of business cycle fluctuations, while their role is more important for explaining variations in forward-looking variables, such as stock prices and the term spread.

In the second chapter, jointly written with Stephane Dées, studies the importance of animal spirits - defined as changes in expectations not supported by changes in fundamentals - for producing business cycles. We find that animal spirits are more important for business cycle fluctuations than permanent shocks. We use a novel identification scheme in a vector-autoregressive framework that exploits the fact that the econometrician has a richer data-set than consumers.

In the third chapter, jointly written with Roberto De Santis, studies the extent and direction of spillovers, contagion and connectedness in European and US sovereign debt markets from 2005 to 2014. We use a new method that allows us to identify orthogonal country specific shocks in a panel of countries, employing restrictions on the relative size of the contemporaneous impact effect. We find that connectedness declined steadily between 2009 and 2012, indicating increased financial fragmentation. We find that Greece was a key source of systemic risk in 2010, explaining 20-30% of the variance of sovereign yields in stressed countries, while in 2011-2012 Italy, not Spain, was a key source of systemic risk.

To Barbara and Sara

Acknowledgments

My special gratitude goes to my supervisors Fabio Canova and Evi Pappa for their support and guidance during my studies. It was the luckiest coincidence in my professional life when both of you joined the institute and took over my supervision. I will always be grateful for all your comments and effort that improved my work and all the support that you gave me during the job market and in everything else.

Writing a thesis was not only a professional achievement, but also a personal adventure. This adventure would not be the same without Barbara who sacrificed her personal career in order to support me during the years in Florence and the least I could do is to dedicate this thesis to you and to our beautiful daughter Sara who was born during this adventure.

I am also thankful to my family, especially to my mother who always made me believe that I can achieve important things in my life and to my father for teaching me that this is impossible without hard work. To my brother Janez, sisters Vida and Vesna and Barbara's parents Metka and Jože, a special thanks for making our time in Florence much more enjoyable with regular visits. I would also like to thank my uncle Viljem for all the late night discussions which sparked my interest in economics.

This thesis would be impossible without Igor Masten and Hessel Oosterbeek who encouraged me during my masters studies in Ljubljana and Amsterdam to proceed with PhD studies. I am also grateful to the EUI Economics department faculty, in particular to my supervisor over the first year, Helmut Lütkepohl, and to Árpad Ábrahám and Juan J. Dolado for their support during the job market. I would also like to thank Rana Sajedi for in-depth thesis review and to Jessica Spataro and Lucia Vigna for their prompt help with all administrative issues. I am greatly indebted to my co-authors Stephane Dées and Roberto De Santis for their contribution - it was a great pleasure to work with you.

The experience of the PhD was much more enjoyable thanks to Kirill, Romanos, Vasja, Wojciech and all other great classmates and friends from EUI. I wish our discussions, trips and ('bistecca') dinners not only stay in my memory but that we will find time to meet and enjoy together also in the future.

Contents

Introduction

The drivers of economic and financial fluctuations are one of the central topics studied in economic research. In the last three decades mainstream economic literature has emphasized supply side factors - like technological changes - as the most important drivers of economic fluctuations. However, in recent years demand side factors have regained attention in the profession. In particular, the notion that changes in expectations about economic fundamentals, independently of actual changes in those fundamentals, may be an important factor causing business cycles gained increasing attention. This thesis studies the importance of such non-fundamental factors in producing economic and financial fluctuations.

The first chapter investigates how the economy reacts to the arrival of news about future technological progress. To study the effects of so-called news shocks in the data I use information contained in the term spread. The term spread is a difference between long-term and short-term yields and it was well known, especially among economic forecasters, that its movements are useful for predicting changes in economic activity. Building on these insights I show that in a standard Dynamic Stochastic General Equilibrium model the surprise increase in technology decreases the term spread, while when technology is only expected to increase in the future the term spread increases. The theoretical predictions serve to rationalize a sign restriction identification scheme to obtain news shocks in the data. I find that the economy expands following a news shock, but the bulk of the effect is delayed until technology starts to actually improve. News shocks explain around 30 percent of business cycle fluctuations, while their role is more important for explaining variations in forward-looking variables, such as stock prices and the term spread.

Changes in expectations may be caused by factors other than the arrival of news about future technological progress. For example, spells of optimism may be caused by misperceptions about potential long-term economic growth or misperceptions about the performance of firms on the stock exchange. In the second chapter, jointly written with Stephane Dées, we study the importance of animal spirits - defined as changes in expectations not supported by changes in fundamentals - for producing business cycles. We propose a novel econometric methodology that allows us to study the effects of animal spirits without imposing too much structure on the data. We find that animal spirits -

in the model defined as noise shocks - are more important for business cycle fluctuations than permanent shocks - in the model defined as technology shocks.

In the third chapter, which is a result of collaboration with Roberto De Santis, we turn our attention to financial markets. During the Eurozone debt crisis it became clear that the problems of one country can endanger the whole Eurozone, despite most countries having relatively sound economic fundamentals. We provide a first step in understanding those events by studying the extent and direction of spillovers, contagion and connectedness in European and US sovereign debt markets from 2005 to 2014. We propose a new identification method that allows us to identify orthogonal country specific shocks. The proposed method generates more intuitive results compared to previous methods, since it shows that Greece was a key source of systemic risk in 2010, while previous methods suggest the role of Greece declined in this period. Moreover, we find that connectedness, defined as the variation of asset prices in one country stemming from shocks in asset markets of another country, declined steadily between 2009 and 2012, indicating increased financial fragmentation during the Eurozone's debt crisis.

Chapter 1

Can the Term Spread Reveal the Effect of News Shocks?

1.1 Introduction

In the last decade, the notion that news about future technological progress may have significant effects on business cycles has attracted a lot of attention. Previously, economists demonstrated the role of the term spread - defined as the difference between long-term and short-term yields - for predicting changes in economic activity. Despite the clear link between the two topics, the two strands of the literature evolved independently. This paper explicitly connects these two related topics. I show that the movements in the term spread can be generated by both standard surprise TFP shocks and anticipated TFP news shocks. Using this insight and the information contained in the term spread, I explore the effect that news has in the US economy.

The idea that business cycles can be generated by expectations about future technological changes can be found in Pigou [1926]. For the next 80 years the idea faded from the mainstream business cycle literature until it was recently revived by Beaudry and Portier [2006]. They show empirically that news shocks can cause business cycles, and that they account for more than half of output fluctuations. The 'news' literature has since expanded rapidly.

The theoretical literature has focused primarily on the fact that real business cycle (RBC) models cannot generate news driven business cycles, i.e. increase in consumption, investment, hours and output, following a positive news shock. Beaudry and Portier [2007] show how the RBC model can be modified in order to produce this result. The same goal was achieved in Jaimovich and Rebelo [2009], using a different modification to the standard model. These authors extend the closed economy in Jaimovich and Rebelo [2008] to an open economy environment.

There is no consensus about the empirical effects of news shocks, especially about

the short-run response of output and investment to news shocks and about the relative importance of news shocks in producing business cycles. On the one hand, Beaudry and Portier [2006] and Beaudry and Lucke [2010] find that positive news shocks have an expansionary effect on the economy, and that news shocks account for a large share of business cycle fluctuations. The same finding is also reported by Schmitt-Grohe and Uribe [2012], who estimate a full structural model. On the other hand, Barsky and Sims [2011] and Forni et al. [2011] find that news shocks cause investment and output to decrease and consumption to increase, therefore supporting the predictions of the standard RBC models.

Closest to this paper is the empirical work of Kurmann and Otrok [2013]. To the best of my knowledge, they were the first to note the relation between information contained in the term spread and news shocks. Namely, they extract the shock that explains most of the fluctuations in the term spread and show that this shock is closely related to TFP news shocks. However, their work lacks a theoretical foundation for why news shocks can cause movements in the term spread. They also do not establish the relation between the standard surprise TFP shock and the term spread.

This paper contributes to both the theoretical and empirical strands of the 'news' literature. On the theoretical side, I show that the term spread depends crucially on the expected change in the marginal utility of consumption. This conclusion, initially obtained in a simple model, is confirmed in a general DSGE framework. In the model the term spread arises endogenously: a positive surprise TFP shock decreases the term spread on impact, while a positive news shock is accompanied by an increase in the term spread. [1]

The main empirical contribution of this paper is a novel strategy to extract the news shock. The fact that there are different responses of the term spread to the surprise and the news TFP shocks enables me to identify both shocks using a sign restriction identification scheme. In contrast, previous empirical studies exploring the effect of the news shock apply restrictions to TFP data in order to separate the surprise and the news TFP shock. This is problematic since TFP data is an artificial construct and therefore prone to large measurement errors that can affect empirical inference.

I show that the effects of my identified news shocks are in line with predictions from standard DSGE models. News shocks are important in producing cyclical fluctuations at medium term horizons, but their instantaneous effect on output and investment is quantitatively small. The instantaneous response of output and investment depends on the identification restrictions used. The news shocks account for about 30 percent of business cycle fluctuations in the real economy, while standard surprise TFP shocks account for

[1] The increase of the term spread after the positive news shock is in line with previous empirical work that found that the term spread is useful for economic forecasting. A good overview can be found in Wheelock et al. [2009].

about 50 percent. The quantitative importance of the news shock in producing business cycles is therefore smaller than in Beaudry and Portier [2006]. Yet cycles of some variables such as stock prices and the term spread are, to a large extent, attributed to the news shock.

Section 1.2 describes a benchmark model in which I show how the movements of the term spread arise. In the next section, I extend the results to a standard DSGE model. Section 1.4 presents the empirical model and identification strategy. In Section 1.5 I present the main results and in Section 1.6 I check the robustness of these results. Section 1.7 concludes.

1.2 What affects the term spread?

This section provides intuition about the interaction between the term spread and macroeconomic fluctuations. Using the framework discussed in Ljungqvist and Sargent [2004], I show under what conditions the response of the term spread is positive or negative following exogenous shocks. This serves to explain why and how the term spread reacts to the news shock and the surprise TFP shock.

Consider two kinds of risk-free bonds, a one-period and a two-period bond. The budget constraints in period t and $t+1$ are:

$$c_t + R_{1,t}^{-1} B_{1,t} + R_{2,t}^{-1} B_{2,t} + y_t \geq W_t \tag{1.2.1}$$

$$W_{t+1} = B_{1,t} + R_{1,t+1}^{-1} B_{2,t} + y_{t+1} \tag{1.2.2}$$

where c_t is consumption, y_t is an exogenous income and W_t is wealth. $R_{1,t}^{-1}$ is the price of the one-period bond $B_{1,t}$, a perfectly riskless claim to one unit of consumption at time $t+1$. Similarly $R_{2,t}^{-1}$ is the time t price of the two-period bond, a perfectly riskless claim to one unit of consumption at time $t+2$. Agents are allowed to sell the two-period bond before it matures, but its price in the next period, $R_{1,t+1}^{-1}$, is unknown and thus this bong is subject to price risk prior to maturity. In time $t+1$, the price $R_{1,t+1}^{-1}$ follows from a simple arbitrage condition - a two-period bond in period $t+1$ represents an identical claim as a one-period bond issued in period $t+1$.

The first-order necessary condition with respect to $B_{1,t}$ is:

$$R_{1,t}^{-1} = \beta E_t \left[\frac{u'(c_{t+1})}{u'(c_t)} \right] \tag{1.2.3}$$

which is a standard Euler equation. The price of a risk-free bond is obtained by equalizing the marginal loss of today's consumption from purchasing the bond to the discounted expected marginal gain of tomorrow's consumption from selling the bond.

The first-order necessary condition with respect to $B_{2,t}$ is:

$$\begin{aligned} R_{2,t}^{-1} &= \beta E_t \left[\frac{u^{'}(c_{t+1})}{u^{'}(c_t)} R_{1,t+1}^{-1} \right] \\ &= \beta^2 E_t \left[\frac{u^{'}(c_{t+2})}{u^{'}(c_t)} \right] \end{aligned} \tag{1.2.4}$$

where the second equality uses the fact that $R_{1,t+1}^{-1} = \beta E_{t+1} \left[u^{'}(c_{t+2}) / u^{'}(c_{t+1}) \right]$ and the law of iterated expectations. Similarly, it can be shown that:

$$R_{j,t}^{-1} = \beta^j E_t \left[\frac{u^{'}(c_{t+j})}{u^{'}(c_t)} \right] \tag{1.2.5}$$

which is a general expression for the price of j-period bond. In order to define the term spread, I rewrite the price of j-period bond in terms of one-year yield on this instrument. For a zero-coupon bond, the yield to maturity is:

$$R_{j,t}^{*} \equiv R_{j,t}^{1/j} = \beta^{-1} \left[\frac{u^{'}(c_t)}{E_t u^{'}(c_{t+j})} \right]^{1/j} \tag{1.2.6}$$

I define the term spread, TS_t, as the ratio between the 1-year yield of a k-year and a j-year bond:

$$TS_t \equiv \frac{R_{k,t}^{*}}{R_{j,t}^{*}} = \frac{\beta^{-1} \left(u^{'}(c_t) [E_t u^{'}(c_{t+k})]^{-1} \right)^{1/k}}{\beta^{-1} \left(u^{'}(c_t) [E_t u^{'}(c_{t+j})]^{-1} \right)^{1/j}} \tag{1.2.7}$$

When the ratio is larger than one the term spread is positive and when the ratio is less than one the term spread is negative.[2] In the next two propositions, I define conditions determining the sign of the term spread.

Proposition 1. *The term spread equals zero when the expected growth rate of marginal utility is constant, independent of the growth rate.*

Proof. in Appendix in Section A.2.

□

[2] In the empirical section, the term spread is defined as the difference between the yields of the bonds of different maturities.

Proposition 2.

i.) The term spread is positive when the expected growth rate of the marginal utility of consumption is decreasing over time, and it is negative when the expected growth rate of the marginal utility of consumption is increasing over time.

ii.) The term spread is positive when the expected decay of the marginal utility of consumption is increasing in time and the term spread is negative when the expected decay of the marginal utility of consumption is decreasing with time.

Proof. in Appendix in Section A.2. □

1.2.1 The term spread and news shocks

The link between the term spread and news and surprise TFP shocks may not be evident from Propositions 1 and 2. To clarify this, assume a standard CES utility, $u_t = \frac{c_t^{1-\sigma}}{1-\sigma}$. Log-linearizing equation (1.2.7) we have:[3]

$$\widetilde{TS}_t = -\frac{\sigma}{k}\widetilde{c}_t + \frac{\sigma}{k}E_t[\widetilde{c}_{t+k}] + \frac{\sigma}{j}\widetilde{c}_t - \frac{\sigma}{j}E_t[\widetilde{c}_{t+j}] \tag{1.2.8}$$

where $\widetilde{x}_t$ is the deviation of the log of x_t from its steady state value. Let $E_t c_{t+1} = \rho c_t$, where $\rho = r + 1$ and where r is the growth rate of consumption. We can now forecast the values in equation (1.2.8):

$$\begin{array}{rcl} E_t c_{t+k} = \varepsilon \rho^k c_t & \rightarrow & E_t[\widetilde{c}_{t+k}] = ln(\varepsilon) + k\ ln(\rho) + \widetilde{c}_t \\ E_t c_{t+j} = \rho^j c_t & \rightarrow & E_t[\widetilde{c}_{t+j}] = j\ ln(\rho) + \widetilde{c}_t \end{array} \tag{1.2.9}$$

where ε allows the growth rate of consumption between periods t and $t+k$ to differ from the growth rate of consumption between periods t and $t+j$. Inserting the expected values from equation (1.2.9) into equation (1.2.8), we get:

$$\widetilde{TS}_t = ln(\varepsilon) \tag{1.2.10}$$

which implies that the term spread in this setup depends only on the difference between the expected growth rates of consumption. Whenever ε is equal to one - whenever the expected growth rate of consumption is constant - the term spread is zero. An increasing growth rate of consumption, $\varepsilon > 1$, implies that the term spread is positive, while the term spread is negative for the decreasing growth rate of consumption.

The first and second panels of Figure 1.1 show the response of consumption following a news shock and a surprise TFP respectively. The news shock is assumed to anticipate the TFP shock five periods ahead. I assume the short-term bond matures in one period,

[3]Log-linearizing equation 1.2.7 implies that the variance and higher moments of consumption do not matter for evaluating the expected value of marginal utility, which simplifies the presentation.

$j = 1$, while the long-term bond matures in five periods, $k = 5$. The news shock and the surprise 'TFP' shock in this model are shocks to the income process.

Given that the supply of bonds is fixed and the agent does not have any other assets to finance the increase of consumption, consumption stays unchanged until the news shock is realized as an actual increase in income. In other words, only in the fifth period, when the anticipated increase in income actually materializes, does consumption increase considerably.

Figure 1.1: IRF of consumption for the surprise TFP and the news shock

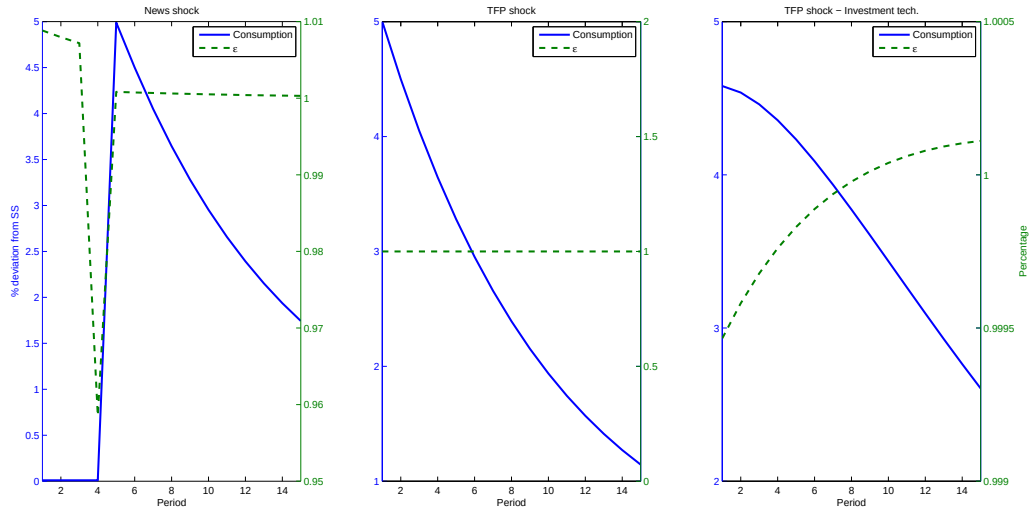

The dashed line shows the value of ε. After the news shock ε is above one and thus the term spread is positive. In this simplified model the result is straightforward: the growth rate of consumption between periods t and $t+1$ is zero, while the growth rate of consumption between period t and $t+5$ is positive. Thus $\varepsilon > 1$ due to the higher expected growth rate of consumption and the term spread is positive. To the best of my knowledge, all DSGE models available in the literature are characterized by a mild increase of consumption immediately after the news shock and a large increase after the news shock actually realizes as an increase of TFP. This acceleration of consumption implies that the news shock increases the term spread.

In the benchmark model, due to the absence of alternative assets, consumption is a one-to-one function of the income process. Therefore, the response of consumption following a standard TFP shock simply follows the assumed income process. After the shock, the income process and consumption follow an exponential decay, implying that $\varepsilon = 1$. Thus, the term spread is equal to zero in all periods.

The one-to-one relationship between the income process and consumption is altered with the introduction of capital to the model. As can be seen in the third panel in Figure 1.1, consumption now increases on impact to the TFP shock, but in the next periods the

decay of consumption increases. The increasing decay implies $\varepsilon < 1$ and thus a negative term spread.

In general, the effect of the two shocks will depend on the assumed utility function. The utility function determines how increases in the level of consumption, and possibly labor, translate into the marginal utility on which the interest rate depends. The behavior of the term spread also crucially depends on the assumed maturities used to construct the term spread. When the period in which the news shock is realized as an actual increase of TFP, $t + p$, is between the maturities of short-term and long-term bond, $j < p < k$, the term spread is more likely to increase after the news shock. This was the case in the model illustrated above, which implied that the term spread always increased following the news shock, regardless of the other parameters of the model.

1.3 The Model

The model presented in this section is a standard DSGE model with the addition of some non-standard features. The first of these is the presence of bonds with different maturities. Secondly, I add the modifications, like utility characterized by a low wealth effect, that are typically used in the news literature, for example in Jaimovich and Rebelo [2009]. With these modifications the model becomes more flexible as different combinations of the parameters imply different responses of the model's variables to the news shock.

1.3.1 Household

The household maximizes their expected lifetime utility, discounting the future by β, subject to a budget constraint. The household's utility depends positively on consumption, C_t, and negatively on hours worked, N_t:

$$U(C, N) = E_t \sum_{t=0}^{\infty} \beta^t \frac{(C_t - \psi N_t^{\theta} X_t)^{1-\omega}}{1-\omega} \tag{1.3.1}$$

where

$$X_t = C_t^{\gamma} X_{t-1}^{1-\gamma} \tag{1.3.2}$$

The 'non-standard' form of the utility function was introduced by Jaimovich and Rebelo [2009]. The presence of the variable X_t implies that the preferences are not time-separable and are characterized by a low wealth effect which depends on the parameter γ. The strength of the wealth effect crucially affects the response of the model to the news shock and will be discussed below.[4]

[4]The specification of utility in 1.3.1 nests two special cases of utility functions commonly used in the real business cycle literature; when $\gamma = 0$, we obtain the preferences proposed in Greenwood et al. [1988],

The budget constraint is given by:

$$C_t + I_t + \tau_t + \sum_{q=1}^{N} B_{q,t} = W_t N_t + Q_t K_{t-1} + \sum_{q=1}^{N} R_{q,t-q} B_{q,t-q} - \Phi(N) \tag{1.3.3}$$

Purchases of consumption, C_t, investment, I_t, lump-sum taxes, τ_t and bonds of maturity 1 to N, $\sum_{q=1}^{N} B_{q,t}$, are financed by labor income, $W_t N_t$, income from invested capital, $Q_t K_{t-1}$ and interest payments on outstanding bonds, $\sum_{q=1}^{N} R_{q,t-q} B_{q,t-q}$.

The law of motion for capital is:

$$K_t = I_t + (1-\delta) K_{t-1} \tag{1.3.4}$$

where δ is a depreciation rate.

I assume a quadratic labor adjustment cost:

$$\Phi(N) = \frac{\phi_n}{2}(N_t - N_{t-1})^2 \tag{1.3.5}$$

The presence and size of the labor adjustment cost crucially affects the response of the labor supply to the news shock, as will be seen below.

1.3.2 Firm

The competitive firm uses a standard Cobb-Douglas production function to produce the final goods for consumption:

$$F_t(K, N) = Z_t K_{t-1}^{\alpha} N_t^{1-\alpha} \tag{1.3.6}$$

where Z_t is TFP and follows a first order auto-regressive process:

$$ln(Z_t) = \rho \; ln(Z_{t-1}) + \zeta_{t-p} + \epsilon_t \tag{1.3.7}$$

where ϵ_t is a standard unanticipated technology shock. The news shock, ζ_{t-p}, is modeled as an anticipated TFP shock, which is realized p periods ahead. The maximization problem of a firm yields:

$$Q_t = \alpha Z_t K_{t-1}^{\alpha-1} N_t^{1-\alpha} \tag{1.3.8}$$

$$W_t = (1-\alpha) Z_t K_{t-1}^{\alpha} N_t^{-\alpha} \tag{1.3.9}$$

where Q_t is the return to capital and W_t is the wage.

which are known as the GHH preferences. The main propriety of the GHH preferences is the absence of the wealth effect, as labor supply only depends on the real wage. On the other hand, when $\gamma = 1$, we obtain the preferences proposed in King et al. [1988]. In this case, when $\theta = 1$ the utility function corresponds to utility of the form $U(C) = ln(C) + \psi ln(1-N)$.

The equilibrium condition for stock prices, SP_t, is:

$$SP_t = E_t M_t (Y_{t+1} + SP_{t+1}) \tag{1.3.10}$$

where M_t is a stochastic discount factor defined as:

$$M_t = \beta \frac{u^{'}(c_{t+1})}{u^{'}(c_t)} \tag{1.3.11}$$

where $u^{'}(c_t)$ is the marginal utility from consumption. In equilibrium the stock price will be equal to:

$$SP_t = \sum_{s=1}^{\infty} \beta^s Y_{t+s} \tag{1.3.12}$$

1.3.3 Government

The government budget constraint is:

$$\tau_t + \sum_{q=1}^{N} B_{q,t} = G_t + \sum_{q=1}^{N} R_{q,t-q} B_{q,t-q} \tag{1.3.13}$$

The government issues a full set of bonds with maturities $q \in [1, 2, ..., N]$ and levies a lump-sum tax, τ_t, to finance unproductive government consumption, G_t, and interest payments. In order to close the model, I assume the following rules for government debt and consumption expenditure:

$$G_t = \overline{gg} \left[\frac{Y_{t+l}}{Y_{ss}} \right]^{\gamma_g} \tag{1.3.14}$$

$$B_{q,t} = \overline{gb} \left[\frac{Y_{t+l}}{Y_{ss}} \right]^{\gamma_b} \; for \; q \in [1, 2, ..., N] \tag{1.3.15}$$

where $\overline{gb}$ is the steady state quantity of bonds of maturity N, and $\overline{gg}$ is the steady state value of government consumption. Y_{ss} represents the steady state value of output. Whenever $l > 0$, the government reacts to expected output. This allows the government a more active role in the case of a news shock. The extent of the government's reaction is captured by the parameters γ_b and γ_g. When $\gamma_b = 0$ the supply of bonds is fixed and when $\gamma_b = 1$ the ratio of government debt over output is fixed. For positive values of γ_b, government reaction is pro-cyclical, while for negative values government reaction is counter-cyclical. The same holds true for government consumption.

1.3.4 Baseline parameterization

In this subsection, I present the baseline parameterization of the model to explain the main mechanisms in the model. In the next subsection, I use different combinations of parameters to show the robustness of the term spread's response in the model.

The baseline parameter values are shown in Table A.2. 'Standard' parameters, such as the discount factor and the share of capital in production, are set to values commonly used in the literature. Turning to 'non-standard' parameters, the parameter γ, which controls the size of the wealth effect, is set to one, meaning that the wealth effect is the strongest. In the baseline specification, I assume the supply of bonds and government consumption expenditures are fixed: $\gamma_b = 0$ and $\gamma_g = 0$. Finally, the long-term bonds are assumed to have a maturity of five periods, $N = 5$, and the news shock is assumed to anticipate the TFP shock four periods in advance, $p = 4$. The term spread is constructed as the ratio between the annualized interest rate on a five-period bond and the interest rate on a one-period bond.

The responses to the surprise TFP and the news shock are presented in Figures A.1 and A.2. The responses of macro variables after the surprise TFP shock are standard - output, consumption and investment all increase after the a positive shock to TFP. At the same time, stock prices and labor supply also increase. The most interesting result concerns the response of the term spread; as expected from the discussion in Section 1.2, the term spread decreases following the TFP shock.

The model presented in this paper also reproduces standard results with regard to the response of macro variables to the news shock. While consumption increases after the news shock, the news shock generates a drop in output and investment, a common result in standard DSGE models. The result is a consequence of the wealth effect and consumption smoothing. The news shock increases the expected lifetime income and therefore, via the wealth effect, tends to depress the labor supply. At the same time, due to consumption smoothing, investment becomes negative and therefore the marginal productivity of labor decreases slightly. The decrease of labor supply and investment implies output decreases on impact. A lower wealth effect and labor adjustment costs would lead to increases in output following the news shock. This will be considered in the next section. Stock prices also increase after the news shock.

The most relevant result is that the term spread increases following the news shock. As explained above, the result is the consequence of the expected increase of the growth rate of consumption. Here we see that this continues to hold with the non-separable utility specification.

1.3.5 Robustness to the change of parameters

In this section I show that the response of the term spread as predicted in Section 1.2 is robust to different parameter values. Different combinations of parameters imply a different response from some variables, such as output, to the news shock. However, the response of the term spread to the news shock is qualitatively unaffected by changing parameter values.

I consider the following combinations of parameters:

- Wealth effect: $\gamma \in [0.001, 0.5, 1]$
- Government's debt reaction: $\gamma_b \in [-1, 0, 1]$
- Government's consumption reaction: $\gamma_g \in [-1, 0, 1]$
- Labor adjustment cost: $\psi_n \in [0, 20, 200]$
- Persistence of technology: $\rho \in [0.7, 0.9]$

The impulse responses for all the models ($3 \times 3 \times 3 \times 3 \times 2 = 162$) are shown in Figures A.3 and A.4. Focusing on the responses to the news shock, we can see that the response of output to the news shock can be positive or negative depending on parameters. The most important parameters for the response of output are the parameter γ, controlling the strength of the wealth effect, and the labor adjustment cost parameter ψ_n, controlling the response of labor supply. Consider the combinations when $\gamma = 0.001$ and $\psi_n = 200$. Due to the convex labor adjustment cost, labor supply starts to increase immediately after the news shock, lowering the costs associated with the increase of labor supply. The increase of labor is further eased by the fact that the wealth effect is low and therefore the increase of the expected lifetime income does not work strongly to depress the labor supply. As a consequence of the increased labor supply, output increases.

Similar explanations can be considered when the reaction of the government is changed. For example, when government debt reacts pro-cyclically to the news shock, this implies agents have to give up some consumption in order to buy bonds. The increase of agents' savings depresses the increase of consumption following the news shock.

The response of macroeconomic variables to the news shock thus depend on the combinations of parameters. This is not the case for the response of the term spread to the news shock. Figure A.4 shows that regardless of the combination of parameters, the qualitative response of the term spread does not change - the term spread increases following the news shock. Furthermore, the response of the term spread is qualitatively robust also in the case of the surprise TFP shock - regardless of parameters, the term spread decreases after the TFP shock. These results show that predictions in Section 1.2 are not the consequence of the choice of model parameters. Therefore, the restrictions that rely

on the sign of the response of the term spread can be confidently used in the empirical part.

1.4 Does positive news lead to expansions?

The theoretical results discussed above allow me to identify news shocks in the data using an identification strategy that does not depend on restricting the response of TFP data. To date, news shocks have been identified by imposing zero restrictions on TFP. However, since TFP measures are artificial constructs that are prone to large measurement errors, these restrictions can lead to incorrect conclusions. This is particularly true in cases when measurement errors are correlated with news shocks, as will be shown below.

The empirical analysis is done with a large-scale factor model. Factor models do not suffer from the problem of non-invertibility, which is an inherent problem when researching the effects of news shocks on the real economy. The non-invertibility of the moving average process is essentially a problem of missing information, as the econometrician does not have the same information set as agents. To solve the problem of non-invertibility, Forni et al. [2011] propose a large-dimensional factor model. The factor model uses a large amount of information so, intuitively, insufficient information is unlikely.

1.4.1 Factor model

The exposition of the factor model and the methodology used to extract the structural shock closely follows Forni and Gambetti [2010]. Each time series in the data set, x_{it}, is assumed to be the sum of two components:

$$x_{it} = \chi_{it} + \xi_{it} \tag{1.4.1}$$

where χ_{it} is the common component and ξ_{it} is the idiosyncratic component. The idiosyncratic component can be thought of as a variable specific shock or a measurement error. The common components are the linear combination of r static factors:

$$\chi_{it} = a_{1i}f_{1t} + a_{2i}f_{2t} + \ldots + a_{ri}f_{rt} = \boldsymbol{a_i f_t} \tag{1.4.2}$$

where a_{si} and f_{st} for $s = 1 \ldots r$ are factor loadings and static factors, respectively. The dynamic relation between macroeconomic variables implies a VAR representation for the factors:

$$\boldsymbol{f_t} = D_i \boldsymbol{f_{t-1}} + \ldots + D_i \boldsymbol{f_{t-p}} + \boldsymbol{\epsilon_t} \tag{1.4.3}$$

$$\boldsymbol{\epsilon_t} = R\boldsymbol{u_t} \tag{1.4.4}$$

where $\boldsymbol{u_t}$ is a vector of q dynamic factors and R is an $r \times q$ matrix, with $q \leq r$, implying the number of dynamic factors is less than or equal to the number of static factors. Equations (1.4.2), (1.4.3) and (1.4.4) can be combined as:

$$x_{it} = \boldsymbol{b_i(L)u_t} + \xi_{it} \tag{1.4.5}$$

where

$$b_i(L) = a_i(I - D_1L - \ldots - D_pL^p)R \tag{1.4.6}$$

The dynamic factors, $\boldsymbol{u_t}$ can be interpreted as structural shocks, and $\boldsymbol{b_i(L)}$ are the related impulse responses.

1.4.2 Number of static and dynamic factors

One of the main issues in estimating dynamic factor models is choosing the number of static and dynamic factors, r and q. There are a number of tests available in the literature, but the selected number of static and dynamic factors usually differs considerably between different tests.

The most popular test for the number of static factors was proposed by Bai and Ng [2002]. The test IC(1) proposed in their paper suggests that there are 20 static factors in my data, while the test IC(2) suggests using 18 static factors. On the other hand, the BIC test tailored for panel data setup, BIC(3), selects only 10 static factors. Finally, the test for the number of static factors proposed in Onatski [2009] favors 10 static factors. Therefore, the number of static factors should be in the range $r \in [10, 20]$.

Similar results apply to testing the number of dynamic factors. While the tests proposed in Bai and Ng [2007], depending on the number of static factors, suggest that there are 5 or 8 dynamic factors, the test proposed by Onatski [2009] favors 4 dynamic factors. Thus, the number of dynamic factors should be in the range $q \in [4, 8]$.

The goal of this paper is to be as agnostic as possible; the strategy I pursue is to use all of the proposed specifications. More precisely, at each bootstrap draw, explained in Step 4 in Section 1.4.4, the number of static and dynamic factors is randomly selected in the range proposed by the tests. As the number of bootstrap replications is large, each suggested model is used and the final results correspond to an 'average' model. Therefore, the presented distribution of impulse response functions (IRFs) and forecast error variance decompositions (FEVDs) in the next section also contain uncertainty about the model.

Alternatively, I could choose one model out of the $5 \times 11 = 55$ models and possibly choose the one that best fits my prior beliefs. From the Bayesian perspective this corresponds to prior model selection with probability assigned to only one model. The proposed method instead assigns equal probability to each proposed model which is preferable if one wants to be agnostic. The results, not reported here, show that the difference between

the models characterized by different number of static and dynamic factors is not large, and different specifications mainly affect standard errors.[5]

1.4.3 VAR lag length

The last issue with respect to the model concerns the number of lags used in VAR, p. The Akaike information criterion (AIC) suggests using 4 lags, while the Bayesian information criterion (BIC) suggest using only one lag. Conditional on the results of the Monte Carlo exercise, discussed below, which shows that a longer lag length may be preferable to a shorter one, I decided to use four lags in the baseline model, $p = 4$. I perform robustness checks with shorter and longer lag lengths.

1.4.4 Estimation

The estimation procedure consists of four steps. In the first two steps, I estimate the dynamic factor model. The third step takes into account the identification uncertainty and is based on methodology proposed in Rubio-Ramrez et al. [2010]. The fourth step takes into account the estimation uncertainty. The steps are:

1. **Estimate static factors:** using the chosen number of static factors, $\widehat{r}$, discussed above, the first $\widehat{r}$ static factors are estimated using principal component analysis as $\widehat{\boldsymbol{f_t}} = \widehat{A_n}' X^*$ where X^* is data sample and $\widehat{A_n}$ is $n \times r$ matrix of factor loadings.

2. **Estimate dynamic factors:** a $VAR(p)$ is estimated using the static factors, $\widehat{\boldsymbol{f_{t-p}}}$, to obtain an estimate of $D(L)$ and the residuals $\boldsymbol{\epsilon_t}$, $\widehat{D(L)}$ and $\widehat{\boldsymbol{\epsilon_t}}$ respectively. Using the chosen number of dynamic factors, $\widehat{q}$, discussed above, the estimation of a non-structural representation of the common components is achieved by using the spectral decomposition of $\widehat{\Gamma^\epsilon}$, the sample variance-covariance matrix of $\widehat{\boldsymbol{\epsilon_t}}$. This is done by calculating eigenvalues of $\widehat{\Gamma^\epsilon}$, denoted by γ_j^ϵ for $j = 1, 2, ..., \widehat{q}$. The diagonal $\widehat{q} \times \widehat{q}$ matrix M is then constructed by placing $\sqrt{\gamma_j^\epsilon}$ in the decreasing order in the $(j,j)^{th}$ position. The $\widehat{r} \times \widehat{q}$ matrix $\widehat{K}$ is constructed with the corresponding normalized eigenvector in the columns. Defining $\widehat{S} = \widehat{K}\widehat{M}$, the reduced form impulse responses can be written as:

$$\widehat{C_n}(L) = \widehat{A_n}\widehat{D}(L)^{-1}\widehat{S} \tag{1.4.7}$$

3. **Sign restrictions:** the non-uniqueness of the representation in (1.4.6) is used to derive the distribution of impulse response functions.

   (a) First, a $q \times q$ matrix P is constructed with draws from a standard normal distribution, $\mathcal{N}(0,1)$.

[5] Results for each possible model can be obtained from the author on request.

(b) The QR decomposition of P is derived, such that $P = QR$ and $QQ' = I$.

(c) The impulse response function in (1.4.7) is post-multiplied by Q. The impulse response function is retained if it satisfies the sign restrictions, discussed below.

(d) For every accepted impulse response function, the FEVD is calculated.

(e) The steps 3a-3d are repeated 1000 times. The retained impulse response functions make up the IRF distribution.

4. **Estimation uncertainty:** to account for estimation uncertainty, I repeat steps 1-3 1000 times, each time with a new data sample, X^*, artificially constructed from the original data. To construct the data samples, I follow Forni and Gambetti [2010] and adopt a standard non-overlapping block bootstrap technique. The full $T \times n$ matrix of data, $X = [x_{it}]$, is partitioned into S sub-matrices X_s, $s = 1 \dots S$, of dimension $\tau \times n$, where τ is the integer part of T/S.[6] An integer h_s between 1 and S is drawn randomly, with replacement, S times to obtain the sequence $h_1, \dots h_S$. A new artificial sample of dimension $\tau S \times n$ is then generated as $X^* = [X'_{h1} \dots X'_{hS}]$.

The point estimates and confidence bands of the IRFs are the median and relevant percentiles of the distribution of retained IRFs. The same procedure is used to construct the mean estimates and the related confidence bands of the FEVDs.

1.4.5 Identification

Identification of surprise and news TFP shocks is achieved by sign restrictions and by restrictions on forecast error variance decomposition.

Sign restrictions

The structural decomposition in (1.4.6) is not unique. To see this, assume H is an orthogonal $q \times q$ matrix such that $HH' = I$. Multiplying $\boldsymbol{b_i(L)}$ by H we can obtain an alternative structural decomposition, where $R\boldsymbol{u_t}$ now becomes $S\boldsymbol{v_t}$ with $S = RH'$ and $\boldsymbol{v_t} = H\boldsymbol{u_t}$.

To obtain a unique structural decomposition, the researcher needs to impose $q(q-1)/2$ restrictions, which is identical to the problem of identification in a Structural Vector Auto-Regression model (SVAR). In the present paper, rather than imposing restrictions to obtain a unique identification, I obtain the distribution of plausible impulse response functions by imposing sign restrictions, as in Faust [1998], Canova and Nicoló [2002] and Uhlig [2005].

In the theoretical sections I showed that, regardless of the parameterization of the model, the term spread responds positively to a positive news shock and negatively to

[6] In the present paper I choose a fairly high value of $\tau = 21$, as I want to retain the relevant lagged auto- and cross-covariances, which are especially important to explore the effect of the news shock.

a positive surprise TFP shock. Different combinations of the model's parameters, for the most part, do not affect the sign of the response of consumption and stock prices - for most of the parameter combinations consumption and stock prices respond positively to both news and surprise TFP shocks. It is worth pointing out that positive response of consumption is also found in typical news models, like those in Beaudry and Portier [2007] and Jaimovich and Rebelo [2009]. In the baseline sign restriction scheme I assume that both consumption and stock prices increase following both shocks. However, I also perform robustness checks where I restrict only one of the two variables to respond positively.

On the other hand, the response of other variables, like output and investment, crucially depends on certain parameters of the model. In the empirical investigation I thus want to leave the response of output and investment to the news shock unrestricted. The restrictions I employ are presented in Table 1.1.

Table 1.1: Sign restrictions - baseline identification scheme

	Stock prices	Consumption	Term spread
TPF **surprise** shock	$>$	$>$	$<$
TFP **news** shock	$>$	$>$	$>$

The sign restrictions are imposed on (log) levels of variables and for one year.[7] The fact that I use 116 time series implies that stock prices, consumption and the term spread are captured by more than one series. Stock prices may be represented in the data by the real stock price index, S&P500, the US Share Price Index, NADJ, and the US Dow Jones Industrials Share Price Index. Consumption is represented by Real Personal Consumption Expenditures, while the term spread is represented by the three measures discussed above. The sign restrictions are applied to all of these variables.

Restrictions on Forecast Error Variance Decomposition

Although the theory suggests that the sign restrictions proposed above should be able to separate surprise and news TFP shocks, separation of these shocks from other possible shocks may be problematic. For example, a monetary shock may well have the same dynamics as news TFP shock for the restricted variables.

In order to separate TFP shocks from other shocks, like monetary or fiscal shocks, I add the restriction that the two TFP shocks explain at least 80 percent of the FEV of TFP. A similar approach to identify investment-specific news shock was used in Ben Zeev [2014].

[7] Imposing sign restrictions only for one quarter does not qualitatively change the results, except standard error bands become wider. Results can be obtained from the author on request.

1.4.6 Monte Carlo simulation Results

Before estimating the model on the US data, I carry out an exercise to show that the proposed methodology works on simulated data. The data was simulated for 250 periods 200 times with the DSGE model presented in the previous section. I use the baseline parameters as shown in Table A.2. All 26 endogenous variables from the model are used in the Factor model. The selection criteria suggested that the number of static factors is in the range $r \in [3, 6]$ and the number of dynamic factor is in the range $q \in [2, 3]$. The identification restrictions are the same as those used in the baseline empirical model.

Figure A.5 shows the IRFs for the surprise TFP and Figure A.6 shows the IRFs for the news shock. The model-based impulse responses are mostly included in two standard error bands. The theoretical responses of output and investment to the news shock are negative. While the estimated median responses of output and investment are negative, the impact responses are not significant - a consequence of using a partial identification scheme and a small sample. Nevertheless, the estimation methodology performs reasonably well in the presented Monte Carlo and thus it can confidently be used in the empirical exercise.

1.4.7 Data

The US data set consists of 116 time series covering the period from the first quarter of 1959 until the fourth quarter of 2011. Most of the data is from FRED, while time series corresponding to TFP measures is from Fernald [2009]. The real stock price index S&P is from Shiller [2001]. All the series are described in the Appendix in Table A.1. The data used corresponds in large part to data used in Forni and Gambetti [2010].

I use two measures for the term spread on government bonds. The first is constructed as the difference between the yield of government bond with 5-year and 1-year maturity. The second is defined as the difference between the yield of government bond with 10-year maturity and the yield of 3-month treasury bill. The corporate term spread is defined as the difference between the yied on Moody's AAA-graded long term corporate bonds and the interest rate on 3-month commercial paper.

The factor model requires data to be stationary. I follow Stock and Watson [2005] and take the second log-difference of prices and nominal variables and first differences of interest rates and spreads. The exact transformation applied to each series is described in the Appendix in Table A.1. After the transformation all the series appear to be stationary.[8]

The last issue concerns outliers. These are identified as values differing from the mean of each series by 6-times the interquartile range.[9] Identified outliers are then replaced

[8]Stationarity is tested using the ADF and the KPSS tests.

[9]The bulk of outliers were identified in the series of Non-Borrowed Reserves of Depository Institutions, Board of Governors Total Reserves and Board of Governors Monetary Base, which increase dramatically after 2007.

with the corresponding maximum value - in the case of a positive value, with the mean plus 6-times the interquartile range and in the case of a negative value, with the mean minus 6-times the interquartile range.

1.5 Empirical Results

Figures A.7 and A.8 present the impulse responses of selected variables to the identified surprise and the news TFP shock respectively. The lower and upper bands represent one standard deviation from the median, and contain uncertainty about identification, the model and the parameter values.

On impact, the surprise TFP shock produces movements we expect - output, investment, interest rate, labor productivity and TFP all increase. The only prediction not in line with the standard new-Keynesian DSGE model is the response of inflation - the median response of inflation is positive following the positive TFP shock. The positive response of inflation is discussed below.

Besides the sign of responses, it is also interesting to look at the shape of impulse responses. Stock prices, output, consumption, investment, labor productivity and TFP increase on impact, but then the effect starts to fade out. However, the TFP shock still seems to have a permanent effect. On the other hand, the response of the measure of TFP adjusted for utilization turns insignificant after five quarters. The 'transitory nature' of surprise TFP shocks was found also in Barsky and Sims [2011].

The opposite result holds true for the effects of the news shock - the shape of the impulse responses to the news shock in Figure A.8 suggests a permanent increase in the variables of interests, confirming the findings in Beaudry and Portier [2006] and Barsky and Sims [2011]. Thus, the term spread embodies important information that can help separate unanticipated and anticipated TFP increases. A similar conclusion is also found in Kurmann and Otrok [2013] - they show that the shock that explains most of the fluctuations of the slope of the term structure of interest rates is closely related to the news shock about TFP.

Output increases after the news shock, while the large standard errors make it difficult to be explicit about the impact response of investment, although the median response of investment is slightly positive. The interest rate decreases significantly after the news shock. Kurmann and Otrok [2013] find the same result and attribute it to the systematic response of monetary policy to the news shock. TFP adjusted for utilization increases immediately after the news shock, which is not in line with theoretical model.[10] The reason may be that the measure of TFP is contaminated by measurement errors that are positively correlated with news shocks. Below I check whether results change when

[10]This result is not robust - for example considering two standard-error confidence bands, the increase is not significant.

assuming a zero impact effect of news shock on the measure of TFP.

In subsequent periods the effect of the news shock becomes more significant: most of the aggregate variables track predicted movements in observed technology. The small impact and large long-run effects of the news shock are in line with the predictions of most DSGE models. On the other hand, the effect on inflation is negative on impact, similar to what is found in Barsky and Sims [2011].

The identified news TFP shock can be interpreted as a standard 'supply' shock as it leads to a fall in inflation while output increases. On the other hand, transitory effects and the positive responses of inflation and interest rates suggest that the identified surprise TFP shock can be interpreted as a 'demand' shock rather than 'supply' shock. Although the increase of the TFP measure is not in line with the 'demand' shock interpretation of surprise TFP shock, a positive correlation between the measurement errors of TFP and 'demand' shocks can be a reason why TFP increases after the identified surprise TFP shock.

1.5.1 Forecast Error Variance Decomposition

Figure A.9 presents the forecast error variance decomposition for the surprise TFP shock, the news shock and a sum of all other shocks. The relative importance of the two shocks varies for different variables. The contribution of each set of shocks for the FEVD of stock prices is approximately equal and does not vary considerably across forecast horizons. Similar conclusions can be drawn from looking at the FEVD of consumer sentiment, while in the short run news shocks most affect the government term spread and the corporate term spread. All these variables can be described as forward-looking. The fact that news shocks explain a great deal of the FEV in forward-looking variables should not be surprising.

The 'real economy' variables display a different pattern. Approximately half of the first period FEV of output, consumption, investment and both TFP measures is explained by the surprise TFP shock, while the contribution of the news shock to FEV is only around twenty percent. However, the longer the time horizon, the higher the contribution of the news shock to FEV. A higher contribution for longer horizons is consistent with the predictions from most DSGE models.

1.5.2 News or monetary shocks?

The large effect of the news shocks on the forecast error variance of interest rates may suggest that I have identified monetary shocks and not a news TFP shock. However, there are at least two reasons that this is not the case. The 'real economy' variables, together with all the measures of TFP and labor productivity, are permanently affected by the news shock. At the same time, the decrease of interest rates in the first periods

following the news shock is reversed afterwards. Lastly, the news shock causes inflation to fall, which we do not expect from an expansionary monetary shock. Therefore, the results confirm the hypothesis put forward by Kurmann and Otrok [2013], who argue that monetary policy systematically reacts to news shocks.

1.6 Robustness check

In this section, I explore the robustness of the results to changes in the identification assumptions and to different lag lengths for the VAR of static factors.

1.6.1 Relationship to previous literature

To explore the relationship between the results presented here and those obtained from other models, I apply the identification strategies of two key papers in the literature to my model and compare the results.

Beaudry and Portier [2006]

In their baseline model, Beaudry and Portier [2006] use a VECM(2) including the level of TFP and stock prices. To separate the news shock from surprise TFP shocks they assume that the news shock does not affect TFP on impact, but possibly only with a lag. When they include output in the system and thus estimate a VECM(3), they have to assume two other exclusion restrictions. They assume that the third structural shock has no long-run effect on either TFP or consumption. Due to the identification approach used in this paper, I can discard this extra restriction and use only those that separate surprise and news TFP shocks.

First, I use the identification restrictions used in the paper. That is, I impose that both TFP and stock prices increase following the surprise TFP shock, while the news shock does not affect TFP on impact. The exact restrictions used are in Table 1.2.

Table 1.2: Sign restrictions - comparison with Beaudry and Portier [2006]

	TFP	Stock prices	(corporate) Term spread	Output
TFP shock	$>$	$>$	? ($<$)	?
NEWS shock	0	$>$	? ($>$)	?

Figure A.10 presents the impulse responses for the TFP shock. TFP and stock prices increase in the first periods and afterwards decrease slightly, but the effect seems permanent. Output increases on impact and in the next periods settles at a higher level. The effect of the surprise TFP shock on the term spread is insignificant, but the median response suggests the term spread decreases on impact.

The impulse responses for the news shock are shown in Figure A.11. When only restrictions on stock prices and TFP are used, the effect of news shock is not identified precisely and except for stock prices, all responses are insignificant.

As a second exercise, I also restrict the response of the term spread for the two shocks. The term spread is assumed to decrease after the surprise TFP shock and increase after the news shock, as shown in brackets in Table 1.2. Contrary to the results obtained when the term spread is not restricted, the information contained in the term spread enables me to estimate the effect of the news shock much more precisely. As can be seen from Figure A.13, TFP starts to increase following the news shock and after about six periods settles at a permanently higher level. The news shock has a similar effect on output, although the median response suggests that on impact output decreases and only later starts to increase.

To conclude, the information contained in the term spread is useful and empirical inference about the effect of news shocks can be considerably improved relative to the case when only the restrictions of Beaudry and Portier [2006] are employed.

Barsky and Sims [2011]

Barsky and Sims [2011] identify the news shock as the shock orthogonal to observed technology innovations that best explains variation in future observed technology. I follow this strategy and identify the surprise and the news TFP shock without using restrictions on the term spread.[11]

I follow closely Barsky and Sims [2011] by estimating a VAR in levels with four lags and four variables: TFP adjusted for utilization, consumption, output and the corporate term spread (numbers 8, 3, 2 and 10 in Table A.1 in the Appendix). The only difference is that I include the term spread, while Barsky and Sims [2011] include hours worked per person as the last variable in their VAR.

Figures A.14 and A.15 show the impulse responses to the surprise TFP and the news TFP shock respectively. The term spread responds as predicted by theory - it decreases significantly after the surprise TFP shock and it increases significantly after the news TFP shock. This result confirms the suitability of the empirical methodology used in this paper and shows that the information contained in the term spread is useful for separating surprise TFP shocks from news TFP shocks.

1.6.2 'Zero' restrictions

To facilitate the comparison of my results with those obtained in other papers, I add the zero impact restriction of the news shock on TFP. This is a standard identification restriction used in the 'news' literature. Exclusion restrictions are sometimes ad hoc, but in the

[11] I would like to thank Nadav Ben Zeev for providing me with codes used in this subsection.

case of identifying the news shock this restriction is theoretically sound. Nevertheless, one should believe that the estimated TFP measure is a good approximation to theoretical counterpart to be confident in such an identification restriction.

The results are presented in Figures A.16 and A.17. The large number of identification restrictions results in a big shrinkage of standard errors. The response to the surprise TFP shock follows theoretical predictions. Output, consumption, investment, interest rates and stock prices all increase and stay permanently higher following the TFP shock. The only qualitative difference between the case when zero restriction is not used is that inflation now decreases, although the effect is not significant.

More interesting are the responses to the news shock. Contrary to the previous results, the impact response of output now becomes insignificant. In addition, the zero restriction allows me to pin down the impact effect on investment; the news shock seems to be associated with a decrease of investment on impact.

The result that investment decreases on impact following the news shock is in line with the findings in Barsky and Sims [2011] and Forni et al. [2011], but contrary to what is in Beaudry and Portier [2006]. However, the result crucially depends on the quality of the TFP measure. For example, in case of a positive correlation between measurement errors in TFP and the news shock, the assumption of a zero impact effect on TFP is incorrect. Using such a restriction results in the wrong conclusions about the impact effect; the true impact effect on output may be positive, but the estimated effect would suggest a negative response, which was also confirmed by Monte Carlo exercises not shown here. Constraining the response of TFP by zero restriction implies reduced response of other variables interrelated with TFP, like output and investment.

1.6.3 Only sign restrictions

As with the zero restrictions, the restrictions on the FEV of TFP assumes that the measure of TFP is precisely estimated. While those restrictions helped in identifying the shocks, the methodology used in this paper allows to completely dispense with any restrictions on TFP.

Figures A.18 and A.19 show the impulse responses to the surprise and the news TFP shock when only sign restrictions from Table 1.1 are used, and the FEV is left unrestricted. Except for wider error bands, the results are not considerably different from the baseline restrictions.

Figure A.20 shows that the FEVD is more affected by the change in identification assumptions. On the one hand, the relative importance of surprise versus news TFP shocks does not change considerably. On the other hand, the absolute shares of FEVD explained by both TFP shocks decreases substantially. While in the baseline model the two TFP shocks explain around 80 percent of the variation in output, consumption and

investment, this share falls to around 60 percent when only sign restrictions are used.

The decrease of the absolute share of FEV explained by both TFP shocks is the expected result when restrictions on FEVD are not used. However, given that now only 40 percent of the FEV of TFP is explained by both TFP shocks, adding the baseline restriction that 80 percent of the FEV of TFP should be explained by the TFP shocks seems an appropriate restriction.

1.6.4 Alternative sign restrictions

As we saw, different combinations of the model's parameters can affect the sign of the response of consumption and stock prices. In contrast to restrictions on the term spread, one may still argue that constraints on consumption and stock prices are too restrictive. In this section I thus relax restrictions on the response of consumption and stock prices and show that this does not considerably change the results.

Figures A.21 and A.22 present the case when the response of consumption is not restricted. The shape of the responses are similar to the baseline model, while the standard error bands are wider. The response of consumption is positive on impact, which suggests that the restriction used in the baseline results is not too far from the truth.

Figures A.23 and A.24 present the case when the response of stock prices is not restricted. Again, the shape of the responses is similar to the baseline model, while the standard error bands are wider. The impact effect of stock prices to the news shock is significant and in line with the restriction used in the baseline model.

Despite the similarities, one can notice a difference in these two cases. When only sign restrictions on the response of stock prices are used, the news shock seems to be anticipated with a longer time lag than in the case when only the response of consumption is restricted. In fact, the impact responses of most variables, such as output, TFP and investment, to the news shock are smaller when sign restrictions are only used on stock prices. Stock prices appear more forward-looking than consumption, thus capturing the arrival of news sooner than consumption. If one of the two restrictions has to be chosen, restricting stock prices seems preferable.

1.6.5 Lag length

Figures A.25 and A.26 show the results when eight lags are used to estimate the VAR for the static factors. Compared to the baseline model with 4 lags, the median responses do not change dramatically. The main differences are wider standard errors bands, which is not surprising given that up to 126 parameters are estimated.

Similar conclusions can be drawn from looking at Figures A.27 and A.28, which show responses for the VAR with one lag. While the responses of other variables to both shocks are similar to the baseline model, the response of TFP adjusted for utilization to the news

shock differs considerably. First of all, the response is insignificant, but also the median response differs in shape; there is no evidence that after the news shock TFP adjusted for utilization increases. The reason may be that a short lag length cannot capture well the effect of the news shock.

1.7 Conclusions

In the theoretical section, I have shown that the term spread responds differently to the surprise TFP and the news shock. On the one hand, the news that technology will improve in the future increases the term spread. On the other hand, the term spread decreases after the standard surprise TFP shock.

I use this robust response of the term spread to identify the effects of news and TFP shocks in US data. I find that standard surprise TFP shocks are the most important driver of business cycles, while news shocks account for about 30 percent of business cycle fluctuations in the US. However, cycles of some variables, like stock prices and the term spread, can to a large extent be attributed to news shocks.

The instantaneous effect of news shocks on output and investment is quantitatively small and the sign of this effect depends on the identification restrictions. Which restriction to use depends on how much one believes in the quality of the TFP data. Contrary to this, the effect of the news shock at medium-term horizons is clear. Aggregate variables mainly follow TFP movements: consumption, output and investment increase following the news shock.

For future work it would be interesting to find other financial variables that responds differently to unanticipated and anticipated shocks, regardless of the parameters of the model. Such a variable could then be used to strengthen the identification of the news shock. The methodology used in this paper could also be applied to identify other structural shocks that are characterized by anticipation effects, for example government spending shocks. Lastly, it would be interesting to check whether the information about expectations contained in the term spread could improve the forecasting capabilities of DSGE models.

Appendix A

Appendix: Can the Term Spread Reveal the Effect of News Shocks?

A.1 Appendix - Data

Table A.1: The list of data series and their transformations used in the paper

no.	Tra.	Mnemonic	Long Label
1	5	REALS&P	Real stock price index S&P500 (Robert Shiller)
2	5	GDPC1	Real Gross Domestic Product, 1 Decimal
3	5	PCECC96	Real Personal Consumption Expenditures
4	5	GPDI/DEF	Real Gross Private Domestic Investment (GPDI)
5	2	FEDFUNDS	Effective Federal Funds Rate
6	2	UMCSENT	University of Michigan: Consumer Sentiment (UMCSENT)
7	5	DTFP	Business sector TFP (produced by John Fernald)
8	5	DTFPUTIL	Utilization-adjusted TFP (produced by John Fernald)
9	2	GS10-FEDFUNDS	Government term spread
10	2	CPN3M-CPN3M	Corporate term spread
11	5	GNPC96	Real Gross National Product
12	5	NICUR/GDPDEF	National Income/GDPDEF
13	5	DPIC96	Real Disposable Personal Income
14	5	OUTNFB	Nonfarm Business Sector: Output
15	5	FINSLC1	Real Final Sales of Domestic Product, 1 Decimal
16	5	PRFI/DEF	Real Private Residential Fixed Investment (PRFI)
17	5	PNFI/DEF	Real Private Nonresidential Fixed Investment (PNFI)
18	5	GPDIC1	Real Gross Private Domestic Investment, 1 Decimal
19	5	PCND/DEF	Real Personal Consumption Expenditures: Nondurable Goods
20	5	PCDG/DEF	Real Personal Consumption Expenditures: Durable Goods
21	5	PCES/DEF	Real Personal Consumption Expenditures: Services
22	5	GPSAVE/GDPDEF	Gross Private Saving/GDP Deflator
23	5	FGCE/DEF	Real Federal Consumption Expenditures & Gross Investment (FGCE)
24	5	FGEXPND/GDPDEF	Federal Government: Current Expenditures/ GDP deflator
25	5	FGRECPT/GDPDEF	Federal Government Current Receipts/ GDP deflator
26	2	FGDEF	Federal Real Expend-Real Receipts
27	1	CBIC1	Real Change in Private Inventories, 1 Decimal
28	5	EXPGSC1	Real Exports of Goods & Services, 1 Decimal
29	5	IMPGSC1	Real Imports of Goods & Services, 1 Decimal
30	5	CP/GDPDEF	Corporate Profits After Tax/GDP deflator
31	5	NFCPATAX/GDPDEF	Nonfinancial Corporate Business: Profits After Tax/GDP deflator
32	5	CNCF/GDPDEF	Corporate Net Cash Flow/GDP deflator
33	5	DIVIDEND/GDPDEF	Net Corporate Dividends/GDP deflator
34	5	HOANBS	Nonfarm Business Sector: Hours of All Persons
35	5	OPHNFB	Nonfarm Business Sector: Output Per Hour of All Persons
36	5	UNLPNBS	Nonfarm Business Sector: Unit Nonlabor Payments
37	5	ULCNFB	Nonfarm Business Sector: Unit Labor Cost
38	5	WASCUR/CPI	Compensation of Employees: Wages & Salary Accruals/CPI

* 1=no transformation 2=first differences 5=first differences of logs 6= second differences of logs *

Table A.1: The list of data series and their transformations used in the paper

no.	Tra.	Mnemonic	Long Label
39	6	COMPNFB	Nonfarm Business Sector: Compensation Per Hour
40	5	COMPRNFB	Nonfarm Business Sector: Real Compensation Per Hour
41	6	GDPCTPI	Gross Domestic Product: Chain-type Price Index
42	6	GNPCTPI	Gross National Product: Chain-type Price Index
43	6	GDPDEF	Gross Domestic Product: Implicit Price Deflator
44	6	GNPDEF	Gross National Product: Implicit Price Deflator
45	5	INDPRO	Industrial Production Index
46	5	IPBUSEQ	Industrial Production: Business Equipment
47	5	IPCONGD	Industrial Production: Consumer Goods
48	5	IPDCONGD	Industrial Production: Durable Consumer Goods
49	5	IPFINAL	Industrial Production: Final Products (Market Group)
50	5	IPMAT	Industrial Production: Materials
51	5	IPNCONGD	Industrial Production: Nondurable Consumer Goods
52	2	AWHMAN	Average Weekly Hours: Manufacturing
53	2	AWOTMAN	Average Weekly Hours: Overtime: Manufacturing
54	2	CIVPART	Civilian Participation Rate
55	5	CLF16OV	Civilian Labor Force
56	5	CE16OV	Civilian Employment
57	5	USPRIV	All Employees: Total Private Industries
58	5	USGOOD	All Employees: Goods-Producing Industries
59	5	SRVPRD	All Employees: Service-Providing Industries
60	5	UNEMPLOY	Unemployed
61	5	UEMPMEAN	Average (Mean) Duration of Unemployment
62	2	UNRATE	Civilian Unemployment Rate
63	5	HOUST	Housing Starts: Total: New Privately Owned Housing Units Started
64	2	TB3MS	3-Month Treasury Bill: Secondary Market Rate
65	2	GS1	1-Year Treasury Constant Maturity Rate
66	2	GS10	10-Year Treasury Constant Maturity Rate
67	2	AAA	Moody's Seasoned Aaa Corporate Bond Yield
68	2	BAA	Moody's Seasoned Baa Corporate Bond Yield
69	2	MPRIME	Bank Prime Loan Rate
70	6	BOGNONBR	Non-Borrowed Reserves of Depository Institutions
71	6	TRARR	Board of Governors Total Reserves, Adjusted for Changes in Reserve
72	6	BOGAMBSL	Board of Governors Monetary Base, Adjusted for Changes in Reserve
73	6	M1SL	M1 Money Stock
74	6	M2MSL	M2 Minus
75	6	M2SL	M2 Money Stock
76	6	BUSLOANS	Commercial and Industrial Loans at All Commercial Banks
77	6	CONSUMER	Consumer (Individual) Loans at All Commercial Banks
78	6	LOANINV	Total Loans and Investments at All Commercial Banks
79	6	REALLN	Real Estate Loans at All Commercial Banks
80	6	TOTALSL	Total Consumer Credit Outstanding
81	6	CPIAUCSL	Cons. Price Index : All Items
82	6	CPIULFSL	Cons. Price Index : All Items Less Food
83	6	CPILEGSL	Cons. Price Index : All Items Less Energy
84	6	CPILFESL	Cons. Price Index : All Items Less Food & Energy
85	6	CPIENGSL	Cons. Price Index: Energy
86	6	CPIUFDSL	Cons. Price Index : Food
87	6	PPICPE	Producer Price Index Finished Goods: Capital Equipment
88	6	PPICRM	Producer Price Index: Crude Materials for Further Processing
89	6	PPIFCG	Producer Price Index: Finished Consumer Goods
90	6	PPIFGS	Producer Price Index: Finished Goods
91	6	OILPRICE	Spot Oil Price: West Texas Intermediate
92	5	USSHRPRCF	US Dow Jones Industrials Share Price Index (EP) NADJ
93	5	US500STK	US Standard & Poor Index if 500 Common Stocks
94	5	USI62...F	US Share Price Index NADJ
95	5	USNOIDN.D	US Manufacturers New Orders for Non Defense Capital Goods (BCI 27)
96	5	USCNORCGD	US New Orders of Consumer Goods & Materials (BCI 8) CONA
97	1	USNAPMNO	US ISM Manufacturers Survey: New Orders Index SADJ
98	5	USCYLEAD	US The Conference Board Leading Economic Indicators Index SADJ
99	5	USECRIWLH	US Economic Cycle Research Institute Weekly Leading Index
100	2	GS1-FEDFUNDS	Spread between 1-year treasury and FEDFUNDS
101	2	BAA-FEDFUNDS	Spread between BAA rared corporate bond and FEDFUNDS
102	5	GEXPND/GDPDEF	Government Current Expenditures/ GDP deflator
103	5	GRECPT/GDPDEF	Government Current Receipts/ GDP deflator
104	2	GDEF	Governnent Real Expend-Real Receipts
105	5	GCEC1	Real Government Consumption Expenditures & Gross Investment
106	5	PE	Adjusted Price-Earnings ratio (Robert Shiller)

* 1=no transformation 2=first differences 5=first differences of logs 6= second differences of logs *

Table A.1: The list of data series and their transformations used in the paper

no.	Tra.	Mnemonic	Long Label
107	2	GS5-GS1	5-Year - 1-Year Treasury Constant Maturity Rate
108	5	IST	Equipment-investment share of business output (produced by John Fernald)
109	2	UTIL	Utilization (produced by John Fernald)
110	5	dLP	Business- sector labor productivity (produced by John Fernald)
111	5	TFP_INV	TFP in equip and con. durables (produced by John Fernald)
112	5	TFP_CON	TFP in non equip and con. durables (produced by John Fernald)
113	5	TFP_INV_U	Util. adj. TFP in equip and con. durables (produced by John Fernald)
114	5	TFP_CON_U	Util. adj. TFP in non equip and con. durables (produced by John Fernald)
115	2	UTIL_INV	Utilization in equip and con. durables (produced by John Fernald)
116	2	UTIL_CON	Utilization in non equip and con. durables (produced by John Fernald)

* 1=no transformation 2=first differences 5=first differences of logs 6= second differences of logs *

A.2 Appendix - Proofs of propositions from Section 1.2

Proposition 1. *The term spread equals zero when the expected growth rate of marginal utility is constant, independent of the growth rate.*

Proof. Let us start with the definition of a constant growth rate:

$$\frac{u'(c_t) - u'(c_{t-1})}{u'(c_{t-1})} = r \ \forall t \tag{A.2.1}$$

for some constant r. Defining $\rho = (1 + r)$, I can write marginal utility at time t as:

$$u'(c_t) = u'(c_0)\rho^t \tag{A.2.2}$$

Using this equation we can now forecast the values in equation 1.2.7:

$$\begin{aligned} E_t u'(c_{t+k}) &= u'(c_0)\rho^{t+k} \\ E_t u'(c_{t+j}) &= u'(c_0)\rho^{t+j} \end{aligned} \tag{A.2.3}$$

Equation (1.2.7) can now be solved:

$$\begin{aligned} \widetilde{TS}_t \equiv \frac{\widetilde{R}_{k,t}}{\widetilde{R}_{j,t}} &= \frac{\left(\left(u'(c_0)\rho^t\right)\left[(u'(c_0)\rho^{t+k})\right]^{-1}\right)^{1/k}}{\left(\left(u'(c_0)\rho^t\right)\left[(u'(c_0)\rho^{t+j})\right]^{-1}\right)^{1/j}} \\ &= \frac{(\rho^{-k})^{1/k}}{(\rho^{-j})^{1/j}} \\ &= 1 \ \forall \ \rho \in \mathbb{R} \end{aligned} \tag{A.2.4}$$

which says that regardless of the expected growth rate of marginal utility, r, term spread is zero when growth rate is constant.

□

Proposition 2.

i.) The term spread is positive when the expected growth rate of the marginal utility of consumption is decreasing in time and the term spread is negative when the expected growth rate of the marginal utility of consumption is increasing with time.

ii.) The term spread is positive when the expected decay of the marginal utility of consumption is increasing in time and the term spread is negative when the expected decay of the marginal utility of consumption is decreasing with time.

Proof. The changing rate of growth rate can be defined as:

$$\frac{u'(c_t) - u'(c_{t-1})}{u'(c_{t-1})} = r\phi(t) \tag{A.2.5}$$

where $\phi(t)$ is some function of time. Marginal utility at time $t + k$ and $t + j$ can be solved as:

$$E_t u'(c_{t+k}) = u'(c_0)[1 + r\phi(t + k)]^{t+k} \tag{A.2.6}$$

$$E_t u'(c_{t+j}) = u'(c_0)[1 + r\phi(t + j)]^{t+j} \tag{A.2.7}$$

The expected values in equation 1.2.7 can now be solved:

$$\begin{aligned}\widetilde{TS}_t \equiv \frac{\widetilde{R}_{k,t}}{\widetilde{R}_{j,t}} &= \frac{\left((u'(c_0)[1+r\phi(t)]^t)[u'(c_0)[1+r\phi(t+k)]^{t+k}]^{-1}\right)^{1/k}}{\left((u'(c_0)[1+r\phi(t)]^t)[u'(c_0)[1+r\phi(t+j)]^{t+j}]^{-1}\right)^{1/j}} \\ &= \frac{\left(([1+r\phi(t)]^t)[([1+r\phi(t+k)]^{t+k})]^{-1}\right)^{1/k}}{\left(([1+r\phi(t)]^t)[([1+r\phi(t+j)]^{t+j})]^{-1}\right)^{1/j}}\end{aligned} \tag{A.2.8}$$

in order for the term spread to be positive, we need:

$$\left(\frac{[1+r\phi(t)]^t}{[1+r\phi(t+k)]^{t+k}}\right)^{1/k} > \left(\frac{[1+r\phi(t)]^t}{[1+r\phi(t+j)]^{t+j}}\right)^{1/j} \tag{A.2.9}$$

I assume without the loss of generality that period $t = 0$, so condition in (A.2.9) boils down to:

$$[1+r\phi(k)] < [1+r\phi(j)] \tag{A.2.10}$$

Starting with the first part of proposition 2 which states that for a positive growth rate, $r > 0$ and $\phi(t) > 0 \ \forall \ t$, the term spread is positive when the expected growth rate the marginal utility of consumption is decreasing in time. The decreasing growth rate of the marginal utility of consumption corresponds to the case when the derivative of generic function with respect to time is negative, $\frac{\partial\phi(t)}{\partial t} < 0$. Using the assumption that $k > j$, this implies $\phi(k) < \phi(j)$. This is exactly the condition we need to satisfy the condition (A.2.10) and confirms that for a positive growth rate, $r > 0$ and $\phi(t) > 0 \ \forall \ t$, the term spread is positive when the expected growth rate of the marginal utility of consumption is decreasing in time. The mirror argument can be used to show that for a positive growth rate, the term spread is negative when the expected growth rate of the marginal utility of consumption is increasing in time.

The second part of proposition 2 states that when the growth rate is negative, $r < 0$ and $\phi(t) > 0 \ \forall \ t$, the term spread is positive when the expected decay of the marginal utility of consumption is increasing in time. The condition (A.2.10) is now:

$$[1-r\phi(k)] < [1-r\phi(j)] \tag{A.2.11}$$

The increasing decay of the marginal utility of consumption corresponds to the case when the derivative of generic function with respect to time is positive, $\frac{\partial\phi(t)}{\partial t} > 0$. Using the assumption that $k > j$, this implies $\phi(k) > \phi(j)$. This is exactly the condition we need to satisfy the condition (A.2.11) and confirms that for a negative growth rate, $r < 0$ and $\phi(t) > 0 \ \forall \ t$, the term spread is positive when the expected decay of the marginal utility of consumption is increasing in time. The mirror argument can be used to show that for a negative growth rate, the term spread is negative when the expected decay of the marginal utility of consumption is decreasing in time. □

A.3 Appendix - Model

A.3.1 Baseline parameters

Table A.2: Baseline Parameter's values

Parameter	Value	Parameter	Value	Parameter	Value
β	0.95	ω	1	gb	$0.3y_{ss}$
α	0.36	ϕ_n	0	gg	$0.2y_{ss}$
δ	0.1	γ_b	0	p	5
γ	1	γ_g	0	q	5
θ	1.5	ρ	0.9	l	5
ψ	0.8	σ	0.05		

A.3.2 Baseline IRF

Figure A.1: IRF to the TFP shock - baseline parameters

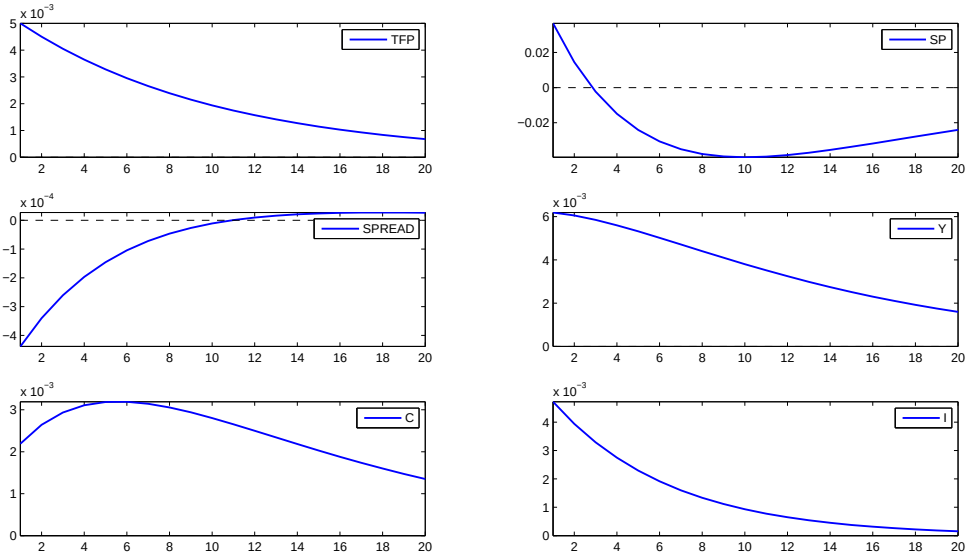

The figure presents the impulse responses to the TFP shock of TFP, stock prices, term spread, output, consumption and investment for the model presented in Section 1.3 with baseline parameters.

Figure A.2: IRF to the news shock - baseline parameters

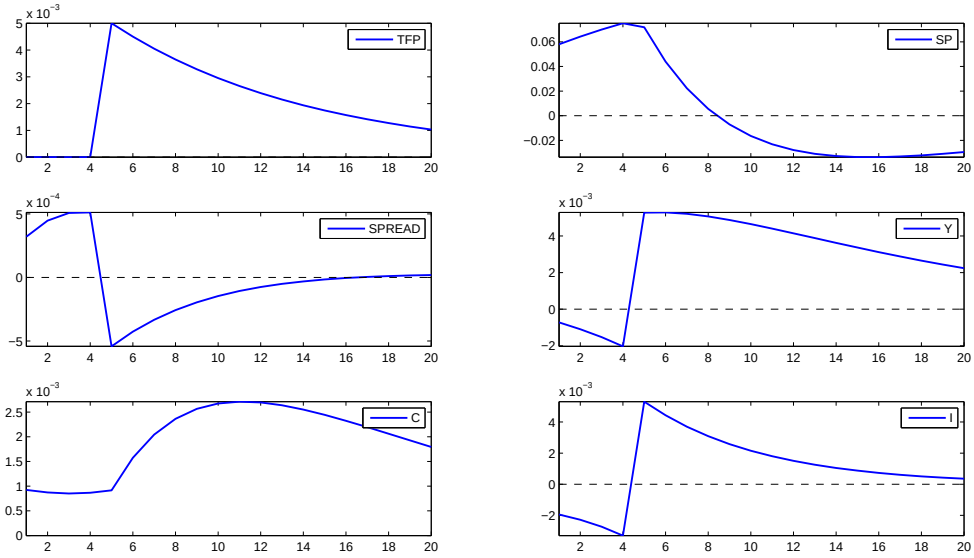

The figure presents the impulse responses to the news shock of TFP, stock prices, term spread, output, consumption and investment for the model presented in Section 1.3 with baseline parameters. The news shock is assumed to anticipate the TFP shock 4 periods ahead.

A.3.3 IRF with different combinations of parameters

Figure A.3: IRF to the TFP shock - different combinations of parameters

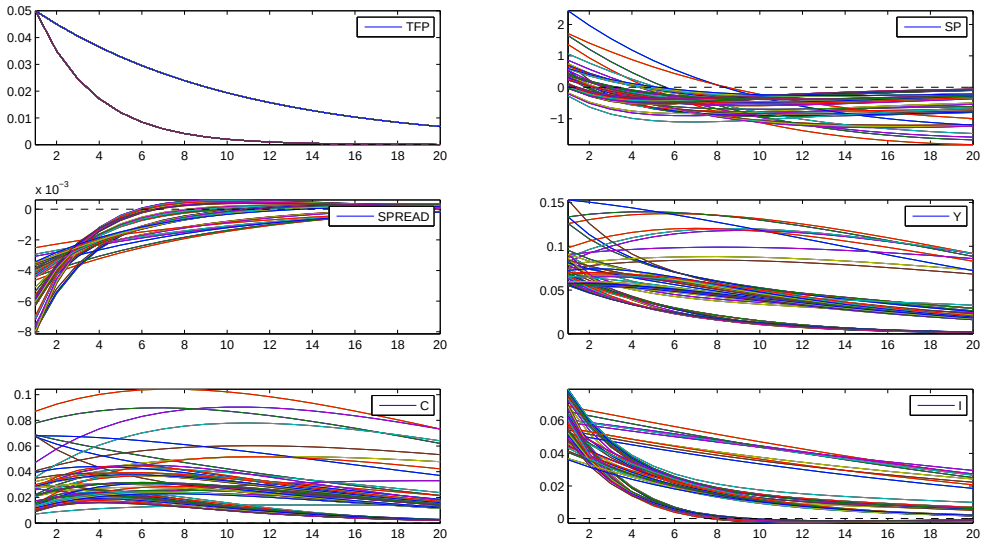

The figure presents the impulse responses to the TFP shock of TFP, stock prices, term spread, output, consumption and investment for different combinations of parameters presented in Section 1.3.5.

Figure A.4: IRF to the news shock - different combinations of parameters

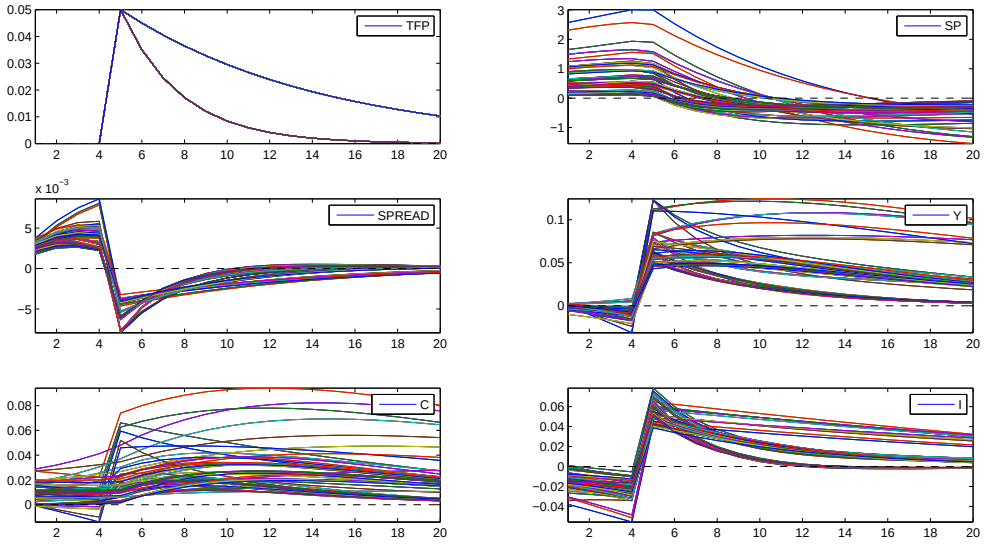

The figure presents the impulse responses to the news shock of TFP, stock prices, term spread, output, consumption and investment for different combinations of parameters presented in Section 1.3.5.The news shock is assumed to anticipate the TFP shock 4 periods ahead.

A.4 Appendix -Monte Carlo simulation

Figure A.5: Impulse responses to tfp shock

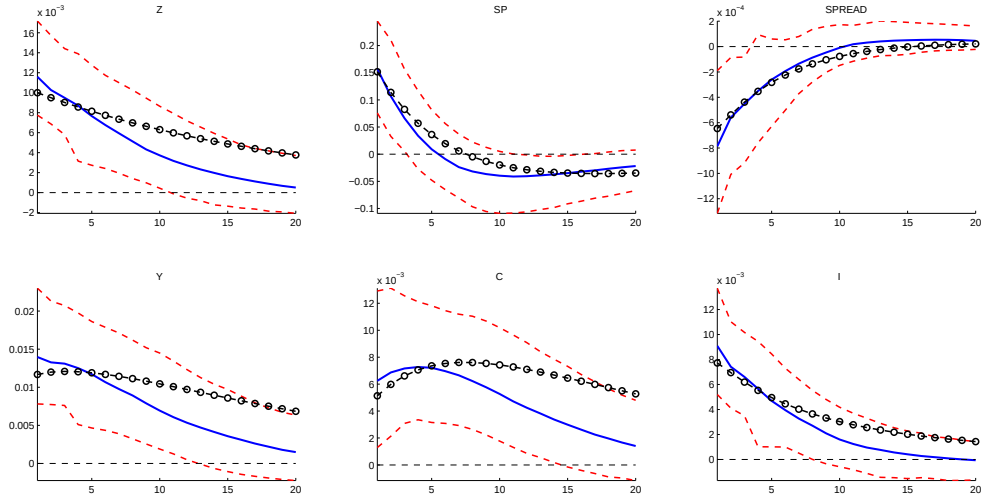

The figure presents the impulse responses to surprise TFP shock of TFP, stock prices, term spread, output, consumption and investment. The data was simulated with the model presented in Section 1.3 for 250 periods. The news shock is assumed to anticipate TFP shock 4 periods ahead. The sign restrictions are the same as used in baseline factor model. The dashed lines correspond to identification,model and parameter uncertainty of two-standard deviation. The lines with the circles corresponds to true impulse responses.

Figure A.6: Impulse responses to news shock

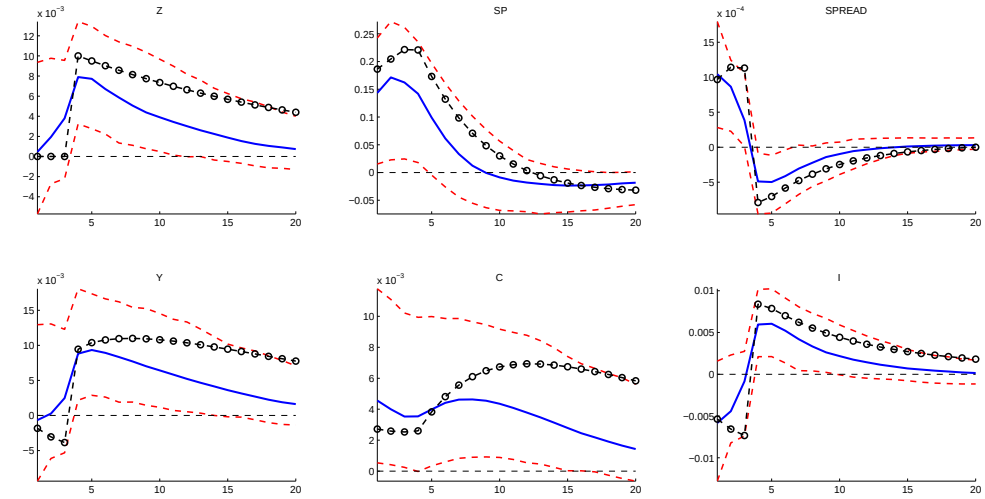

The figure presents the impulse responses to news TFP shock of TFP, stock prices, term spread, output, consumption and investment. The data was simulated with the model presented in Section 1.3 for 250 periods. The news shock is assumed to anticipate TFP shock 4 periods ahead. The sign restrictions are the same as used in baseline factor model. The dashed lines correspond to identification,model and parameter uncertainty of two-standard deviation. The lines with the circles corresponds to true impulse responses.

A.5 Appendix - Factor model

Figure A.7: Impulse responses to TFP shock for selected variables - baseline

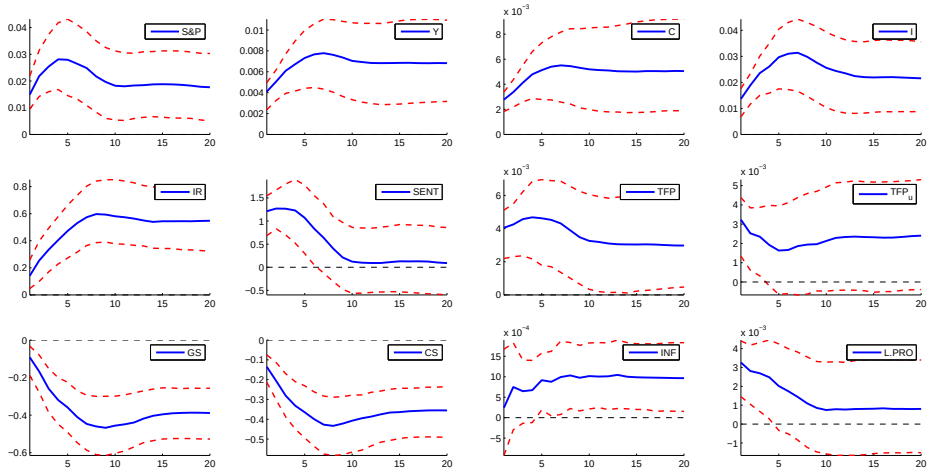

The figure presents the impulse responses to TFP shock of (log) S&P real stock prices, (log) output, (log) consumption and (log) investment in the first row, interest rate, consumer confidence, (log) TFP and (log) TFP adjusted for utilization in the second raw, government term spread, corporate term spread, inflation and (log) labor productivity in the last raw. In order, the number in the table A.1 of presented variables is: 1,2,3,4,5,6,7,8,9,10, 81 and 110. The variables are standardized. The dashed lines correspond to identification,model and parameter uncertainty of one-standard deviation.

Figure A.8: Impulse responses to news shock for selected variables - baseline

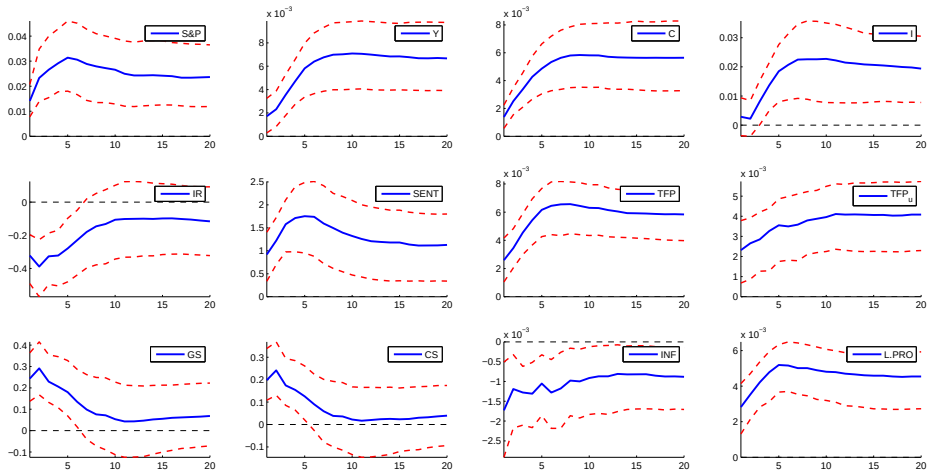

The figure presents the impulse responses to news shock of (log) S&P real stock prices, (log) output, (log) consumption and (log) investment in the first row, interest rate, consumer confidence, (log) TFP and (log) TFP adjusted for utilization in the second raw, government term spread, corporate term spread, inflation and (log) labor productivity in the last raw. In order, the number in the table A.1 of presented variables is: 1,2,3,4,5,6,7,8,9,10, 81 and 110. The variables are standardized. The dashed lines correspond to identification,model and parameter uncertainty of one-standard deviation.

Figure A.9: Forecast Error Variance Decomposition - baseline

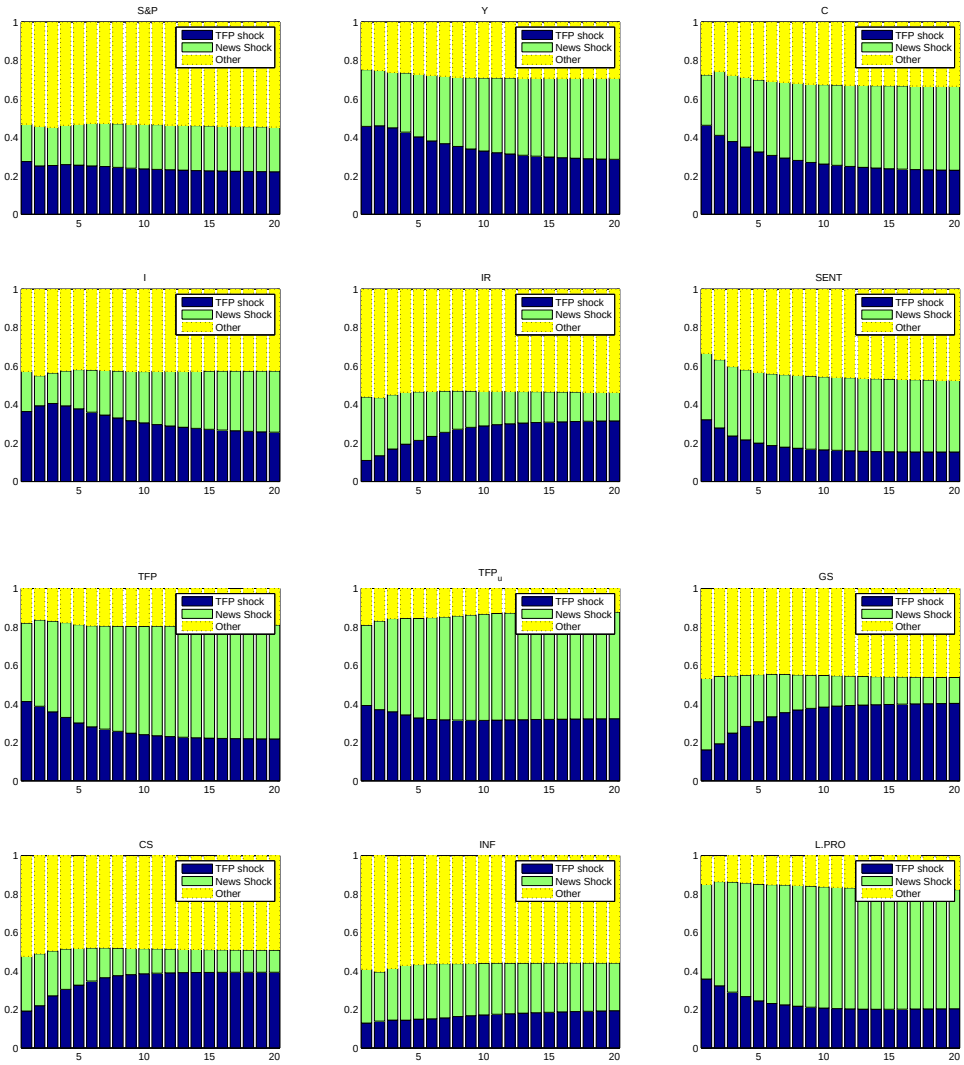

The figure presents Forecast Error Variance Decomposition for the TFP shock, the news shock and other shocks of (log) S&P real stock prices, (log) output and (log) consumption in the first row, (log) investment,interest rate and consumer sentiment in the second row, (log) TFP, (log) TFP adjusted for utilization and government term spread in the third raw, corporate term spread, inflation and (log) labor productivity in the last raw. In order, the number in the table A.1 of presented variables is: 1,2,3,4,5,6,7,8,9,10, 81 and 110. The variables are standardized.

A.6 Appendix - Comparison with Beaudry and Portier [2006]

Figure A.10: IRF to TFP shock for selected variables - comparison with Beaudry and Portier [2006]

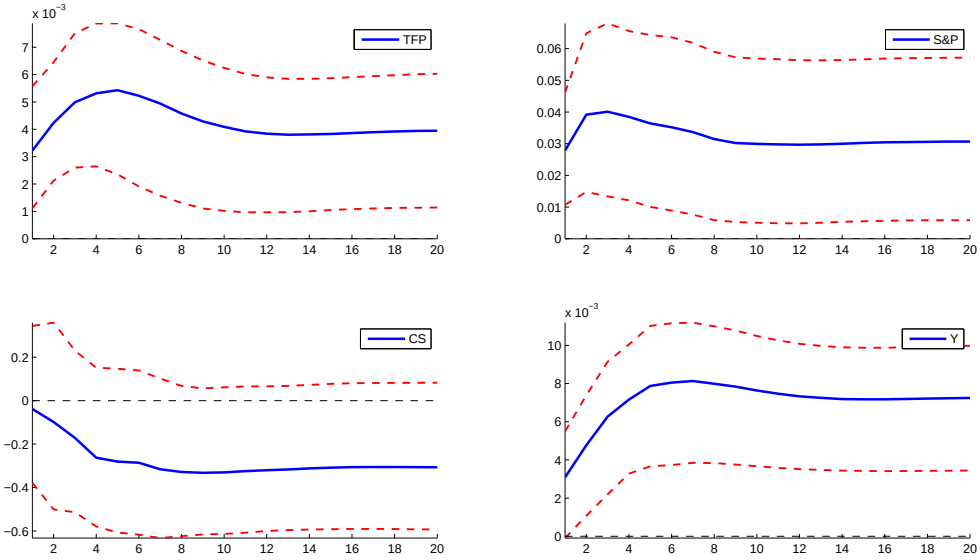

The figure presents the impulse responses to TFP shock of (log) TFP, (log) S&P real stock prices, corporate term spread and (log) output. In order, the number in the table A.1 of presented variables is: 8,1,10, 2. The dashed lines correspond to identification and parameter uncertainty of one-standard deviation.

Figure A.11: IRF to news shock for selected variables - comparison with Beaudry and Portier [2006]

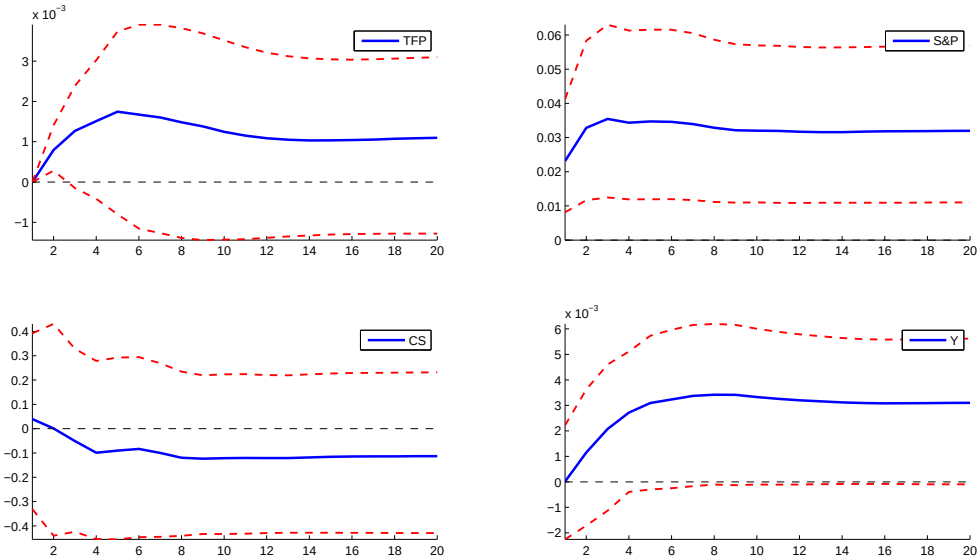

The figure presents the impulse responses to TFP shock of (log) TFP, (log) S&P real stock prices, corporate term spread and (log) output. In order, the number in the table A.1 of presented variables is: 8,1,10, 2. The dashed lines correspond to identification and parameter uncertainty of one-standard deviation.

Figure A.12: Impulse responses to TFP shock for selected variables - comparison with Beaudry and Portier [2006]

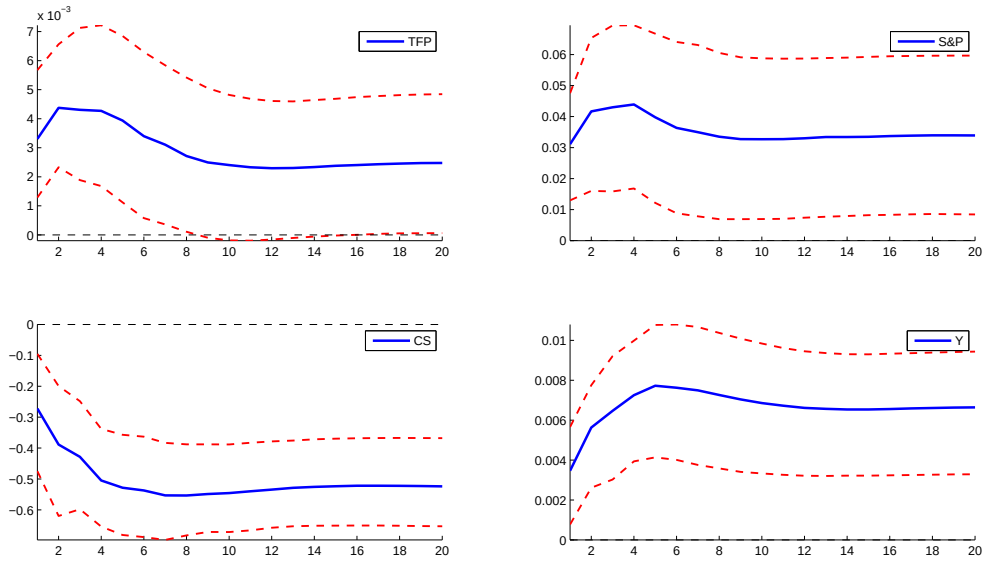

The figure presents the impulse responses to TFP shock of (log) TFP, (log) S&P real stock prices, corporate term spread and (log) output. In order, the number in the table A.1 of presented variables is: 8,1,10, 2. The dashed lines correspond to identification and parameter uncertainty of one-standard deviation.

Figure A.13: Impulse responses to news shock for selected variables - comparison with Beaudry and Portier [2006]

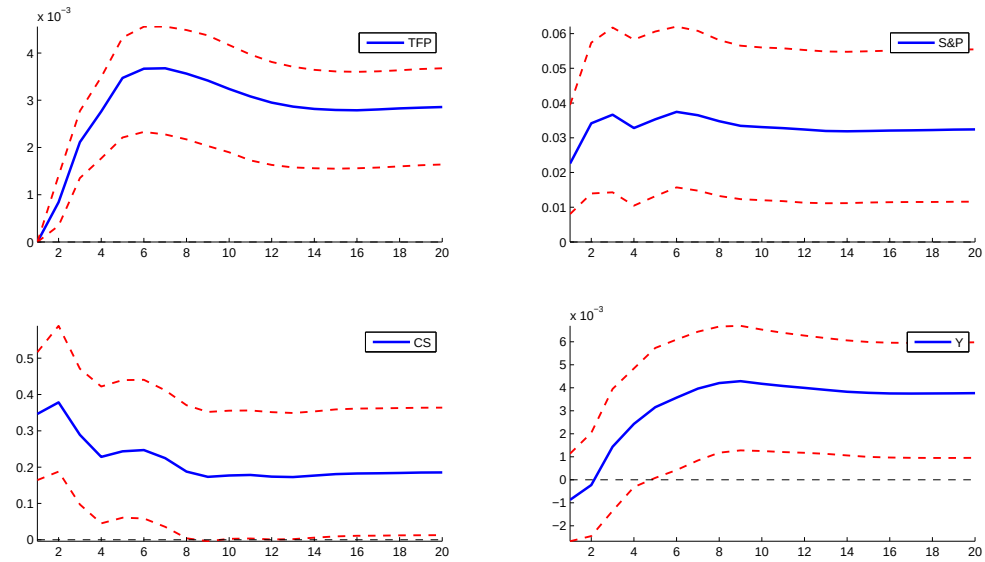

The figure presents the impulse responses to TFP shock of (log) TFP, (log) S&P real stock prices, corporate term spread and (log) output. In order, the number in the table A.1 of presented variables is: 8,1,10, 2. The dashed lines correspond to identification and parameter uncertainty of one-standard deviation.

A.7 Appendix - Comparison with Barsky and Sims [2011]

Figure A.14: Impulse responses to surprise TFP shock for selected variables - comparison with Barsky and Sims [2011]

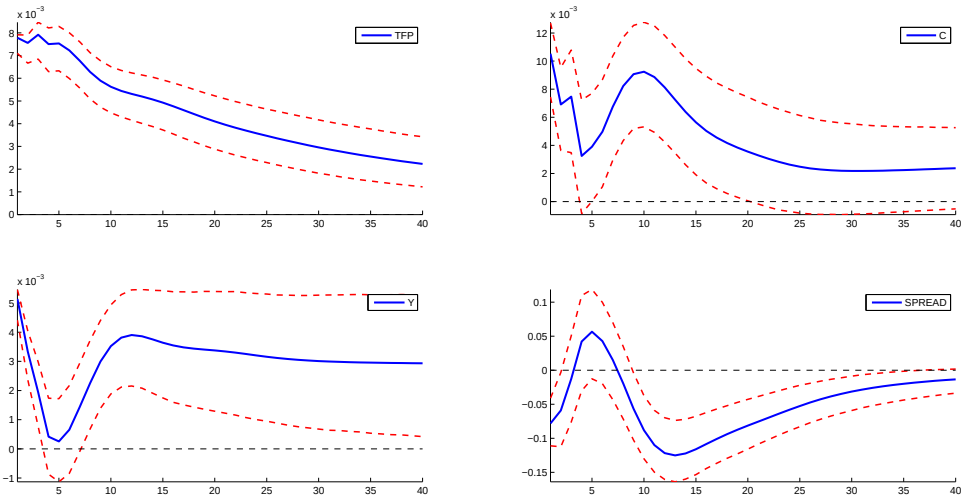

The figure presents the impulse responses to surprise TFP shock of (log) TFP, (log) consumption, (log) output and corporate term spread. In order, the number in the table A.1 of presented variables is: 8,3,2, 10. The solid lines correspond to point estimates. The dashed lines correspond to parameter uncertainty of one-standard deviation.

Figure A.15: Impulse responses to news shock for selected variables - comparison with Barsky and Sims [2011]

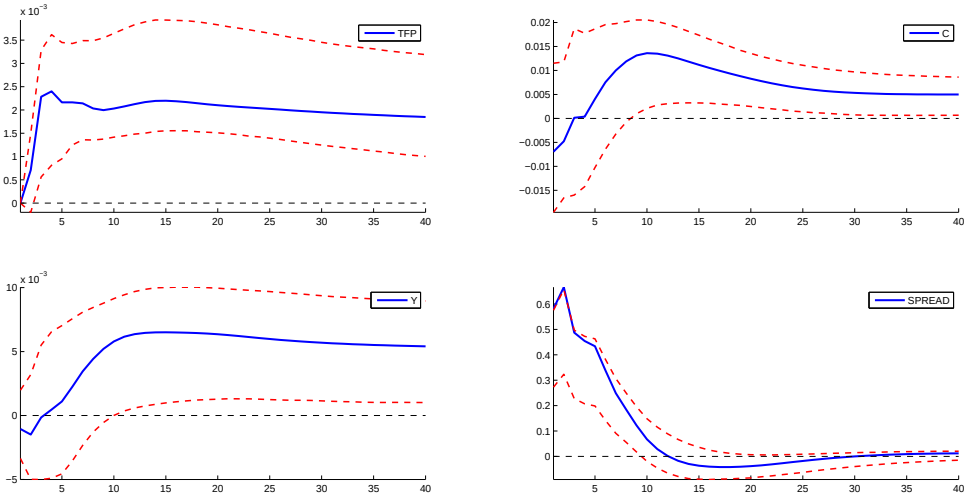

The figure presents the impulse responses to news TFP shock of (log) TFP, (log) consumption, (log) output and corporate term spread. In order, the number in the table A.1 of presented variables is: 8,3,2, 10. The solid lines correspond to point estimates. The dashed lines correspond to parameter uncertainty of one-standard deviation.

A.8 Appendix - Robustness check

Figure A.16: Impulse responses to the surprise TFP shock for selected variables - zero restrictions

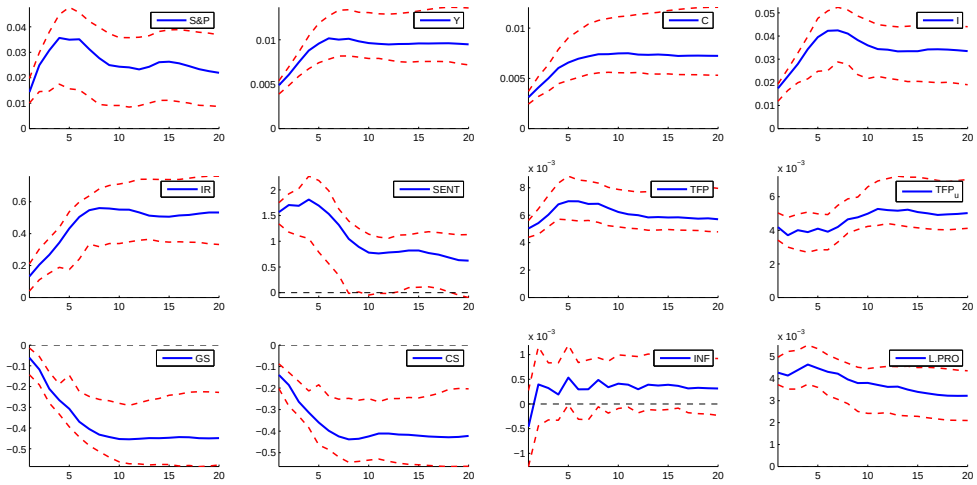

The figure presents the impulse responses to TFP shock of (log) S&P real stock prices, (log) output, (log) consumption and (log) investment in the first row, interest rate, consumer confidence, (log) TFP and (log) TFP adjusted for utilization in the second raw, government term spread, corporate term spread, inflation and (log) labor productivity in the last raw. In order, the number in the table A.1 of presented variables is: 1,2,3,4,5,6,7,8,9,10, 81 and 110. The variables are standardized. The dashed lines correspond to identification,model and parameter uncertainty of one-standard deviation.

Figure A.17: Impulse responses to the news shock for selected variables - zero restrictions

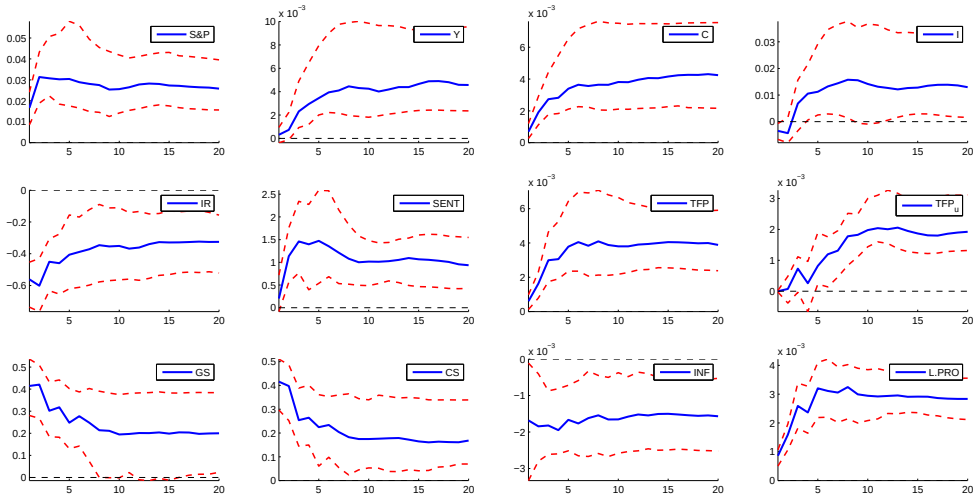

The figure presents the impulse responses to news shock of (log) S&P real stock prices, (log) output, (log) consumption and (log) investment in the first row, interest rate, consumer confidence, (log) TFP and (log) TFP adjusted for utilization in the second raw, government term spread, corporate term spread, inflation and (log) labor productivity in the last raw. In order, the number in the table A.1 of presented variables is: 1,2,3,4,5,6,7,8,9,10, 81 and 110. The variables are standardized. The dashed lines correspond to identification,model and parameter uncertainty of one-standard deviation.

Figure A.18: Impulse responses to the surprise TFP shock for selected variables - only sign restrictions

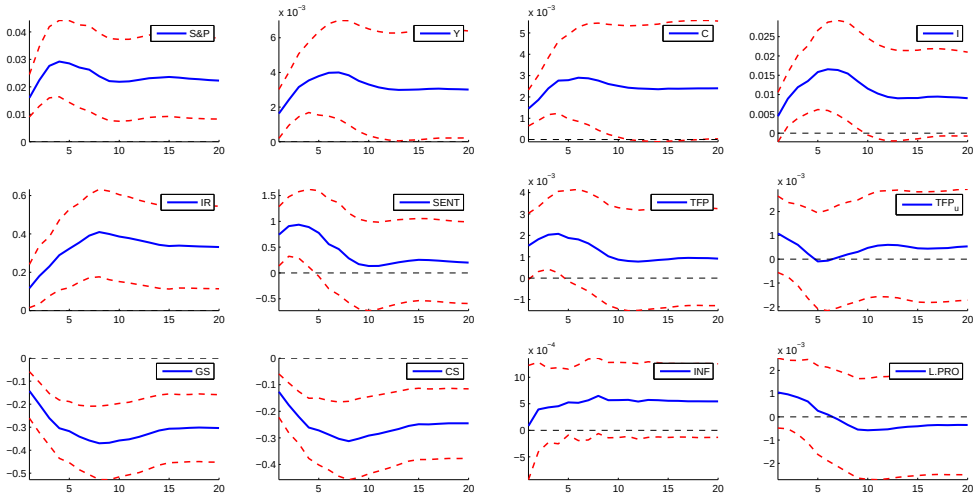

The figure presents the impulse responses to TFP shock of (log) S&P real stock prices, (log) output, (log) consumption and (log) investment in the first row, interest rate, consumer confidence, (log) TFP and (log) TFP adjusted for utilization in the second raw, government term spread, corporate term spread, inflation and (log) labor productivity in the last raw. In order, the number in the table A.1 of presented variables is: 1,2,3,4,5,6,7,8,9,10, 81 and 110. The variables are standardized. The dashed lines correspond to identification,model and parameter uncertainty of one-standard deviation.

Figure A.19: Impulse responses to news shock for selected variables - only sign restrictions

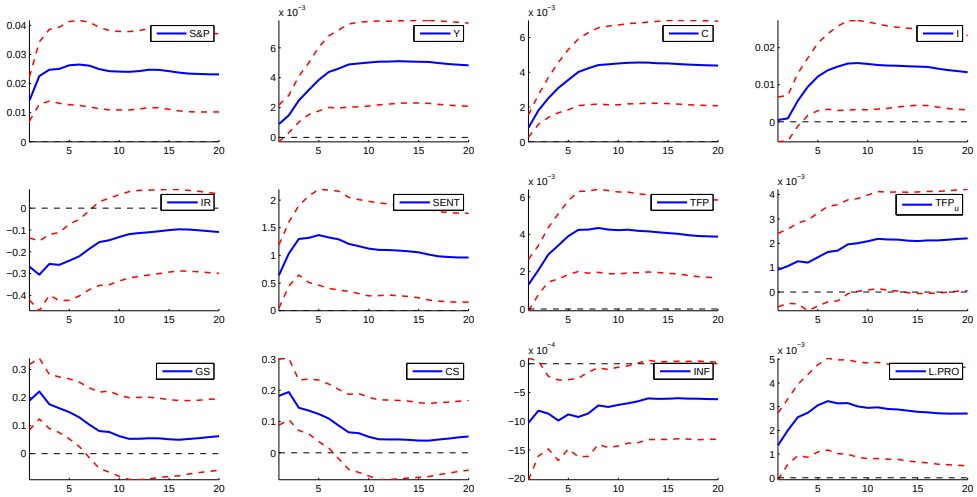

The figure presents the impulse responses to news shock of (log) S&P real stock prices, (log) output, (log) consumption and (log) investment in the first row, interest rate, consumer confidence, (log) TFP and (log) TFP adjusted for utilization in the second raw, government term spread, corporate term spread, inflation and (log) labor productivity in the last raw. In order, the number in the table A.1 of presented variables is: 1,2,3,4,5,6,7,8,9,10, 81 and 110. The variables are standardized. The dashed lines correspond to identification,model and parameter uncertainty of one-standard deviation.

Figure A.20: Forecast Error Variance Decomposition - only sign restrictions

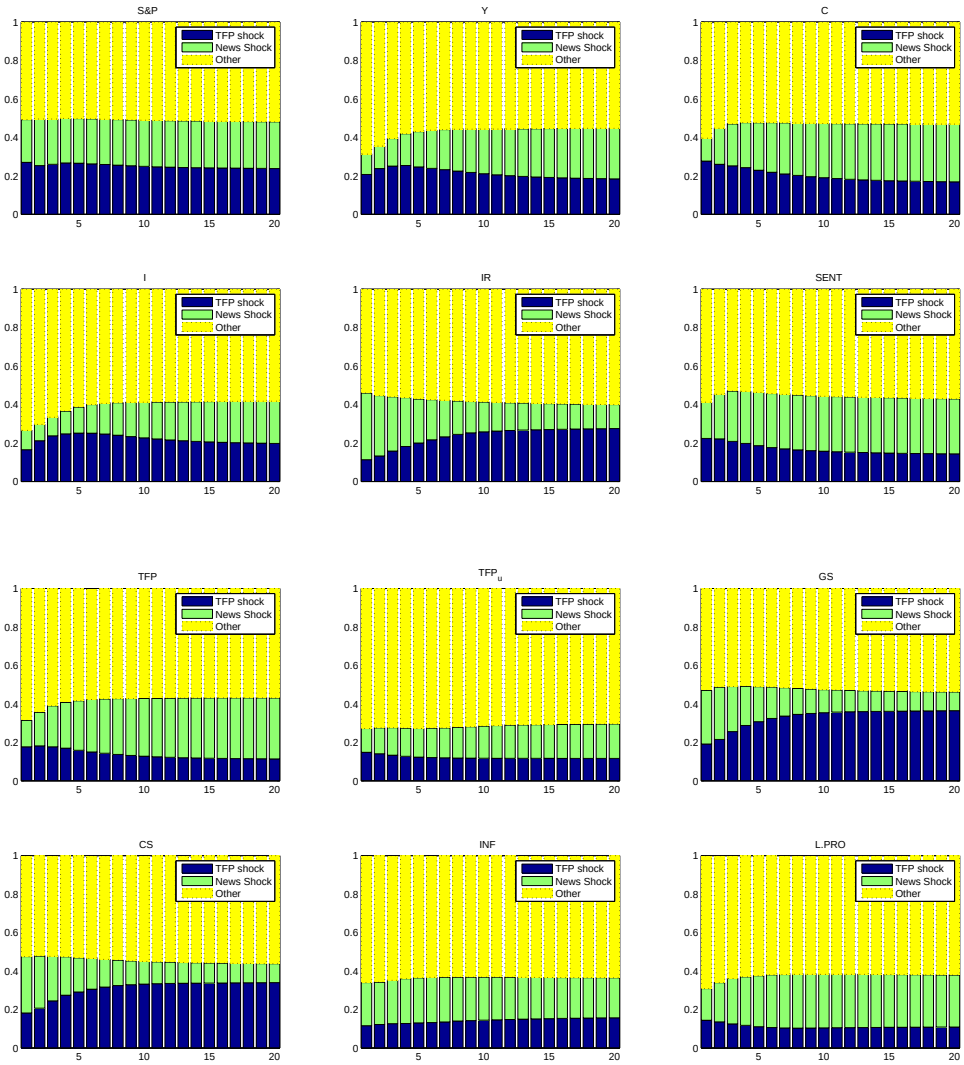

The figure presents Forecast Error Variance Decomposition for the TFP shock, the news shock and other shocks of (log) S&P real stock prices, (log) output and (log) consumption in the first row, (log) investment,interest rate and consumer sentiment in the second row, (log) TFP, (log) TFP adjusted for utilization and government term spread in the third raw, corporate term spread, inflation and (log) labor productivity in the last raw. In order, the number in the table A.1 of presented variables is: 1,2,3,4,5,6,7,8,9,10, 81 and 110. The variables are standardized.

Figure A.21: Impulse responses to TFP shock for selected variables - restrictions only on SP

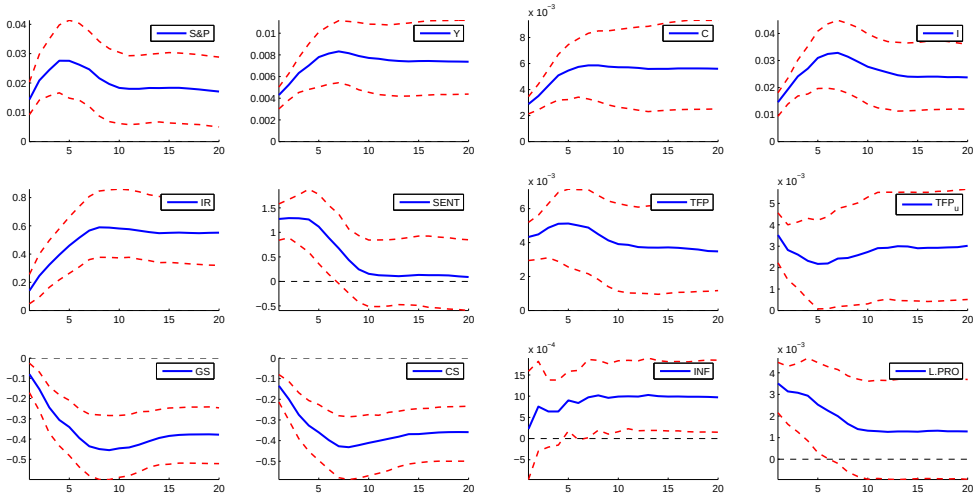

The figure presents the impulse responses to TFP shock of (log) S&P real stock prices, (log) output, (log) consumption and (log) investment in the first row, interest rate, consumer confidence, (log) TFP and (log) TFP adjusted for utilization in the second raw, government term spread, corporate term spread, inflation and (log) labor productivity in the last raw. In order, the number in the table A.1 of presented variables is: 1,2,3,4,5,6,7,8,9,10, 81 and 110. The variables are standardized. The dashed lines correspond to identification,model and parameter uncertainty of one-standard deviation.

Figure A.22: Impulse responses to news shock for selected variables - restrictions only on SP

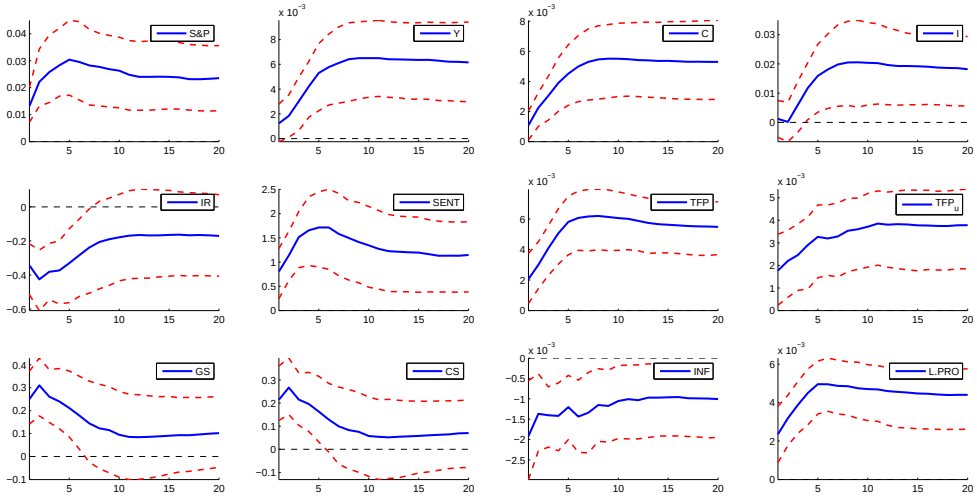

The figure presents the impulse responses to news shock of (log) S&P real stock prices, (log) output, (log) consumption and (log) investment in the first row, interest rate, consumer confidence, (log) TFP and (log) TFP adjusted for utilization in the second raw, government term spread, corporate term spread, inflation and (log) labor productivity in the last raw. In order, the number in the table A.1 of presented variables is: 1,2,3,4,5,6,7,8,9,10, 81 and 110. The variables are standardized. The dashed lines correspond to identification,model and parameter uncertainty of one-standard deviation.

Figure A.23: Impulse responses to TFP shock for selected variables - restrictions only on Consumption

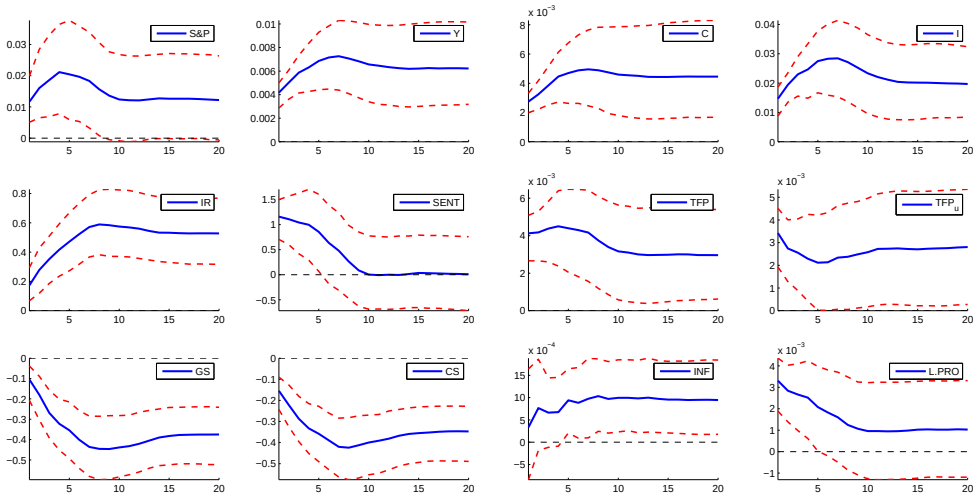

The figure presents the impulse responses to TFP shock of (log) S&P real stock prices, (log) output, (log) consumption and (log) investment in the first row, interest rate, consumer confidence, (log) TFP and (log) TFP adjusted for utilization in the second raw, government term spread, corporate term spread, inflation and (log) labor productivity in the last raw. In order, the number in the table A.1 of presented variables is: 1,2,3,4,5,6,7,8,9,10, 81 and 110. The variables are standardized. The dashed lines correspond to identification,model and parameter uncertainty of one-standard deviation.

Figure A.24: Impulse responses to news shock for selected variables - restrictions only on Consumption

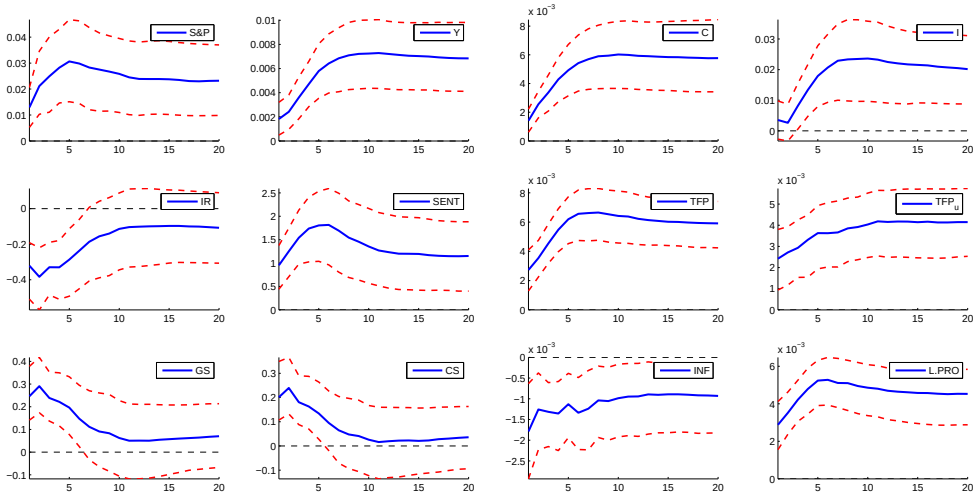

The figure presents the impulse responses to news shock of (log) S&P real stock prices, (log) output, (log) consumption and (log) investment in the first row, interest rate, consumer confidence, (log) TFP and (log) TFP adjusted for utilization in the second raw, government term spread, corporate term spread, inflation and (log) labor productivity in the last raw. In order, the number in the table A.1 of presented variables is: 1,2,3,4,5,6,7,8,9,10, 81 and 110. The variables are standardized. The dashed lines correspond to identification,model and parameter uncertainty of one-standard deviation.

Figure A.25: Impulse responses to TFP shock for selected variables - baseline with 8 lags

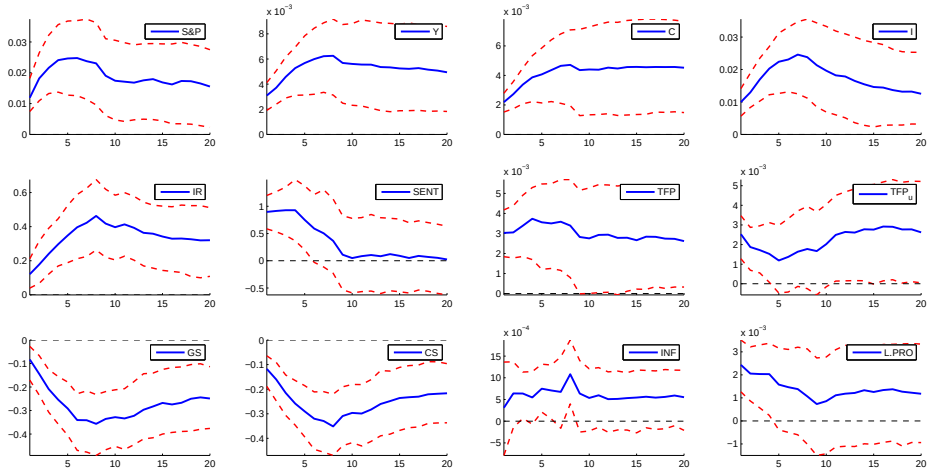

The figure presents the impulse responses to TFP shock of (log) S&P real stock prices, (log) output, (log) consumption and (log) investment in the first row, interest rate, consumer confidence, (log) TFP and (log) TFP adjusted for utilization in the second raw, government term spread, corporate term spread, inflation and (log) labor productivity in the last raw. In order, the number in the table A.1 of presented variables is: 1,2,3,4,5,6,7,8,9,10, 81 and 110. The variables are standardized. The dashed lines correspond to identification,model and parameter uncertainty of one-standard deviation.

Figure A.26: Impulse responses to news shock for selected variables - baseline with 8 lags

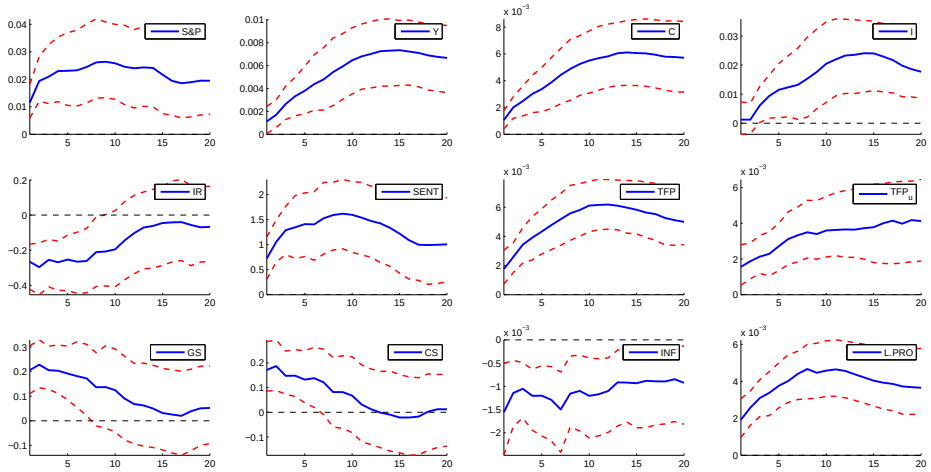

The figure presents the impulse responses to news shock of (log) S&P real stock prices, (log) output, (log) consumption and (log) investment in the first row, interest rate, consumer confidence, (log) TFP and (log) TFP adjusted for utilization in the second raw, government term spread, corporate term spread, inflation and (log) labor productivity in the last raw. In order, the number in the table A.1 of presented variables is: 1,2,3,4,5,6,7,8,9,10, 81 and 110. The variables are standardized. The dashed lines correspond to identification,model and parameter uncertainty of one-standard deviation.

Figure A.27: Impulse responses to TFP shock for selected variables - baseline with 1 lag

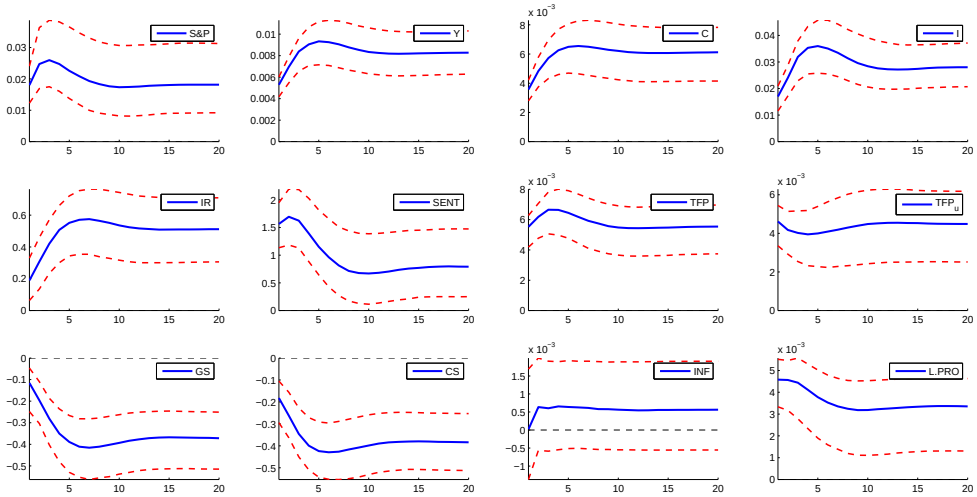

The figure presents the impulse responses to TFP shock of (log) S&P real stock prices, (log) output, (log) consumption and (log) investment in the first row, interest rate, consumer confidence, (log) TFP and (log) TFP adjusted for utilization in the second raw, government term spread, corporate term spread, inflation and (log) labor productivity in the last raw. In order, the number in the table A.1 of presented variables is: 1,2,3,4,5,6,7,8,9,10, 81 and 110. The variables are standardized. The dashed lines correspond to identification,model and parameter uncertainty of one-standard deviation.

Figure A.28: Impulse responses to news shock for selected variables - baseline with 1 lag

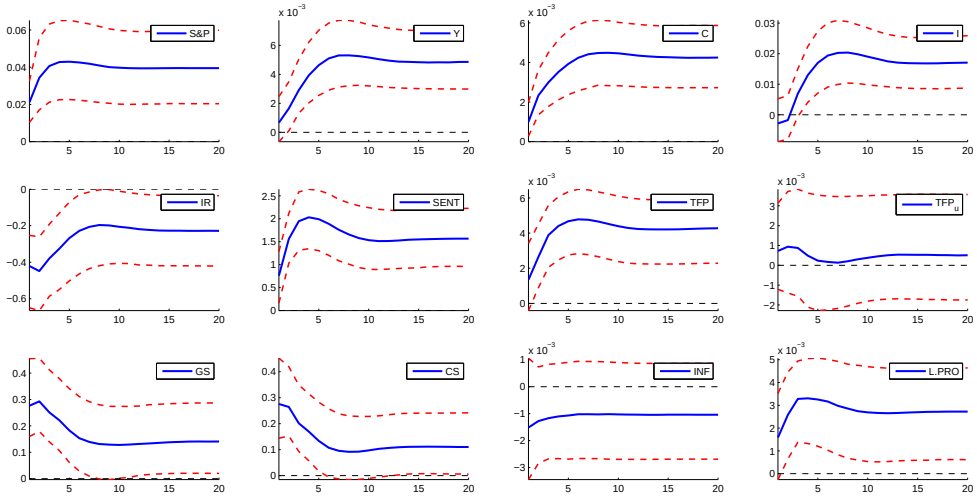

The figure presents the impulse responses to news shock of (log) S&P real stock prices, (log) output, (log) consumption and (log) investment in the first row, interest rate, consumer confidence, (log) TFP and (log) TFP adjusted for utilization in the second raw, government term spread, corporate term spread, inflation and (log) labor productivity in the last raw. In order, the number in the table A.1 of presented variables is: 1,2,3,4,5,6,7,8,9,10, 81 and 110. The variables are standardized. The dashed lines correspond to identification,model and parameter uncertainty of one-standard deviation.

Chapter 2

Animal Spirits, Fundamental Factors and Business Cycle Fluctuations

joint with Stephane Dées

2.1 Introduction

The 2008/09 financial crisis and the Great Recession that followed has led many observers and academics to interpret the recession as a sharp decline in aggregate demand resulting from a collapse in confidence. This gave rise to a self-fulfilling shock to expectations.[1] This suggests that the way that households and firms form expectations of the future may therefore be an independent driving force of the business cycle.

The idea that agents' beliefs may be a source of economic fluctuations has a long history. Pigou [1929] was among the first to stress that expectations were key in explaining business cycles, as psychological factors (i.e. undue optimism and pessimism) lead entrepreneurs to make errors when forming their expectations about future profits. These errors generate cycles through rises and falls in investment. These psychological factors are also very often called "animal spirits", following Keynes [1936]. Although the Real Business Cycle theory does not incorporate such psychological factors in its explanation of economic fluctuations, Pigou's ideas have recently been reintroduced into the theory of cycles in the context of equilibrium business cycle models, notably by Beaudry and Portier [2006] or Jaimovich and Rebelo [2009]. In these models, although technology remains the only determinant of output in the long run, news about future fundamentals can imply a change in expectations, which affects agents' behaviors in the short run in anticipation of the fundamental change. However, economic agents receive only noisy signals about future technology, leading to expectational errors (Lorenzoni [2009]). If the information subsequently appears to have been wrong, i.e. it was just noise, the agents readjust their

[1] See e.g. ECB [2013],Farmer [2012] and Bacchetta et al. [2012]

expectations and decisions accordingly. Conversely, if the information proves correct, the economy adjusts gradually to the level of activity consistent with technology. These changes in expectations generate economic fluctuations, both in the short and the long term.

Blanchard et al. [2013] explore the role of noisy information in cyclical developments empirically, separating fluctuations that are due to genuine changes in fundamentals (news shocks) from those due to temporary expectational errors (noise shocks). They show that identification of the shock is only possible via the estimation of a full structural model, such as the one in Barsky and Sims [2012]. Since economic agents face a signal extraction problem when separating news from noise shocks, the econometrician, using the same data, cannot use structural VARs to recover such shocks. However, although this point is valid in real time, the econometrician can potentially have access to a richer dataset in hindsight.

Based on this idea, this paper shows that a structural VAR model can be used to identify news and noise shocks. First, while economic agents can observe only current and past data, the econometrician can also observe "future" data. In other words, by using the data from the whole sample, the econometrician can have a better estimate of the technological trends than the economic agents. Second, economic agents only observe real-time data, while the econometrician also has access to revised data.

Recent papers have also proposed alternative ways to solve the issue put forward by Blanchard et al. [2013]. Forni et al. [2013] use a modification of the structural VAR method to disentangle real from noise shocks, using future data and future residuals. However, their methodology is only applicable in economies in which the true state of the economy can eventually be exactly retried. In this paper we show that our methodology can be used to approximately identify news and noise shocks in more general models, such as that of Blanchard et al. [2013], in which the true state of economy can never be retrieved. Enders et al. [2013] identify noise shocks in a standard VAR model by including 'nowcast errors', defined as the difference between actual output growth and growth estimated contemporaneously by professional forecasters. Here we also use nowcast errors of output growth to improve the estimates of potential output, but, unlike those authors, we also use the fact that econometricians have access to the later realizations of the time series.

We start our analysis by designing a slightly modified version of the model by Blanchard et al. [2013] and show how a structural VAR can be used to disentangle news and noise shocks. The methodology relies on the forecast errors consumers make when predicting the trend of GDP. These forecast errors are estimated by exploiting the fact that econometricians have access to 'future' and revised data. Applying this method to US data, we find that identified permanent and noise shocks have effects as predicted by the theory. A permanent (technology) shock has an expansionary effect on the economy, which builds through time until variables settle at a new, higher value. A noise shock also

has an expansionary effect on the economy, but the impact fades away over time until all variables settle at their initial value. Nevertheless, noise shocks are more important for business cycle fluctuations, as almost half of output variations at business cycle frequencies can be explained by noise shocks. On the other hand, permanent shocks drive the economy in the long run, but only account for around 20 percent of output variations at business cycle frequencies.

After a presentation of the theoretical model in Section 2.2, in Section 2.3 we explain the problems related to identifying noise shocks in the data with SVAR models. We then show that, by using future observations and revisions of data, we can circumvent those problems and still use SVAR models to extract technology and noise shocks. In Section 2.4, we present empirical evidence on the effects of news and noise shocks, by applying our methodology to US data. We conclude in Section 2.5.

2.2 Model

This section presents a simple model, similar to the model proposed by Blanchard et al. [2013], in which consumers decide their level of consumption based on their expectations about the economy's long-run fundamentals. Long-run economic fundamentals are driven by productivity developments (i.e. technology), which depend on a structural shock with permanent effects and which build up gradually. Consumers do not observe the structural shock but only a noisy signal. This additional source of fluctuations is called a noise shock (or an "animal spirits" shock). As in Blanchard et al. [2013], consumers solve a signal extraction problem and decide their level of consumption on the basis of their expectations about future technology.

2.2.1 The structure of the model

We assume first that consumption is determined by the following Euler equation:

$$c_t = E_t[c_{t+1}|\mathcal{I}_t] \tag{2.2.1}$$

where c_t is consumption and $E_t[c_{t+1}|\mathcal{I}_t]$ is expected consumption in period $t+1$ based on the information set at time t, denoted $\mathcal{I}_t$. The supply side of the economy is completely determined by the demand side, which implies that output, y_t, equals consumption:

$$y_t = c_t \tag{2.2.2}$$

Output depends on utilization, u_t and the level of technology, a_t, in a linear fashion, $y_t = a_t + u_t$. Given the level of technology and consumption, utilization adjusts to produce the demanded level of output. However, in the long-run, output is equal to its

natural level, and utilization is equal to zero, implying:

$$\lim_{t\to\infty} E_t[c_{t+j} - a_{t+j}] = 0 \tag{2.2.3}$$

As is shown in Blanchard et al. [2013], equation (2.2.3) can be derived from a standard New-Keynesian model with Calvo pricing, when the frequency of price adjustment goes to zero. Combining (2.2.1) and (2.2.3) gives:

$$c_t = \lim_{t\to\infty} E_t[a_{t+j}|\mathcal{I}_t] \tag{2.2.4}$$

which implies that consumption depends on expectations about long-run productivity.

The relevant state of the economy is productivity, a_t, which follows the process:

$$a_t = (1+\rho)a_{t-1} - \rho a_{t-2} + \epsilon_t \tag{2.2.5}$$

where $\epsilon_t \sim \mathcal{N}(0, \sigma_\epsilon^2)$ is a technology shock. Given that productivity is modeled as a process with a stochastic trend, the technology shock ϵ_t will have a permanent effect on productivity.

2.2.2 Information structure

The crucial difference with a standard DSGE model lies in the information structure. Consumers do not observe productivity directly, but observe only a noisy signal of productivity, s_t:

$$s_t \;=\; a_t + \upsilon_t \tag{2.2.6}$$

where $\upsilon_t \sim \mathcal{N}(0, \sigma_\upsilon^2)$ is a noise shock. The signal extraction problem can be rewritten as a state-space model:

- State Equation

$$\begin{bmatrix} a_{t|t} \\ a_{t-1|t} \end{bmatrix} = A \begin{bmatrix} a_{t-1|t-1} \\ a_{t-2|t-1} \end{bmatrix} + B \begin{bmatrix} \epsilon_t \\ \upsilon_t \end{bmatrix} \tag{2.2.7}$$

- Observation Equation

$$s_t = C \begin{bmatrix} a_{t|t} \\ a_{t-1|t} \end{bmatrix} + D \begin{bmatrix} \epsilon_t \\ \upsilon_t \end{bmatrix} \tag{2.2.8}$$

where $a_{t|t} = E_t[a_t|\mathcal{I}_t]$ and the matrices A, B, C and D depend on parameters. We assume that consumers know the underlying parameters of the economy and the distributions of shocks, in other words they know the matrices A, B, C and D, and thus they can use a Kalman filter to form expectations about the current state of technology.[2]

[2]Note that we are assuming that consumers do not observe utilization, otherwise agents could differentiate between technology shock and noise shock by observing utilization. Utilization is anyway difficult

Figure B.1 shows, for simulated data, the developments in productivity, i.e. potential output growth, displayed by the smoothed line in the upper panel. Consumers receive a noisy signal, which is by definition very volatile and form their expectations by solving the signal extraction problem. Consumers' expectations about technology are not accurate as they are affected by the noise shock. The lower panel shows the forecast errors made by consumers when predicting the state of the economy.

2.2.3 Model solution

Once we obtain the agent's expectations about the state of technology, by standard Kalman filtering, the solution of the model is straightforward. From Equation (2.2.4) and (2.2.5) we can derive the solution of consumption in terms of the agent's expectations about the state of technology:

$$c_t = \frac{1}{1-\rho}\left(a_{t|t} - \rho a_{t-1|t}\right) \tag{2.2.9}$$

where we have used the same notation as in the setup of the Kalman filter, $a_{t|t} = E_t[a_t|\mathcal{I}_t]$ and $a_{t-1|t} = E_t[a_{t-1}|\mathcal{I}_t]$. The other variables are a linear function of technology:

$$y_t = c_t \tag{2.2.10}$$

$$u_t = a_t - y_t \tag{2.2.11}$$

Figure B.2 shows the response of the model's variables to the technology shock, ϵ_t. The standard deviation of the shock is 0.7 percent.From equation (2.2.6), in the absence of noise shocks, the signal, s_t, is equal to a_t. Consumers underpredict the actual technological improvement in the short term, leading to a negative forecast error. Over time, as the signal confirms the increase in productivity, the expectations converge gradually to the new state of the economy and the forecast error fades away. Consumption improves faster in anticipation of the long-term effects of the technology shock.

Figure B.3 shows the responses to a noise shock. The noise shock is characterized by a one-off change in the signal and no change in productivity. In the short term, consumers believe that the positive signal could potentially be related to a change in technology and their expectations about the state of the economy are positive. Over time, they realise that the signal was just noise and the expectations gradually adjust to the initial state. As a result, the consumers' forecast error is positive in the short term and returns gradually to zero over time. This short term optimism also leads consumption to be positively affected

to observe at the macroeconomic level, even though proxies for utilization of labour can be found (e.g. hours worked). Moreover, we could also remove this assumption by introducing a transitory technological shock, as in Blanchard et al. [2013]. By ignoring this extension, we aimed at keeping the presentation of the signal-extraction problem as simple as possible.

by the noise shock, as the shock has been unduly interpreted as a technology shock. Over time, when the information becomes more accurate, they realize their forecast error and readjust their consumption expenditures.

It is worth noting that, as in Lorenzoni [2009], the only source of exogenous uncertainty is the productivity process a_t and noise shocks have the features of aggregate demand shocks. As with productivity shocks, noise shocks are unobservable because they are related to a noisy signal of productivity. As a result, only these two shocks can lead to forecast errors in the same period about the current state of technology. In a more complex model, we could therefore assume that all other sources of disturbances are observable and do not lead to such forecast errors. Moreover, the general idea developed here can easily be carried over in more complex models with capital accumulation, nominal rigidities or habit persistence. For instance, Blanchard et al. [2013] show that such results are robust when they embed the same productivity process and information structure in a small-scale DSGE model, including investment and capital accumulation, nominal rigidities and a monetary policy rule.

2.3 From the model to a structural VAR

In this section, we focus on the way to identify and estimate the technology and noise shocks. Since consumers only receive a noisy signal about the shocks, it is not possible to recover technology and noise shocks from actual data on c_t and s_t. First, we show that a VAR representation of the model faces an issue of non-invertibility and non-fundamentalness. Second, as the issue is mainly related to the fact that the information set used by consumers is not accurate enough to recover the shocks, we show that having a superior information set can help solve the problem. Third, we show how a structural VAR approach can be used in this context.

2.3.1 Singularity of VAR models

Let us consider running a VAR with consumption, c_t, and the signal, s_t, to obtain the structural shocks. From Equation (2.2.9) we know that consumption is a linear function of expectations about the current and past states of the economy:

$$c_t = f\left(E_t[a_t|\mathcal{I}_t]\right) \tag{2.3.1}$$

As the expectations about the current and past states are formed by a Kalman filtering approach, which is a linear filter, we also know that these expectations are a linear function of current and past signals:

$$E_t[a_t|\mathcal{I}_t] = g(s_t, s_{t-1}, ...) \tag{2.3.2}$$

Equations (2.3.1) and (2.3.2) imply that consumption is a linear function of current and past signals:

$$c_t = f(g(s_t, s_{t-1}, ...)) \tag{2.3.3}$$

Combining Equations (2.2.5) and (2.2.6), we can rewrite the signal process as $s_t = (1+\rho)a_{t-1} - \rho a_{t-2} + \epsilon_t + \upsilon_t$. We can notice that both shocks - technology and noise shocks - affect the signal. Moreover, both shocks affect the signal in the same way, or more formally:

$$\frac{\partial s_t}{\partial \epsilon_t} = \frac{\partial s_t}{\partial \upsilon_t} \tag{2.3.4}$$

For the same size shock, the signal will increase by the same amount to both shocks. As consumption is a linear function of the signal, consumption also responds in the same way to both shocks:

$$\frac{\partial c_t}{\partial \epsilon_t} = \frac{\partial c_t}{\partial \upsilon_t} \tag{2.3.5}$$

In other words, on impact consumers respond in the same way to technology and noise shocks, as they only observe the increase in the signal and are not able to differentiate between the two shocks.

This implies that running a VAR model with consumption and the signal results in a singular system. Moreover, if we extended our model with additional observables, such as stock prices, consumer sentiment or growth forecasts, this would not help to identify the shocks. In particular, so long as those observables are a linear function of the signal, we will have that:

$$\frac{\partial x_t}{\partial \epsilon_t} = \frac{\partial x_t}{\partial \upsilon_t} \tag{2.3.6}$$

To show the problems related to the use of a VAR model in such a case, we perform the following exercise: we use simulated data to estimate a non-singular VAR model with consumption and the signal by adding a measurement error to the signal.[3] Technology and noise shocks are identified by theoretically consistent long-run restrictions: the technology shock is identified as a shock with permanent effects on consumption and the noise shock is a shock with only transitory effects.

The impulse responses of consumption to those shocks are plotted in Figure B.4, which shows that such an approach is not able to correctly identify the two shocks. While the first shock is permanent, it does not build up slowly, as with our theory-based technology shock, but jumps on impact. Similarly, we expect that the identified transitory shock would be a mixture of the measurement error and the theoretical noise shock. Figure B.4 shows that, unlike the structural shock, consumption does not respond at all to the identified transitory shock.

The above principles do not hold for the reaction of consumption in later periods. In

[3]The Measurement error is assumed to be a white noise process with $\mathcal{N}(0, 0.0001\sigma_v^2)$

other words, we have that:

$$\frac{\partial s_{t+j}}{\partial \epsilon_t} \neq \frac{\partial s_{t+j}}{\partial \upsilon_t} \quad \forall\ j = 1, 2, ... \quad \rightarrow \quad \frac{\partial c_{t+j}}{\partial \epsilon_t} \neq \frac{\partial c_{t+j}}{\partial \upsilon_t} \quad \forall\ j = 1, 2, ... \tag{2.3.7}$$

As consumers begin to differentiate between the two shocks, via the Kalman filter, the response of consumption differs in the periods following the shocks.

2.3.2 Consumers vs. Econometricians

The preceding discussion shows that to identify shocks we have to use a superior information set than that available to consumers. To start with an extreme situation, let us assume that the econometrician has access to time series of technology and can infer the consumers' forecast error:

$$\eta_t = E_t[a_t|\mathcal{I}_t] - a_t \tag{2.3.8}$$

Technology responds differently to the two shocks:

$$1 = \frac{\partial a_t}{\partial \epsilon_t} \neq \frac{\partial a_t}{\partial \upsilon_t} = 0 \tag{2.3.9}$$

and since the forecast error is a linear function of technology and the signal, it responds differently to the two shocks:

$$\frac{\partial \eta_t}{\partial \epsilon_t} \neq \frac{\partial \eta_t}{\partial \upsilon_t} \tag{2.3.10}$$

This fact is implicitly used in Enders et al. [2013] and Forni et al. [2013] to justify the identification of noise shocks. In the former paper, the authors use the assumption that forecast errors are observable at the end of the period and therefore the econometrician has access to forecast errors that can be directly included in a VAR. Similarly, Forni et al. [2013] assume that potential output is revealed after one period and therefore the econometrician can retrieve forecast errors. Had we assumed that the econometrician has access to forecast errors, for example by observing utilization, we would also be able to exactly identify the shocks, as is shown by the simulations presented in Figure B.7.

However, in reality, the econometrician cannot observe the true technology and the related forecast errors. In a less extreme situation, we can assume that the econometrician does not have access to perfect information about the state of the economy, but can have access to superior information than the agents.

How well can the econometrician approximate the forecast error by using a superior information set, $\mathcal{I}_t^e$? We can define the forecast errors and the econometrician's estimate of the forecast errors as:

$$\eta_t = E_t[a_t|\mathcal{I}_t] - a_t \quad \rightarrow \quad \hat{\eta}_t = E_t[a_t|\mathcal{I}_t] - E_t[a_t|\mathcal{I}_t^e] \tag{2.3.11}$$

In the extreme case described above, when the econometrician has perfect information, $E_t[a_t|\mathcal{I}_t^e] = a_t$, and the econometrician would be able to exactly recover the forecast error, $\hat{\eta}_t = \eta_t$. Note that, in the opposite extreme, if the econometrician has the same information set as the agents, their estimate of the forecast error is 0.

With a more plausible situation, there are two ways in which the econometrician can use superior information to achieve a more precise estimate of the state of economy, i.e. achieve $var(E_t[a_t|\mathcal{I}_t^e] - a_t) < var(E_t[a_t|\mathcal{I}_t] - a_t)$:

- Using more accurate signals: $var[\upsilon_t|\mathcal{I}_t^e] < var[\upsilon_t|\mathcal{I}_t]$
- Using future observations: $\mathcal{I}_t \subset \mathcal{I}_t^e$

Using more accurate signals

In the real world, consumers and firms have to base their decisions on real-time data. As shown for instance by Diebold and Rudebusch [1991], forecast errors tend to be larger when using real-time data compared with those based on revised data.

It can be shown that:

$$\lim_{\sigma_\upsilon^2 \to 0} E[E_t[a_t|\mathcal{I}_t^e] - a_t] = 0 \tag{2.3.12}$$

which implies that in the limit, when the signal becomes perfectly informative, we can exactly recover the state and the forecast error, η_t. We can also show that:

$$\sigma_\upsilon^2 < \sigma_\upsilon^{2*} \ \rightarrow var[\eta_t|\sigma_\upsilon^2] < var[\eta_t|\sigma_\upsilon^{2*}] \tag{2.3.13}$$

which implies that more informative signals help to decrease the forecast error and the more precise the signal, the greater the decrease in the forecast error.

In order to see how more accurate signals help to estimate the forecast error, we run a simulation where consumers have a signal with the baseline variance, σ_υ^2, while the econometrician can use a signal with smaller variance to predict the state. The estimate of the forecast error is then constructed as $\hat{\eta}_t = E_t[a_t|\mathcal{I}_t] - E_t[a_t|\mathcal{I}_t^e]$, where the difference in consumers' and the econometrician's information sets, $\mathcal{I}_t$ and $\mathcal{I}_t^e$, relates to the difference in the variance of the signal.

Figure B.5 shows how the estimated forecast error evolves according to the quality of the signal. The black lines show the errors implied by the theoretical models after a permanent and a noise shock. When the signal becomes less noisy, the lines move closer to the theoretical impulse responses and the correlation between the estimated and the true forecast errors increase rapidly when the variance of the noise is reduced.[4]

[4]How much the reduction in the variance of the noise shocks contributes to the better estimate of the forecast error depends on the correlation between the improvements in the signal and the noise shock. When newly defined noise shocks with lower variance can be written as $\upsilon_t^* = a\upsilon_t$, implying that the correlation between improvement in the signal and the noise shocks is perfect, the improvement in the

Using future observations

The econometrician can also potentially observe a larger dataset, including 'future' data. By contrast, consumers cannot observe 'future' realizations. If we define $\mathcal{I}_t^{e.j} = \{s_{t+j}, s_{t+j-1}, s_{t+j-2}, ...\}$, we can show:[5]

$$var[E_t[a_t|\mathcal{I}_t^{e.(j+h)}] - a_t] < var[E_t[a_t|\mathcal{I}_t^{e.j}] - a_t] \ \forall \ h = 1, 2, ... \tag{2.3.14}$$

which implies that having access to future signals helps to decrease the forecast error and the more leads are available, the greater the decrease.

In general, future data does not perfectly reveal the true state of technology and therefore the true forecast error, η_t. The gain one obtains by using future observations depends on the variance of the signal - the lower is the variance of the signal, the greater is the improvement in estimation accuracy that we can obtain by including future observations.

We perform another simulation allowing the econometrician to observe different number of leads of the signal. The forecast error is then estimated as:

$$\hat{\eta}_t = E_t[a_t|\mathcal{I}_t] - E_t[a_t|\mathcal{I}_t^{e.j}] \tag{2.3.15}$$

Figure B.6 shows how close to the actual forecast errors the estimated forecast error can become when we increase the number of leads. For the permanent shock, adding four leads is almost sufficient to reproduce the shape of the true forecast error. By contrast, it is more difficult to estimate the forecast error following a noise shock. Nevertheless, four leads imply an impulse response that is qualitatively similar to what the theoretical model gives. Overall, the correlation between the estimated and the true forecast errors is equal to 0.72 with four leads.

It is important to note that it is this improvement in the estimate of a_t that allows the econometrician to estimate the forecast error. In fact, from the definition of $\hat{\eta}_t$, we see that the econometrician's estimate of the forecast error is equal to their correction, relative to the agents, of the estimate the true state. Thus, we can decompose $\hat{\eta}_t$ into a component due to the use of revised data, which we denote by $\hat{\lambda}_t$, and a component due to the use of future data, denoted by $\hat{\kappa}_t$. All the possible differences can be summarized in the following table:

signal contributes the most to the better estimate of the forecast error. In this subsection we assumed correlation between the improvements in the signal and noise shocks is perfect. See also footnote 6.

[5]See Simon [2006], page 271.

Table 2.1: Forecast error estimation

	Kalman Filter	**Kalman Smoother**
Real time data	Consumers' estimate expectation	$\hat{\kappa_t}$
Revised data	$\hat{\lambda_t}$	Econometrician's estimate ($\hat{\eta_t}$)

Using simulated data, Figure B.10 shows the estimate of the forecast error using future signals, and its difference with the true forecast error. As shown in the lower panel, the estimated forecast error matches the patterns of the actual forecast error and the correlation between the two is relatively high (0.8). Similarly, Figure B.11 shows the same graphs for an estimate of the forecast error using a less noisy signal. The correlation between the true forecast error and the estimated one is again high (0.8). Finally, Figure B.12 shows the estimate of the forecast error that combines the previous two estimates. The correlation between this final estimate of the forecast error and the true one is very high (0.93), which supports our strategy.

2.3.3 Approximation with a VAR model

We have seen above that we can approximate the forecast error, $\hat{\eta}_t$, by using more precise data and future values of the signal. We have also shown that if we had access to the series of forecast errors, η_t, we could use a SVAR model to obtain the series of noise and technology shocks. Can we still use a SVAR model if we replace the original forecast errors by approximated forecast errors?

To answer this question, we estimate a SVAR model that includes consumption and instead of the true forecast error, as in Section 2.2, we use estimates of the forecast errors, $\hat{\eta}_t$. The estimates of forecast errors are obtained by using both future observations and more precise signals.[6]

The identification of the shocks is obtained by sign restrictions. From theory, we know that the forecast error responds negatively to the technology shock and positively to the noise shock, while consumption responds positively to both. This implies that we can use the following sign restrictions to identify permanent and noise shocks:

	Permanent shock	Noise shock
Consumption	+	+
Forecast error ($\hat{\eta}_t$)	-	+

[6] The use of future observations may cause VAR with forecast errors to be singular. However, when the improvements in the signal are not perfectly correlated with the noise shocks itself, i.e. the newly defined noise shocks with lower variance cannot be written as $\upsilon_t^* = a\upsilon_t$, the problem of singularity does not appear. The detailed explanation can be found in Appendix B.2. In the following exercises we assume that the correlation between the improvements in the signal and the noise shocks is zero.

In the following example, we use a 50 percent less noisy signal and four leads of the signal to produce the econometrician's estimate of the forecast error, $\hat{\eta}_t$.

Figure B.8 compares the theoretical and the estimated impulse responses to a technology shock (first row) and a noise shock (second row). The shape and size of the two forecast errors are very similar to the theoretical ones, implying that our sign restriction strategy is now able to distinguish between a technology and a noise shock. The response of consumption to these shocks is also similar to what the theoretical model predicts: after a technology shock, consumption increases gradually and is permanently affected by the shock; after a noise shock, consumption increases only in the short term and returns gradually to the baseline state after a few periods. Figure B.9 shows the results of the same exercise by comparing estimated (first row) and theoretical (second row) forecast error variance decompositions (FEVD). The contributions of technological and noise shocks to the forecast error variance is very similar when comparing the estimated and the theoretical decompositions. Noise shocks explain most of the variance of consumption and forecast error in the short-run, while permanent shocks mainly explain the variance of consumption in the long-run.

2.3.4 Comparison with Forni et al. [2013]

In this subsection we show that methodology proposed in Forni et al. [2013] cannot be applied to a general signal extraction model as used in this paper and in Blanchard et al. [2013]. Moreover, we show that our approach can easily accommodate their methodology.

The two crucial equations of the model in Forni et al. [2013] are:

$$a_t = a_{t-1} + \varepsilon_{t-1} \tag{2.3.16}$$

$$s_t = a_t + \upsilon_t \tag{2.3.17}$$

where a_t is the observable technology, s_t is a signal about technology, ε_t is the technology shock and υ_t is the noise shock. The signal extraction problem comes from the fact that the technology shock has delayed effects on technology $\Delta a_t = \varepsilon_{t-1}$. Importantly, contrary to the general model used in this paper, this framework implies that a VAR including the current observable technology and the signal is not singular. This is easy to see as $\frac{\partial s_t}{\partial \varepsilon_t} = \frac{\partial s_t}{\partial \upsilon_t}$, but $\frac{\partial a_t}{\partial \varepsilon_t} \neq \frac{\partial a_t}{\partial \upsilon_t}$ and therefore the problem of singularity of the VAR that was discussed in Section 2.3.1 does not appear in this case.

It is also straightforward to understand why our methodology can be applied to the model described by (2.3.16) and (2.3.17). Indeed, using one lead of technology enables to exactly recover the technology shock, $\Delta a_{t+1} = \varepsilon_t$. This implies that the estimated forecast error is equal to the true forecast error, $\hat{\eta}_t = \eta_t$, and the shocks can be exactly recovered.

2.4 Empirical evidence on US data

Given the positive results of the simulations above, we use our methodology to estimate the effects of news and noise shocks in the US. We first explain how we construct the real-time data on GDP. We then present our methodology to estimate the forecast errors, before presenting the VAR model we use to identify noise and technology shocks. We then present the results, including impulse response analysis, forecast error variance decomposition and historical decomposition, which are consistent with the predictions of our theoretical model. Finally, we show that these results are robust to a different identification strategy.

2.4.1 Real-time data

The first step in our procedure is to obtain the real-time data on GDP. 'Standard' real-time data - the first estimates of GDP available in period t from statistical offices - is normally available only after at least one quarter. In order to be consistent with the model, we have to construct the measure of real GDP in period t that was available exactly in period t. To this end, we use GDP forecasts for the current period from the Survey of Professional Forecasters.

The real time data for real GDP, y_t^{rt}, is constructed as:

$$y_t^{rt} = y_{t-1}^{*}\left(1 + \Delta\hat{y}_t\right) \tag{2.4.1}$$

where y_{t-1}^{*} is the first estimate of real GDP in period $t-1$ as provided by the statistical office and $\Delta\hat{y}_t$ is the forecast for quarterly real GDP growth rate in period t as produced by the Survey of Professional Forecasters.

The calculation of real-time GDP is further complicated by the fact that we are interested in the GDP level, but a consistent series for the GDP level is not available from the SPF. Namely, the level forecasts from SPF are affected by changes in national accounts - for example changes in base years - and it is therefore hard to reconstruct a consistent measure of the real-time level of GDP. To circumvent this problem, we use a consistent revised series and use the growth rates based on the first vintages of the data to move to real-time GDP levels in period $t-1$. Specifically, the first estimate of real GDP in period $t-1$ as provided by the statistical office, y_{t-1}^{*}, is constructed in the following way: $y_{t-1}^{*} = y_{t-5}\left(1 + \Delta^4 y_{t-1}^{*}\right)$ where y_{t-5} is the revised GDP data in period $t-5$ (based on the last available vintage in Q2 2012) and $\Delta^4 y_{t-1}^{*}$ is the yearly growth rate of real GDP between $t-5$ and $t-1$ calculated from the first available vintage for period $t-1$, which is the one available in period t.

2.4.2 Estimating forecast errors

Methodology

The relevant state variable in the model is technology. However, although it would be possible to exactly map the model to the empirical applications by assuming technology as the relevant state, we opt for using trend GDP, or potential output, as the relevant state. The main reason behind this choice is that real-time data for productivity does not exist, except in the case of output per hour worked in the business sector, which is anyway only available since 1998.[7] Moreover, in our opinion, firms and consumers focus on trend GDP rather than technological trend when making economic decisions.

We further assume that consumers use a Kalman filter to construct the estimate of trend GDP.[8] The Kalman filter is set so as to represent a one-sided HP filter, and therefore has some empirical appeal. On the other hand, the econometrician can use the complete data sample, so that the econometrician's estimate of trend GDP is obtained by using a Kalman smoother. There is also a difference in the nature of the data used. Consumers can only use real-time data, while the econometrician can use revised data from later vintages. The correspondance between the model and the empirical application can be summarized as follows:

- **Use of future data** - Consumers only use past data and determine trend GDP with a one-sided filter. The econometrician also uses future data when filtering the GDP series with a two-sided filter.

- **Better signal** - Consumers use real-time data. The econometrician, having access to revised data, uses more accurate information about the state in a given period.

The methodology outlined previously can be applied to actual data. The possible estimates of the forecast errors can then be decomposed as in Table 2.1.

Figure B.13 shows our estimate of $\hat{\kappa_t}$ and Figure B.14 our estimate of $\hat{\lambda}_t$ on US data. These figures allows us to see how the final estimate, shown in Figure B.15, is decomposed into the component due to the use of future signals and the one due the use of less noisy signals. Of course, as the "true" forecast error is not observable in the data, our best estimate of it is the final estimate, $\hat{\eta}_t$. The correlation between $\hat{\kappa_t}$ and $\hat{\eta}_t$ is 0.68 and the correlation between $\hat{\lambda}_t$ and $\hat{\eta}_t$ is 0.92. Figure B.15 also shows the forecast error is pro-cyclical: it is positive and increases in the expansion phase, peaks at the start of a recession (as defined by the NBER) and then falls, reaching a minimum around two of years after the end of the recession phase. A positive, rising error can then be interpreted as an increase in consumers' optimism up to the end of the expansion phase. The error

[7] See https://www.philadelphiafed.org/research-and-data/real-time-center/real-time-data/data-files/OPH/

[8] More detail on the methodology is given in Appendix B.3.1.

becomes negative during the recession and stays negative as long as consumers remain pessimistic about the economy, thus underpredicting the actual state of the economy.

2.4.3 VAR model

We can now estimate a VAR model that includes the following variables:

- Estimated Forecast Errors (FE)
- GDP (Y)
- Private Consumption (C)
- Investment (I)
- Stock prices (S&P500 - SP)
- Fed funds rate (IR)
- CPI inflation (INF)
- Consumer Sentiment (SENT)

The estimated forecast errors are those defined in the previous subsection. The estimation period is from Q1 1970 to Q2 2012. We drop 4 observations at both ends of the sample to account for the lag/lead structure. The system is estimated in differences with three lags, and standard errors are calculated using classic bootstrap methods. The results are robust to changes from differences to levels and using a different number of lags.

Compared to the theoretical model, we enrich the VAR model by including additional variables. This allows us to better identify the shocks and to see their impact on these additional variables, such as stock prices or consumer sentiment. A simple two-variable VAR model, including only the estimate of the forecast error and consumption, has also been estimated. The results, available upon request, are not noticeably different from those presented below.

2.4.4 Identification

The identification of the noise and technology shocks is achieved by sign restrictions. From the theoretical model we know that:

- The forecast error is positive for positive noise shocks (i.e. consumers are too optimistic).
- The forecast error is negative for positive permanent shocks (i.e. consumers are too pessimistic).

The other variables respond similarly to both shocks according to the signs summarized in the following table:

	FE	Y	C	I	SP	SENT
Permanent shock	-	+	+		+	+
Noise shock	+	+	+		+	+

The restrictions are imposed for one year, though changing this does not considerably change the results. The responses of interest rates and inflation are left unrestricted. The estimation methodology is described in Appendix in Section B.4.

Clearly, our VAR model implicitly includes other types of shocks, such as monetary or fiscal shocks. As discussed above, our theoretical model can incorporate other shocks so long as only the shocks considered, technology and noise shocks, are not observable contemporaneously, so that other types of shocks do not affect the forecast errors. The inclusion of other shocks will be discussed as a robustness check in Section 2.4.7.

2.4.5 Empirical results

We now present the estimated impulse response functions, forecast error variance decompositions and historical decompositions.

First, Figure B.16 shows impulse response functions (IRFs) following a 1 standard deviation positive shock to technology. Although we only impose sign restrictions in the short term, the technology shock implies permanent effects on macroeconomic variables, as expected from the theory. Indeed output, consumption and investment are permanently higher. As also expected from the theoretical model, the forecast error is negative with a maximum impact after 5 quarters, before returning towards the baseline. Inflation and interest rates decline on impact but are not permanently affected. Interestingly, both equity prices and consumer sentiment increase permanently following the technology shock.

Figure B.17 shows IRFs following a 1 standard deviation positive noise shock. In this case, the forecast error is positive and increases up to the 10th quarter after the shock. As expected by the theoretical model, the impact on output, investment and consumption is positive in the short term but the effects are short-lived and the variables return to baseline after 8 to 10 quarters. Equity prices and sentiment are also affected positively but, after 5 quarters, the effects are no longer significant. In line with the features of a demand shock, inflation increases in the short term and interest rates are also higher.

The forecast error variance decomposition (FEVD), presented in Figure B.18, shows that the noise shock explains almost half of the business cycle fluctuations in the short term. As expected from the theory, the impact of the technology shock on the business cycle builds up gradually. It explains only up to 20 percent of output variations at business cycle frequencies and half of the fluctuations in the long term, when the noise shock contribution is much smaller.

Figure B.19 shows the series of extracted shocks, with technology shocks in the upper panel and noise shocks in the lower panel. The patterns between these two shocks are very different. A few interesting observations are worth pointing out. First, the technology shock declines just before recessions and sharply increases during the recessions, which could be interpreted as a Schumpeterian creative-destruction mechanism driving the recovery phase. Second, the noise shock tends to be very positive in boom periods, like in the dot-com bubble in the early 2000s and in the housing market boom from the mid-2000s to the financial crisis. Third, noise shocks tend to remain negative for a prolonged period of time after a recession, underlining the role of excess pessimism as a dampening factor in the recovery phases.

Finally, Figures B.20 and B.21 show the historical decomposition of output and the contribution of the two shocks to business cycles fluctuations over time. When the permanent technology shock is removed, US GDP is much lower, especially over the period 1985-2008. This means that our VAR model attributes much of the increase in GDP to positive technology shocks during that period. At the same time, the technology shocks do not contribute so much to short-term fluctuations. By contrast, the noise shock explains most of the output fluctuations at business cycle frequencies.

2.4.6 Robustness check - long run restrictions

As a robustness check, we use a different identification strategy to verify to what extent the previous results depend on the sign restrictions we imposed. We use long-run restrictions instead of sign restrictions to identify the technology and noise shocks.

In particular, restrictions the noise shock is identified by imposing that it has transitory effects on consumption.[9] In a small-scale VAR with only consumption and the forecast error, we identify the permanent and transitory shocks to consumption using the following restrictions on the matrix of long run effects, Ξ:

$$\Xi = \begin{bmatrix} * & 0 \\ * & * \end{bmatrix} \tag{2.4.2}$$

Figure B.22 shows the impulse responses of consumption and the forecast error to the permanent shock, in the upper panel, and the transitory shock, in the lower panel. The responses are qualitatively similar to those obtained with the sign restriction approach. In particular, without imposing the sign restrictions, we again find that a positive permanent technology shock implies negative forecast errors in the short term, while a positive transitory shock increases the forecast error being in this case positive.

[9]Note that while many shocks other than "animal spirits" are compatible with such a restriction, the purpose of this robustness check is to distinguish between the two shocks included in our theoretical model.

2.4.7 Robustness check - additional shock

Our empirical results have so far been based on the identification of the two shocks defined in our theoretical model, distinguishing the noise and technology shocks by their impact on the forecast errors. In our VAR model, which includes more variables, we have so far grouped all other disturbances as "other shocks". As we discussed, the difference is that these other shocks must not have any impact on the forecast errors contemporaneously, as they are supposed to be observable. This is the main constraint given by our theoretical model regarding noise and news shocks. Here, we try to identify some of these other shocks in order to distinguish, among the transitory shocks, those that are related with "animal spirits" from those that are related to more standard shocks, in particular aggregate demand shocks.

Indeed, Lorenzoni [2009] interprets noise shocks, as defined in our paper, as aggregate demand shocks. However, other types of demand shocks may not be related to expectations about future technology. Fiscal shocks or preference shocks may fall into the category of demand shocks that are observable contemporaneously. In this case, the difference between the noise shocks and such a demand shock will only be the effect on the forecast error, which will be positive in the case of a noise shock and zero in the case of an observable demand shock. We use this zero restriction to identify a third shock, which we name an observable demand shock. Figure B.25 shows the IRFs of this newly identified shock. It has positive effects on output and consumption, although these effects are only significant in the short term. Similarly, the positive impact on stock prices and consumer sentiment are significant only in the first quarters following the shock. Figures B.23 and B.24 show the IRFs to the permanent shock and the noise shock in this new system. The responses are relatively similar to those presented earlier. Compared with the noise shock, the effect of the observable demand shock builds up more gradually. As shown by the FEVD, in Figure B.26, the observable demand shock explains a large share of fluctuations in consumption in the medium- to long-term, while the noise shock explains most of the fluctuations in consumption in the short term. The same largely applies to output fluctuations. For consumption, almost half of the fluctuations are explained by these three shocks. For output, they explain almost two-third of the fluctuations. The main conclusions derived earlier still hold in this more comprehensive shock identification exercise.

Two other extended identifications have also been estimated. The first considers an additional shock that has maximum effect on output, and minimal effects on the forecast error. This shock is assumed to also explain investment increases. The purpose of this shock is to potentially account for part of the variation captured in our noise shock in the initial identification scheme. Impulse responses are shown in Figures B.27, B.28 and B.29 and the FEVD is presented in Figure B.30. As with the previous robustness check,

the additional shock, while capturing part of the output fluctuations, does not change the main results, in particular the contribution of the noise shock to output remains broadly unchanged.

A final robustness check distinguishes, in addition to the noise and permanent shocks, a third shock which behaves as a demand shock and a fourth one which behaves like a supply shock. In this exercise, the identification is conducted by assuming that the demand shock leads to an increase in both inflation and interest rates, while the supply shock is assumed to lead to decreases in these two variables. Figures B.31, B.32, B.33 and B.34 show impulse responses to each of these four shocks. Figure B.35 shows the FEVD. While the two additional shocks are able to explain part of the output fluctuations, the contribution of the two main shocks,noise and permanent shocks, remain very close to our baseline exercise.

2.4.8 Comparison with current literature

Our results correspond to a large extent with those found in related literature. In particular, most papers that study the effects of noise versus permanent shocks find that noise shocks could be interpreted as demand shocks and contribute to a large extent to economic fluctuations at business cycle frequency. Noise shocks are therefore more important in explaining the business cycles compared to permanent or technology shocks.

Blanchard et al. [2013] estimate a structural model and find that noise shocks account for more than 50% of short run volatility of consumption, while permanent technology shocks play a smaller role, having almost no effect on quarterly volatility and explaining less than 30% at a 4-quarter horizon. Similar to this paper, they find spells of positive permanent shocks in the first half of 80s and second half of 90s. They estimate a structural model, thus putting structure on the data that can have important effects on the final results. By contrast, we opted for a more parsimonious SVAR model, which suggests why the smoothed series of noise shocks are more informative in our case - we obtain a clearer pattern of positive noise shocks before recessions and negative noise shocks at the start and during recessions. Nevertheless, they also find a succession of negative noise shocks around the recession in the early 1990s, and a spell of positive noise shocks before the 2001 recession.[10]

Given their methodology, Forni et al. [2013] identify two additional shocks, which makes direct comparison slightly more difficult. Nonetheless, overall, their results are similar to those found in our paper. The responses of output, consumption and investment have similar shapes. In the case of the noise shock, the responses are hump-shaped with a relatively small, although significant, impact effect; they reach a maximum after about two years, then decline towards zero after about five years. As predicted by the model,

[10]They do not find similar patterns before the 2007 recession, as they only use data until 2008.

noise shocks spur a wave of private consumption and investment which vanishes once economic agents realize that the signal was just noise. They find that the responses to real shocks are permanent, although real shocks sometimes do not have significantly permanent effects as in our paper.

Enders et al. [2013] use a similar empirical strategy to our paper, but they construct forecast errors only by exploring the fact that real-time data is less precise than revised data. Nevertheless, they also find that nowcast errors react as predicted by theory, as we found in the exercise in Section 2.4.6. Given that they only use the difference between real-time and revised data to improve the estimates of the state, their results are not as revealing as those found in this and other studies. Namely, the distinction between productivity shocks as permanent and optimism shocks as transitory is not as evident as in other studies.

Barsky and Sims [2012] found most contrasting results compared to this and other papers in the literature. They find that "animal spirits" effects are very weak and thus account for essentially none of the relationship between confidence and future consumption or income. The reason for such contrasting results is mostly related to the different methodologies - they estimate a structural model by matching theoretical impulse responses with empirical impulse responses. As discussed above, estimating a structural model imposes structure on the data that may have important effects on the empirical results. While they find noise shocks to be unimportant, they find that permanent shocks are important drivers of business cycles, especially at longer horizons.

Finally, Angeletos et al. [2014] features a model with only two sources of volatility: the usual technology shock and a confidence shock that drives the agents' beliefs about the state of the economy. The confidence shock therefore has a similar interpretation to our noise shock. Interestingly enough, although they use a different model, they also find that confidence shocks can account for about half of GDP volatility at business-cycle frequencies and that their effects look similar to a standard demand shock.

2.5 Conclusion

This paper has presented a model in which consumers receive noisy signals about future economic fundamentals. In this model, business cycle fluctuations can be driven both by news shocks (technology shocks) and noise shocks ("animal spirits" shocks). We have shown that standard structural VAR models cannot be applied in principle to this model to identify the two types of shocks, as the VAR model faces invertibility issues. In other words, if consumers cannot distinguish between the two shocks, the econometrician also faces the same problem. However, by considering that the econometrician can potentially have a richer and more accurate information set, we have shown that a standard SVAR model can recover both technology and noise shocks. Richer information sets relate to the

fact that the econometrician has access to revised data (while consumers take decisions with real-time data) and can include "future" data when estimating the state of the economy (while consumers take decisions with past and current data only).

In the empirical exercise, we have shown that the identified shocks have macroeconomic impacts that are in line with theoretical predictions. We have also shown that noise shocks explain almost half of business cycle fluctuations in the short term, while technology shocks explain only up to 20 percent of output variations at business cycle frequencies. We have also shown that technology shocks turn negative a few years before recessions, while noise shocks are very positive at the cycle peaks and remain negative for some time during recovery phases. The recovery from recessions is mostly led by technology shocks, following Schumpeterian creative-destructive dynamics. These results are robust to the size of the VAR model and to the identification scheme.

Appendix B

Appendix: Animal Spirits, Fundamental Factors and Business Cycle Fluctuations

B.1 Appendix - Model

Figure B.1: Simulated Technology, Signal and Cons. expectations and Forecast error

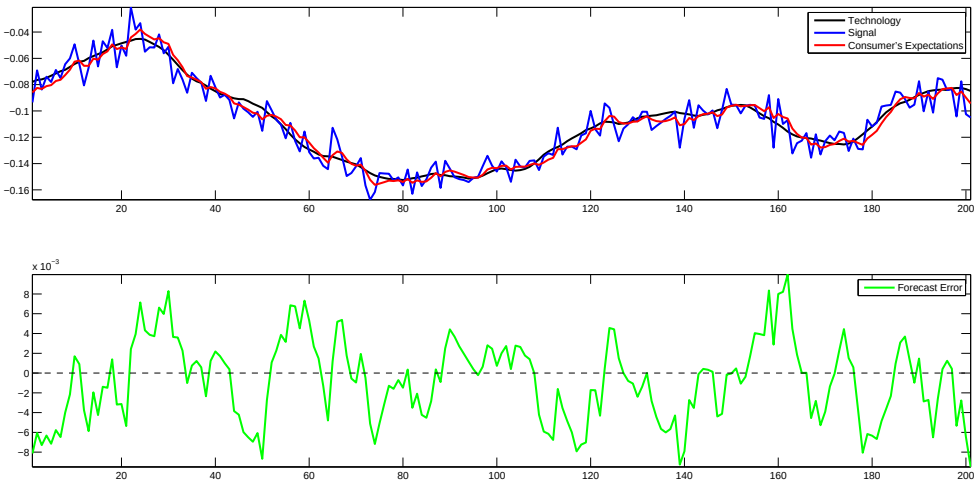

The black line represents the underlying technology process, which agents do not observe. The agents observe a signal (blue line) and via a Kalman filter, they form expectations about the technology (red line). The difference between their expectations and the true state of technology - forecast error - is represented in the graph below with the green line.

Figure B.2: IRFs to the Permanent shock

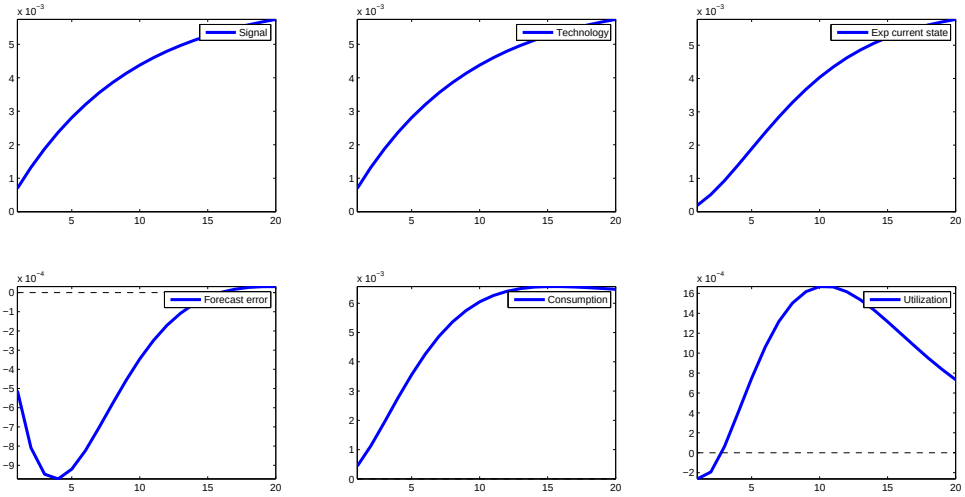

The graph presents the impulse responses of variables to the one-standard deviation permanent shock. The top row presents responses of signal, technology and agent's expectation. The bottom row presents responses of forecast error, consumption and utilization.

Figure B.3: IRF to the Noise shock

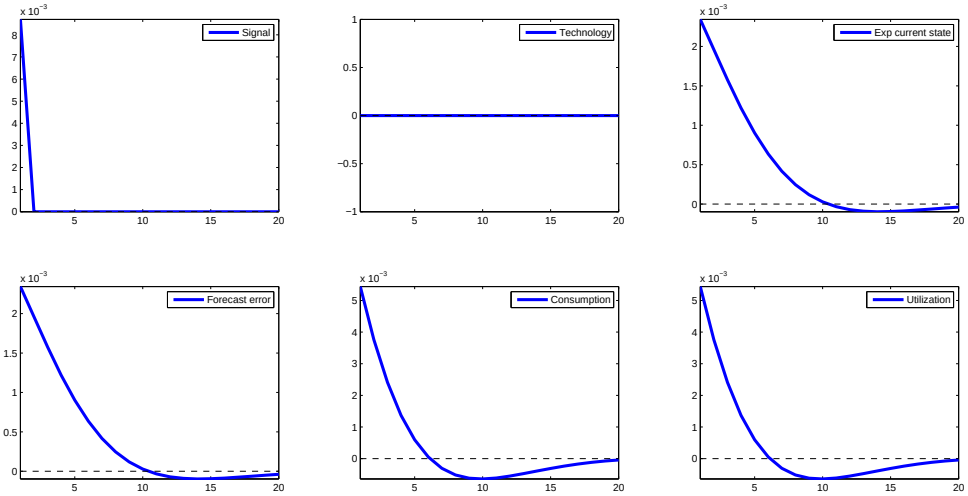

The graph presents the impulse responses of variables to the one-standard deviation noise shock. The top row presents responses of signal, technology and agent's expectations. The bottom row presents responses of forecast error, consumption and utilization.

Figure B.4: IRF of consumption

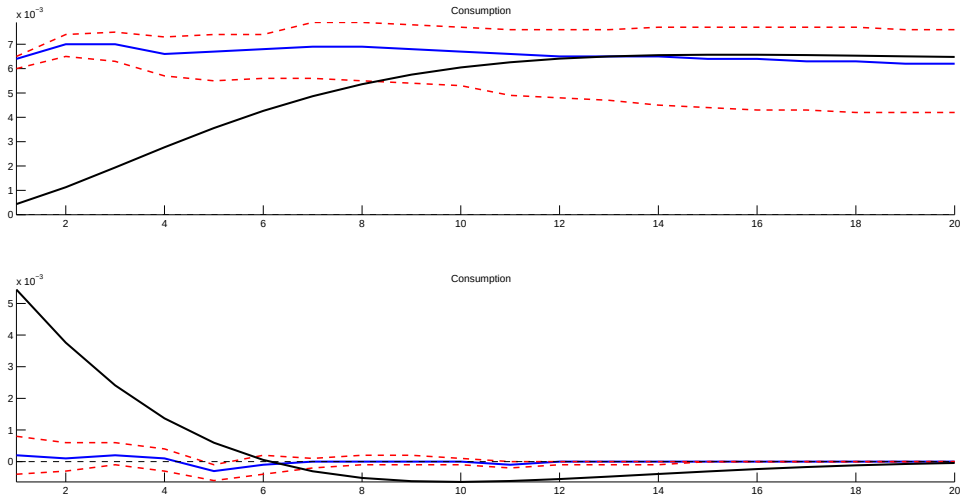

The graph presents the estimated impulse responses of consumption to the permanent (above) and the noise (below) shock. The black lines are theoretical responses. The blue line is point estimate and the red lines are 90% error bands.

B.2 Appendix - Singularity of VAR with leads

To see the problem related to the singularity of VAR models when the future values of signals are used, we define an estimate of the state by a Kalman filter as:

$$\begin{aligned} \hat{x}_t^t &= \hat{x}_{t-1}^t + \mathcal{K}\left(s_t - A\hat{x}_{t-1}^t\right) \\ &= (1 - \mathcal{K}A)\hat{x}_{t-1}^t + \mathcal{K}s_t \end{aligned} \tag{B.2.1}$$

where $\hat{x}_t^t$ is a state estimate in period t using signals up to period t - an estimate derived with a standard Kalman filter. $\mathcal{K}$ is the Kalman gain and s_t is the signal in period t. Similarly, the state estimate in period t using signals up to period $t+1$ can be written as:

$$\begin{aligned} \hat{x}_t^{t+1} &= \hat{x}_{t-1}^{t+1} + \mathcal{K}^0\left(s_t - A^0\hat{x}_{t-1}^{t+1}\right) + \mathcal{K}^1\left(s_{t+1} - A^1\hat{x}_{t-1}^{t+1}\right) \\ &= (1 - \mathcal{K}^0A^0 - \mathcal{K}^1A^1)\hat{x}_{t-1}^{t+1} + \mathcal{K}^0s_t + \mathcal{K}^1s_{t+1} \end{aligned} \tag{B.2.2}$$

where $\hat{x}_t^{t+1}$ is a state estimate in period t using signals up to period $t+1$. $\mathcal{K}^0$ is the Kalman gain related to the signal in period t and $\mathcal{K}^1$ is the Kalman gain related to the signal in period $t+1$.

Consider now that the state estimate, $\hat{x}_t^t$ follows an autoregressive process:[1]

$$\hat{x}_t^t = \beta_1\hat{x}_{t-1}^t + u_t \tag{B.2.3}$$

where u_t is the error term. Comparing equation (B.2.1) with equation (B.2.3), we can see that s_t and u_t span the same linear space.

Shifting by one period and rearranging equations (B.2.1) and (B.2.2) we have:

$$\begin{aligned} \hat{x}_{t-1}^t - (1 - \mathcal{K}A)\hat{x}_{t-2}^t &= \mathcal{K}s_{t-1} \\ \hat{x}_{t-1}^{t+1} - (1 - \mathcal{K}^0A^0 - \mathcal{K}^1A^1)\hat{x}_{t-2}^{t+1} &= \mathcal{K}^0s_{t-1} + \mathcal{K}^1s_t \end{aligned} \tag{B.2.4}$$

where the first row follows from equation (B.2.1) and the second row from equation (B.2.2). From equation (B.2.4), we can see that s_t can be expressed as a linear combination of $\hat{x}_{t-1}^t$, $\hat{x}_{t-2}^t$, $\hat{x}_{t-1}^{t+1}$ and $\hat{x}_{t-2}^{t+1}$. As s_t and u_t span the same linear space, u_t can also be expressed as a linear combination of the latter four variables, which implies a regression of the form:

$$\hat{x}_t^t = \beta_1\hat{x}_{t-1}^t + \beta_2\hat{x}_{t-2}^t + \beta_3\hat{x}_{t-1}^{t+1} + \beta_4\hat{x}_{t-2}^{t+1} + u_t \tag{B.2.5}$$

is characterized by a perfect linear relation between the independent and dependent variables, and the corresponding VAR is therefore singular. A similar reasoning applies also to regressions involving state estimates $\hat{x}_t^{t+2}$, $\hat{x}_t^{t+3}$,... that are constructed by using more

[1]The results in this section are presented only for auto-regressions with the state estimate. However, the forecast error, η_t, and consumption, c_t, are a linear function of the state estimate $\hat{x}_t^i$ and therefore results also hold for auto-regressions with the forecast error and consumption.

leads of the signal. The only difference is that the more leads of the signal are used to construct state estimates, the more lags are needed to achieve a perfect linear correlation.

The improvements in the signal - lower variance of noise shocks - can reduce the problem of singularity. Whenever improvements in the signals are perfectly correlated with the noise shocks itself - newly defined noise shocks with lower variance can be written as $\upsilon_t^* = a\upsilon_t$, where υ_t^* are noise shocks with lower variance, a is a constant and υ_t are old shocks - the reduced variance of the signals does not alter the singularity problem. Namely, s_t can still be expressed as a (different) linear combination of $\hat{x}_{t-1}^t$, $\hat{x}_{t-2}^t$, $\hat{x}_{t-1}^{t+1}$ and $\hat{x}_{t-2}^{t+1}$.

On the other hand, when correlation is not perfect - noise shocks with lower variance cannot be written as $\upsilon_t^* = a\upsilon_t$ - the singularity problem does not appear. To see this, we can write equation (B.2.4) as:

$$\begin{aligned} \hat{x}_{t-1}^t - (1 - \mathcal{K}A)\hat{x}_{t-2}^t &= \mathcal{K}s_{t-1} \\ \hat{x}_{t-1}^{t+1} - (1 - \mathcal{K}^0A^0 - \mathcal{K}^1A^1)\hat{x}_{t-2}^{t+1} &= \mathcal{K}^0s_{t-1}^* + \mathcal{K}^1s_t^* \end{aligned} \tag{B.2.6}$$

where we use the fact that we have access to a different signal in the future, $s_t^* \neq s_t$ (second row). The new signal cannot be written as $s_t^* = cs_t$, where c is some constant. Therefore, it is not possible to form a perfect linear relation between s_t and $\hat{x}_{t-1}^t$, $\hat{x}_{t-2}^t$, $\hat{x}_{t-1}^{t+1}$ and $\hat{x}_{t-2}^{t+1}$.

Figure B.5: Estimated Forecast error from less noisy signal

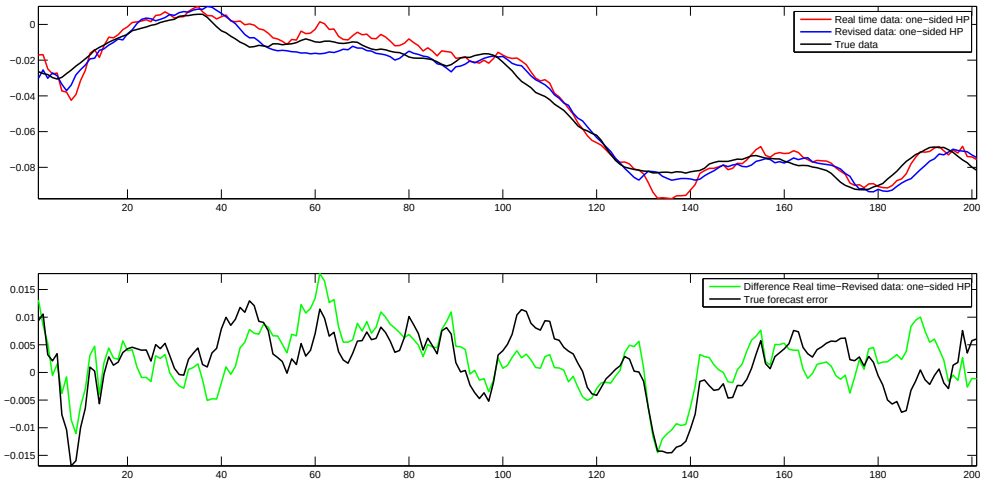

Correlation between Estimated and True Forecast errors

	σ_v^2	$0.75\sigma_v^2$	$0.5\sigma_v^2$	$0.25\sigma_v^2$	$0\sigma_v^2$
$\text{corr}(\eta_t, \hat{\eta}_t)$	0	0.88	0.93	0.94	1

Figure B.6: Estimated Forecast error from using future observations

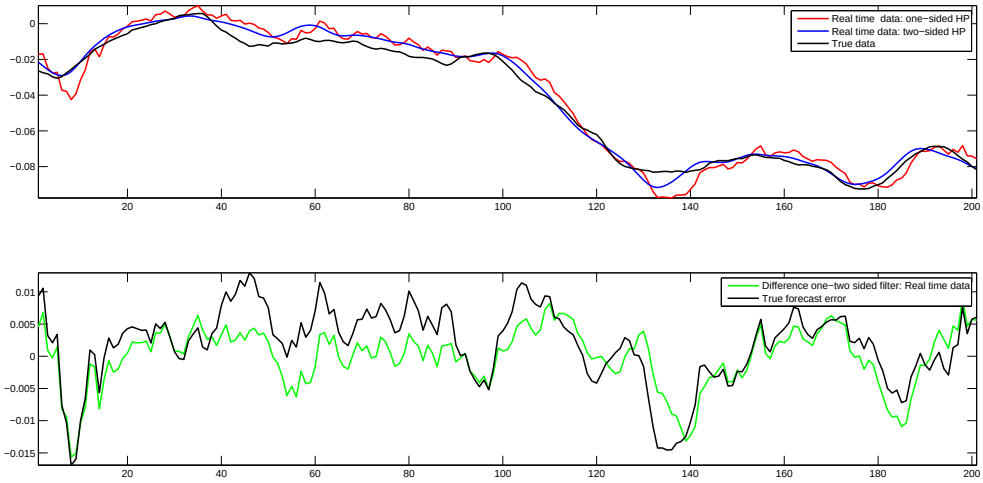

Correlation between Estimated and True Forecast errors

	0 leads	1 lead	2 leads	3 leads	4 leads
$\text{corr}(\eta_t, \hat{\eta}_t)$	0	0.44	0.58	0.67	0.72

Figure B.7: Estimated IRF by using the true forecast errors (simulated data)

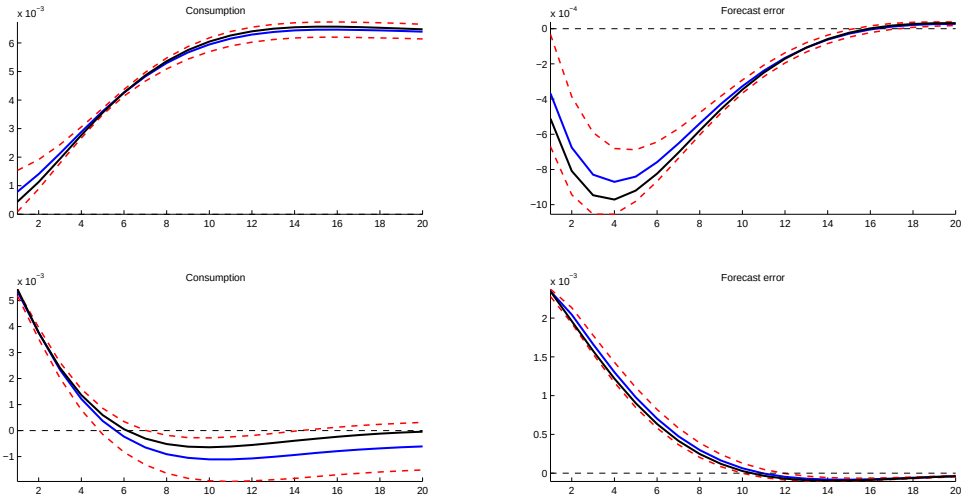

The graph presents the estimated impulse responses of consumption (right) and the forecast error (left) to the permanent (above) and the noise (below) shock. The blue line is point estimate and the red lines are 90% error bands.

Figure B.8: Estimated IRF by using estimated forecast errors (simulated data)

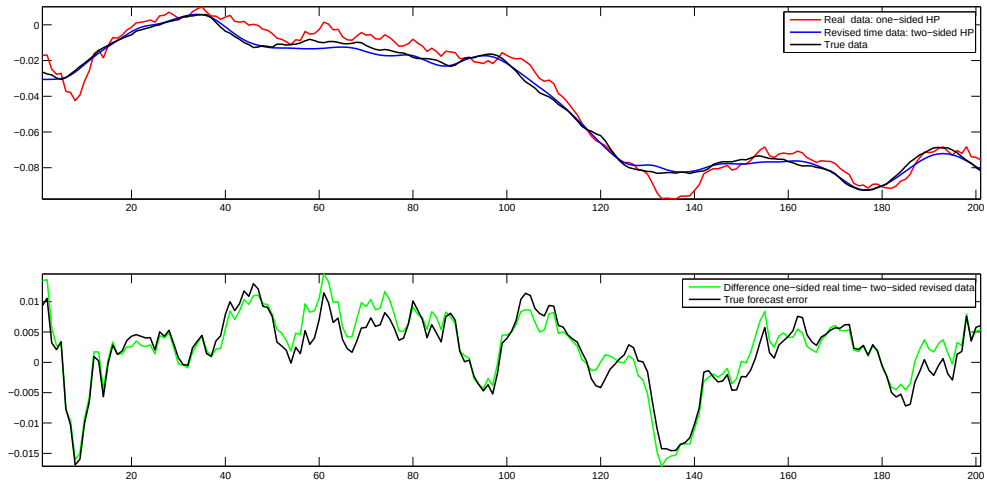

The graph presents the estimated impulse responses of consumption (right) and the forecast error (left) to the permanent (above) and the noise (below) shock. The estimated forecast errors are obtained by using 4 leads of the signal and 50 percent less noisy signal. The black lines are theoretical responses. The blue line is point estimate and the red lines are 90% error bands.

Figure B.9: Simulated data: Estimated FEVD (above) and theoretical FEVD (below)

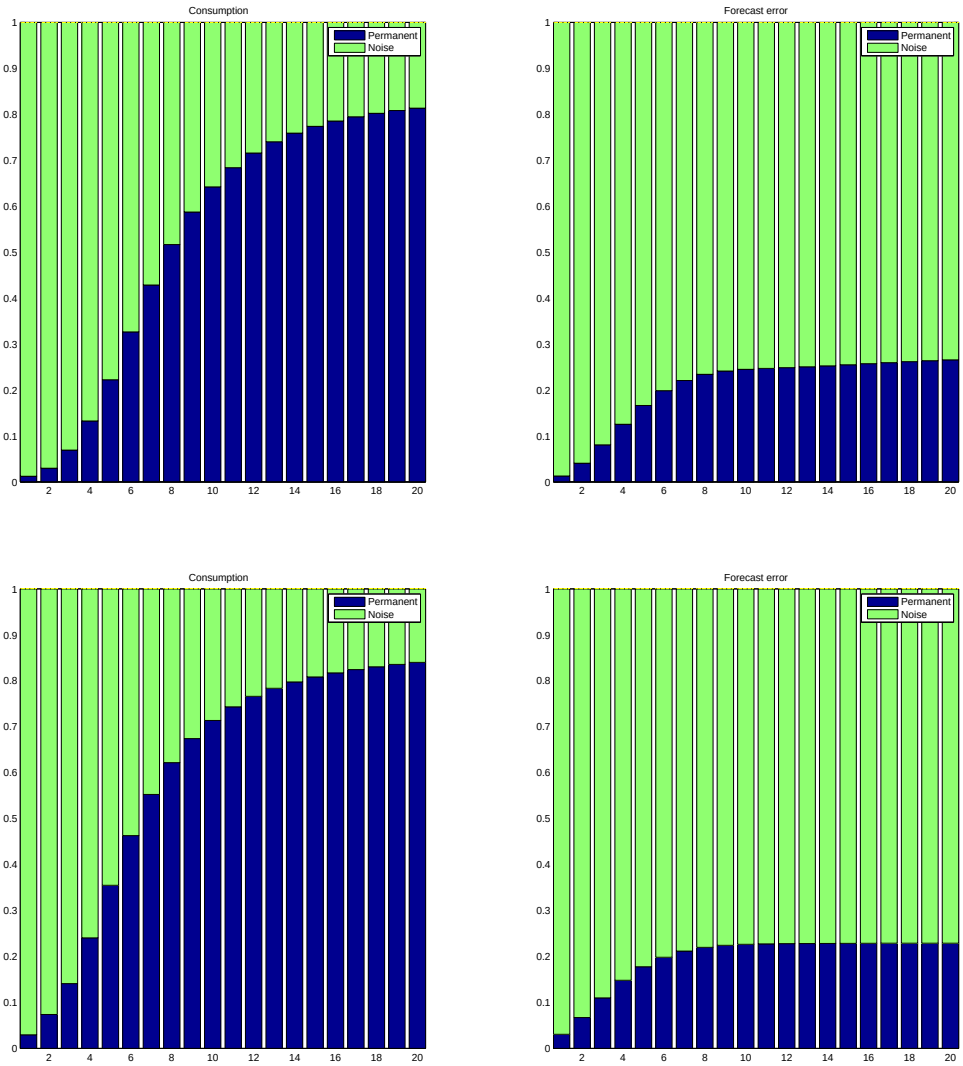

The first row presents the estimated forecast error variance decomposition (FEVD) of consumption (right) and the forecast error (left). The second row presents the theoretical forecast error variance decomposition (FEVD) of consumption (right) and the forecast error (left). The blue area corresponds to the median contribution of the permanent and the green area corresponds to the median contribution of the noise shock. The estimated forecast errors are obtained by using 4 leads of the signal and 50 percent less noisy signal.

B.3 Appendix - Estimation of trend GDP

B.3.1 HP filter in a state space form

The HP-filter widely used in practice decomposes time series y_t, in our case GDP, into a trend component and a cyclical component, can be represented as:[2]

$$y_t = \tau_t + \epsilon_t \tag{B.3.1}$$

$$(1-L)^2\tau_t = \eta_t \tag{B.3.2}$$

where τ_t is a trend component, $\{\epsilon_t\}$ is a white noise sequence (cyclical component) and $\{\eta_t\}$ is a white noise sequence. The following process can be written as a state space:

1. State Equation

$$\begin{bmatrix} \tau_{t|t} \\ \tau_{t-1|t} \end{bmatrix} = \begin{bmatrix} 2 & -1 \\ 1 & 0 \end{bmatrix} \begin{bmatrix} \tau_{t-1|t-1} \\ \tau_{t-2|t-1} \end{bmatrix} + \begin{bmatrix} 1 & 0 \\ 0 & 0 \end{bmatrix} \begin{bmatrix} \epsilon_t \\ 0 \end{bmatrix} \tag{B.3.3}$$

2. Observation Equation

$$y_t = \begin{bmatrix} 1 & 0 \end{bmatrix} \begin{bmatrix} \tau_{t|t} \\ \tau_{t-1|t} \end{bmatrix} + \begin{bmatrix} 0 & 1 \end{bmatrix} \begin{bmatrix} 0 \\ \eta_t \end{bmatrix} \tag{B.3.4}$$

where $\epsilon_t \sim \mathcal{N}(0, \sigma_\epsilon^2)$ and $\eta_t \sim \mathcal{N}(0, \sigma_\eta^2)$. The standard parameter lambda is obtained as, $\lambda = \frac{\sigma_\eta^2}{\sigma_\epsilon^2}$.

The one-sided HP filter is obtained by estimating the state space system by a Kalman filter, while non-casual estimate of the state-space system is obtained by a Kalman smoother. The alternative to obtain non-casual filter estimates of the trend and cyclical component is to use a standard two-sided HP filter.

[2] See Stock and Watson [1999]

Figure B.10: An estimate of forecast error due to the use of future signals - $\hat{\kappa}_t$ (simulated data)

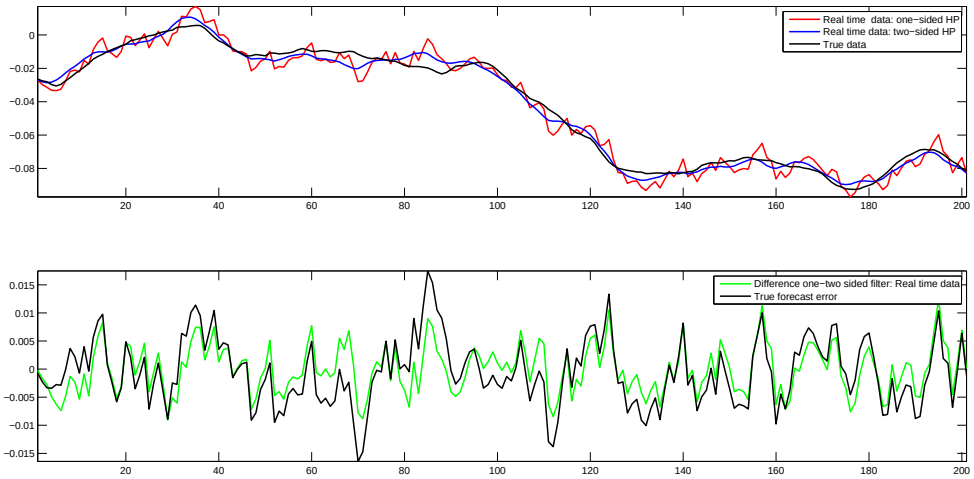

$$corr(\hat{\kappa}_t, \eta_t) = 0.8$$

The black line represents the true technology. The red line represents the expectations that are obtained via Kalman filter with the structure of HP filter. The blue line represents the expectations that are obtained via Kalman smoother with the structure of HP filter. The green line represents the difference between the two series of expectations, which is a proxy for the forecast error estimated due to the usage of future values. The black line are the true forecast errors.

Figure B.11: An estimate of forecast error due to the use of less noisy signals - $\hat{\lambda}_t$ (simulated data)

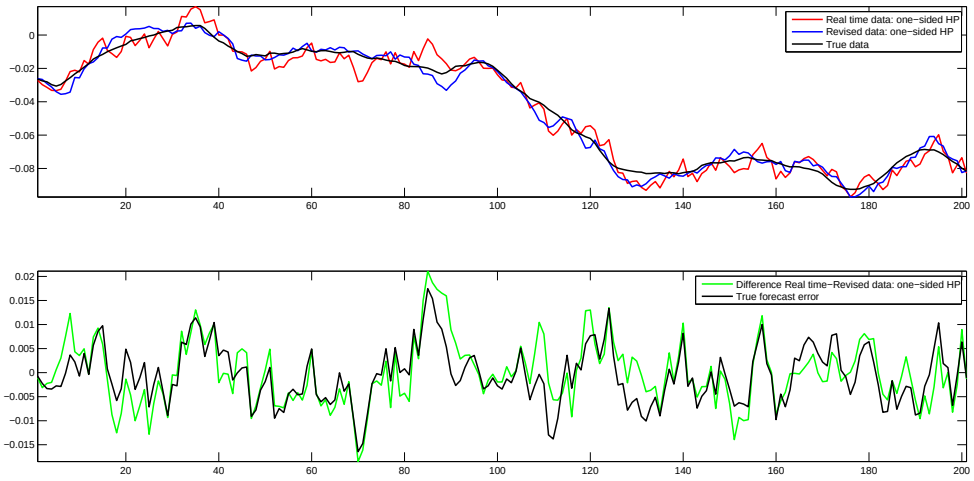

$$corr(\hat{\lambda}_t, \eta_t) = 0.8$$

The black line represents the true technology. The red line represents the expectations that are obtained via Kalman filter with the structure of HP filter using the real-time data. The blue line represents the expectations that are obtained via Kalman filter with the structure of HP filter using the revised data (less noisy signal). The green line represents the difference between the two series of expectations, which is a proxy for the forecast error estimated due to the usage of revised data. The black line are the true forecast errors.

Figure B.12: A final estimate of forecast error - $\hat{\eta}_t$
(simulated data)

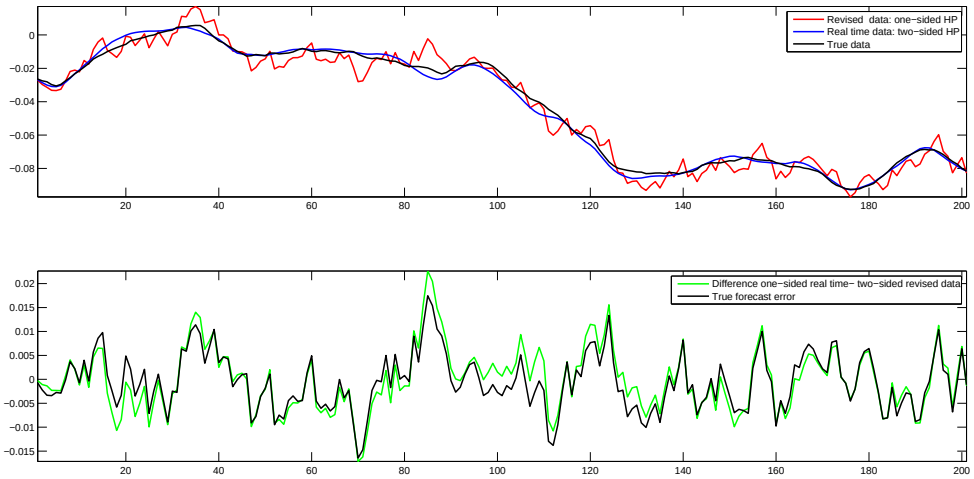

$$corr(\hat{\eta}_t, \eta_t) = 0.93$$

The black line represents the true technology. The red line represents the expectations that are obtained via Kalman filter with the structure of HP filter using the real-time data. The blue line represents the expectations that are obtained via Kalman smoother with the structure of HP filter using the revised data (less noisy signal). The green line represents the difference between the two series of expectations, which is a proxy for the forecast error estimated due to the usage of revised data. The black line are the true forecast errors.

Figure B.13: An estimate of forecast error due to the use of future signals - $\hat{\kappa}_t$
(US data)

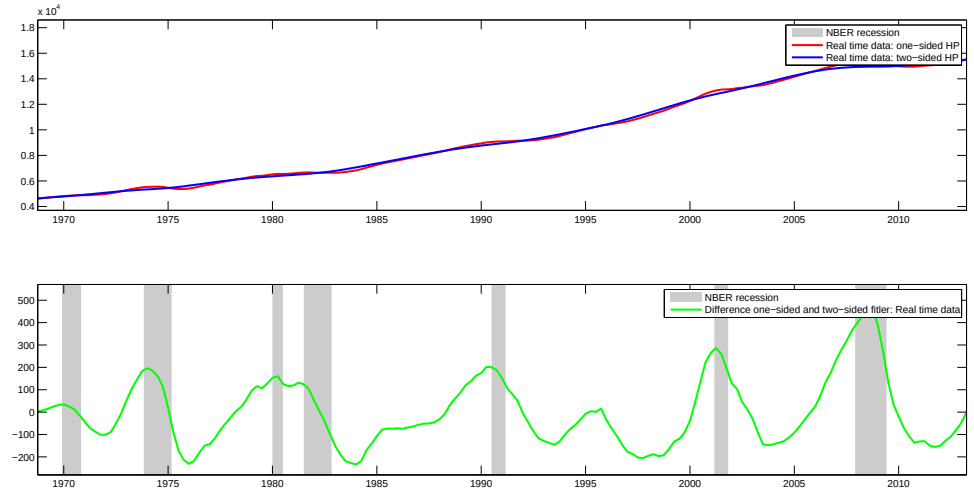

$$corr(\hat{\kappa}_t, \eta_t) = 0.68$$

The red line represents the trend GDP that is obtained via Kalman filter with the structure of HP filter. The blue line represents the trend GDP that is obtained via Kalman smoother with the structure of HP filter. The green line represents the difference between the two estimated trends, which is a proxy for the forecast error estimated due to the usage of future values.

Figure B.14: An estimate of forecast error due to the use of less noisy signals - $\hat{\lambda}_t$ (US data)

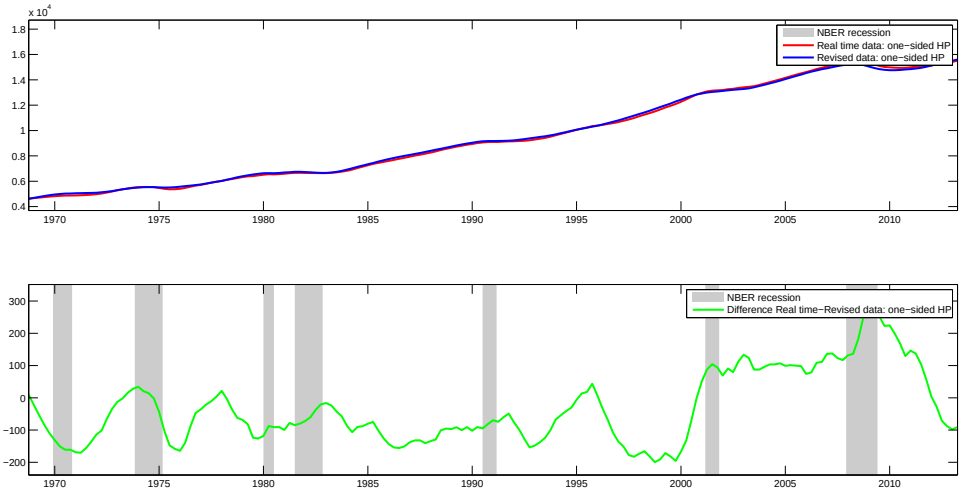

$$corr(\hat{\lambda}_t, \eta_t) = 0.92$$

The red line represents the trend GDP that is obtained via Kalman filter with the structure of HP filter using real-time data. The blue line represents the trend GDP that is obtained via Kalman filter with the structure of HP filter using revised data. The green line represents the difference between the two estimated trends, which is a proxy for the forecast error estimated due to the usage of more precise signals.

Figure B.15: A final estimate of forecast error - $\hat{\eta}_t$ (US data)

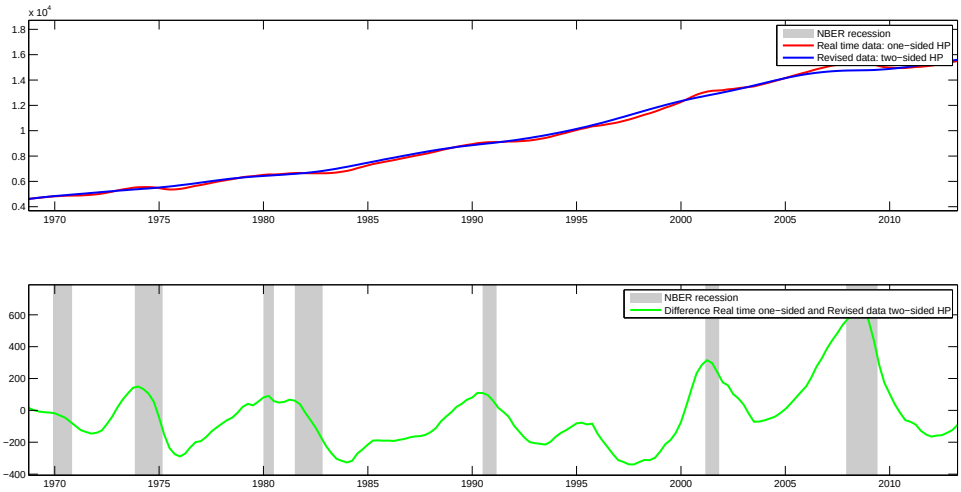

$$corr(\hat{\eta}_t, \eta_t) = 1$$

The red line represents the trend GDP that is obtained via Kalman filter with the structure of HP filter using real-time data. The blue line represents the trend GDP that is obtained via Kalman smoother with the structure of HP filter using revised data. The green line represents the difference between the two estimated trends, which is a proxy for the forecast error.

B.4 Appendix - Estimation algorithm

The estimation procedure is based on a modified version of the sign restriction approach presented in Uhlig [2005]. The modification is that we restrict responses of most variables only by non-negativity constraints - in the spirit of sign restrictions approach proposed in Canova and Nicoló [2002].

The estimation procedure consists of three steps. In the first step, we estimate the reduced form VAR model. In the second step, we identify the structural shocks and take into account identification uncertainty. The third step serves to take into account estimation uncertainty. The steps are:

1. **Estimate reduced-form VAR:** Given the number of chosen lags, $\widehat{p}$, $VAR(\widehat{p})$ is estimated by Ordinary Least Squares (OLS) to obtain an estimate of autoregressive coefficients and the variance-covariance of reduced form errors, $\widehat{\Sigma_u}$.

2. **Identification restrictions:** The non-structural impulse response function, $C(L)$, is related to the structural impulse response function as $B(L) = A_0 C(L)$ and reduced form errors, u_t, are related to structural errors as $u_t = A_0^{-1} B\varepsilon_t$. Impact matrix, $S = A_0^{-1}B$, must satisfy:

$$\Sigma_u = SS' \tag{B.4.1}$$

The first estimate of impact matrix, $\hat{S}$, is obtained by a Cholesky decomposition of the variance-covariance matrix of reduced form errors, $\hat{S} = chol(\hat{\Sigma_u})$. The full set of permissible impact matrices can be construct as, $S* = \hat{S}Q$, where Q is an orthonormal matrix such that, $QQ' = I$.

Define $b_{i,j}(k)$ to be a response of variable i to shock j in period k that follows from the structural lag-polynomial $B(L)B$. Define the function f on the real line per $f(x) = x$ if $x \geq 0$ and $f(x) = 100x$ if $x \leq 0$. Let s_j be the standard error of variable j. Let $J_{S,+}$ be the index set of variables for which identification restricts response to be positive and let $J_{S,-}$ be the index set of variables for which identification restricts response to be negative. Define the penalty function as:

$$\Psi(S) = \sum_{j \in J_{S,+}} \sum_{k=0}^{P} f\left(\frac{b_{i,j}(k)}{s_j}\right) + \sum_{j \in J_{S,-}} \sum_{k=0}^{P} f\left(\frac{b_{i,j}(k)}{s_j}\right) \tag{B.4.2}$$

where P is the horizon over which restrictions should hold. Let $C_{S,+}$ be the index set of variables for which identification restricts response to be non-negative and let $C_{S,-}$ be the index set of variables for which identification restricts response to be non-positive. Define the non-negativity constraints vector as $c(S) = [\frac{b_{i,j}(k)}{s_j}^1, ..., \frac{b_{i,j}(k)}{s_j}^P]$. To identify the model, we solve the following maximization problem:

$$\begin{aligned} S \;=\; & \underset{S}{argmax} && \Psi(S) \\ & subject\ to && c(S) \geq 0 \\ & && SS' = \Sigma_u \end{aligned} \tag{B.4.3}$$

In the current paper only restrictions on forecast error enter the penalty function, while sign restrictions on other variables are applied only as non-negativity constraints. In this way we achieved that most of the forecast variance of forecast error is explained by the two identified shocks, while at the same time achieving that identification is not too restrictive - our methodology restricts only the sign of responses and does not maximize the magnitude - in relation to responses of other variables.

3. **Estimation uncertainty:** to account for estimation uncertainty, we repeat steps 1-2 1000 times, each time with a new artificially constructed data sample, Y^*. To construct data samples, we use re-sampling of errors. To correct for small-sample bias, we use the method described in Kilian [1998]. New data sample is constructed recursively as $y_t^* = \hat{A}_1^* y_{t-1}^* + ... + \hat{A}_N^* y_{t-N}^* + \widehat{u_t}^*$, starting from initial values $[y_0, ..., y_{N-1}]$. $\hat{A}_n^*$ are estimated reduced form autoregressive coefficients. $\widehat{u_t}^*$ are drawn randomly with replacement from estimated reduced form errors, $\widehat{u_t}$.

The IRF's point estimates and the related confidence bands are constructed by retaining the relevant percentiles of a distribution of retained IRFs. The same procedure is used to construct FEVD's point estimates and the related confidence bands.

B.5 Appendix - Baseline results

Figure B.16: US data - IRFs to permanent shock

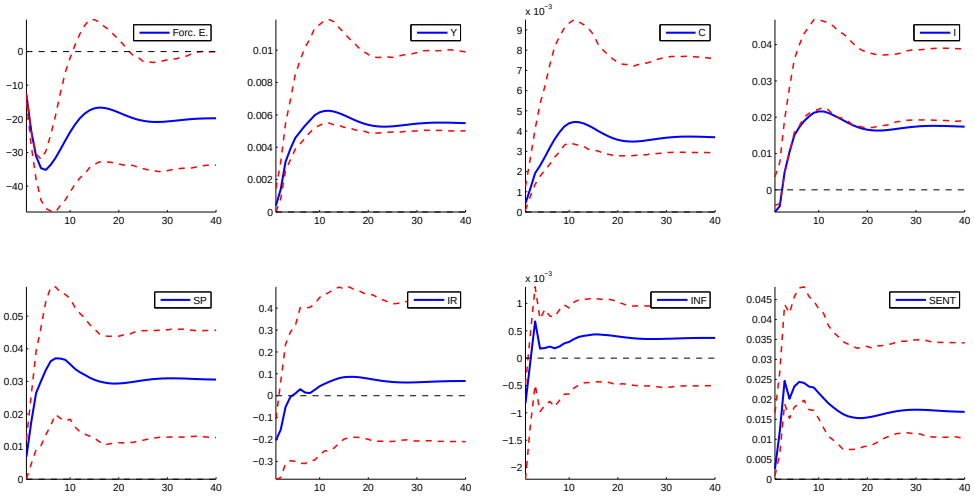

The graph presents the impulse responses to the permanent shock of the estimated forecast error, output and consumption (first row), investment, stock prices and interest rates (second row) and inflation and sentiment (third row).The blue line is the point estimate and the red lines are 90% error bands.

Figure B.17: US data - IRFs to noise shock

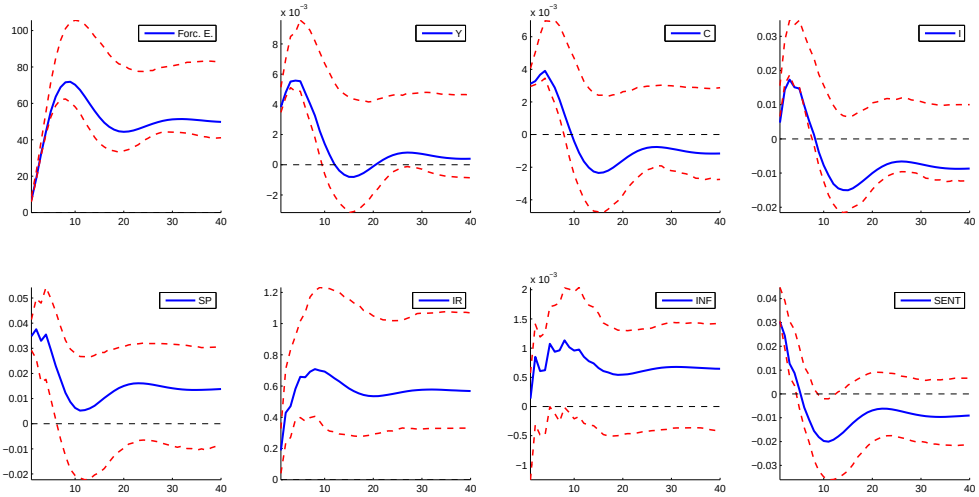

The graph presents the impulse responses to the noise shock of the estimated forecast error, output and consumption (first row), investment, stock prices and interest rates (second row) and inflation and sentiment (third row).The blue line is the point estimate and the red lines are 90% error bands.

Figure B.18: US data - FEVD

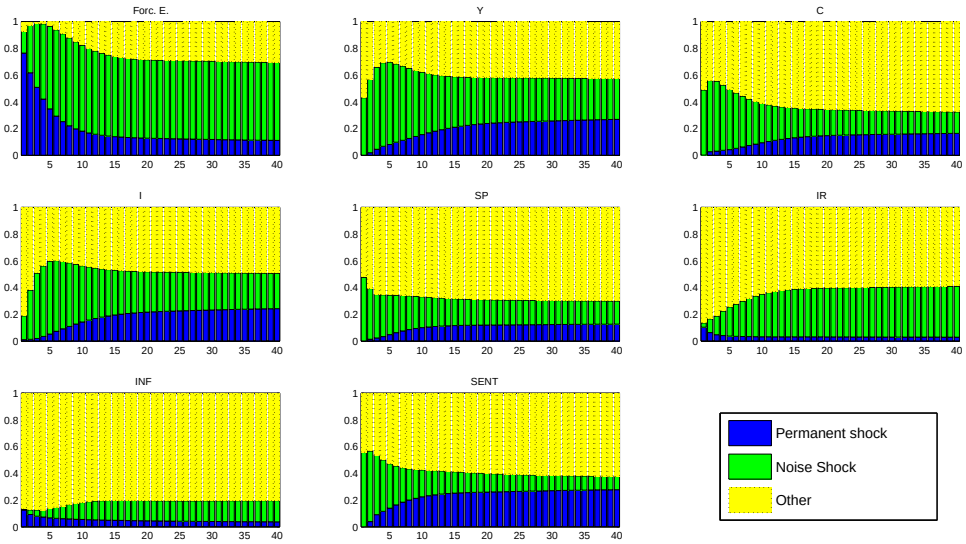

The graph presents the forecast error decomposition of the estimated forecast error, output and consumption (first row), investment, stock prices and interest rates (second row) and inflation and sentiment (third row). The blue area corresponds to the median contribution of permanent shocks, the green area to the median contribution of noise shocks and yellow area to the contribution of all other non-identified shocks.

Figure B.19: US data - extracted shocks (smoothed)

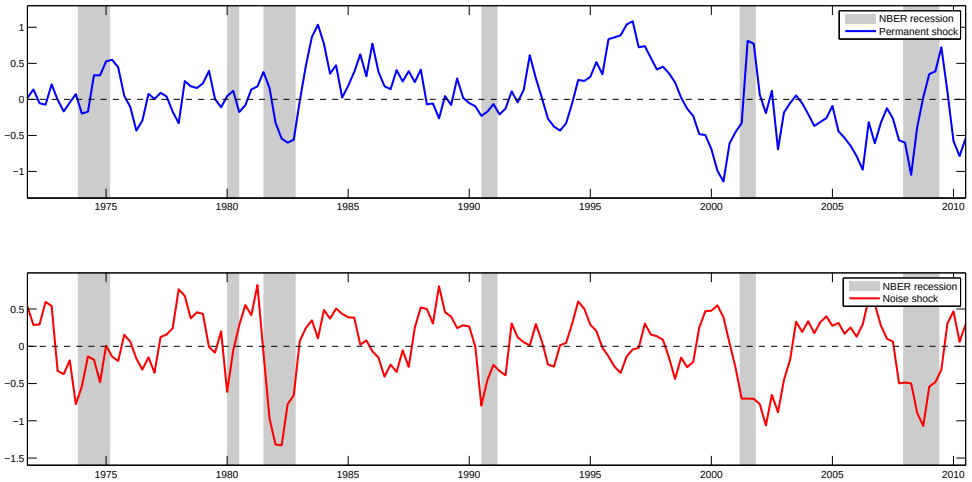

The graph presents the extracted permanent (blue line above) and noise shocks (red line below). The series of shocks are smoothed with moving average filter with 5-period window. The gray areas correspond to NBER-defined recessions.

Figure B.20: US data - historical decomposition of output (permanent shocks off)

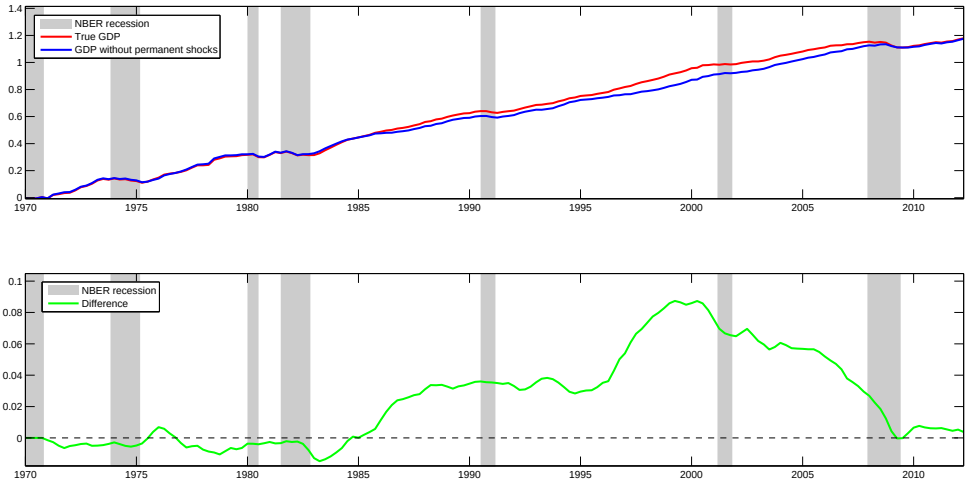

The graph presents the historical decomposition of output. The red line is output, while blue line is output in case when we set permanent shocks to zero in all the periods. The difference between the two series of output is presented with the green line in the graph below.

Figure B.21: US data - historical decomposition of output (noise shocks off)

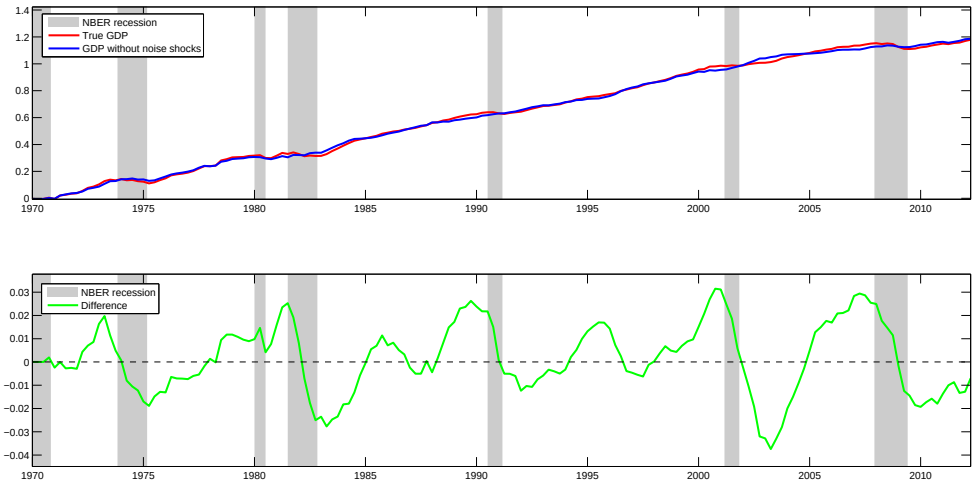

The graph presents the historical decomposition of output. The red line is output, while blue line is output in case when we set noise shocks to zero in all the periods. The difference between the two series of output is presented with the green line in the graph below.

B.6 Appendix - Additional results

Figure B.22: US data - IRFs with long-run restrictions

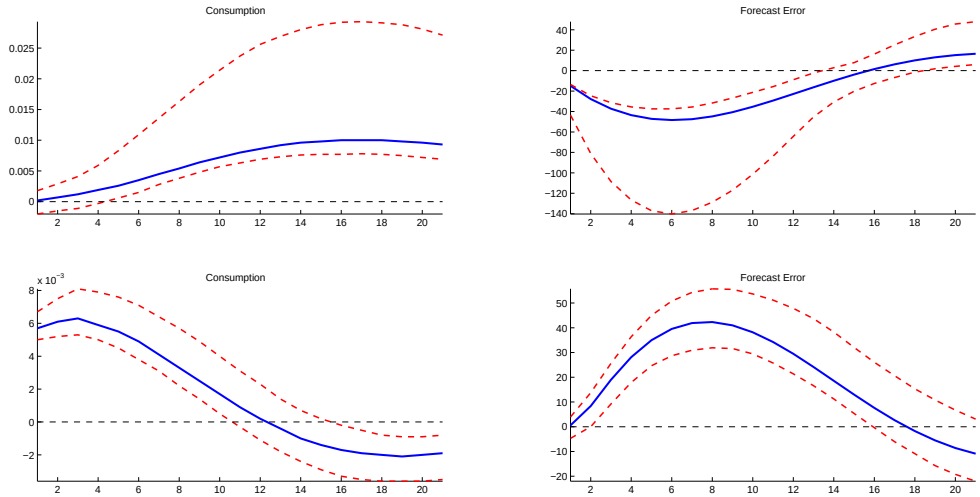

The graph presents the impulse responses of consumption and the estimated forecast error to the permanent shock (above) and to the transitory shock (below). The identification restrictions rely on long-run restrictions. The blue line is the point estimate and the red lines are 90% error bands.

Figure B.23: US data - IRFs to permanent shock (extended identification)

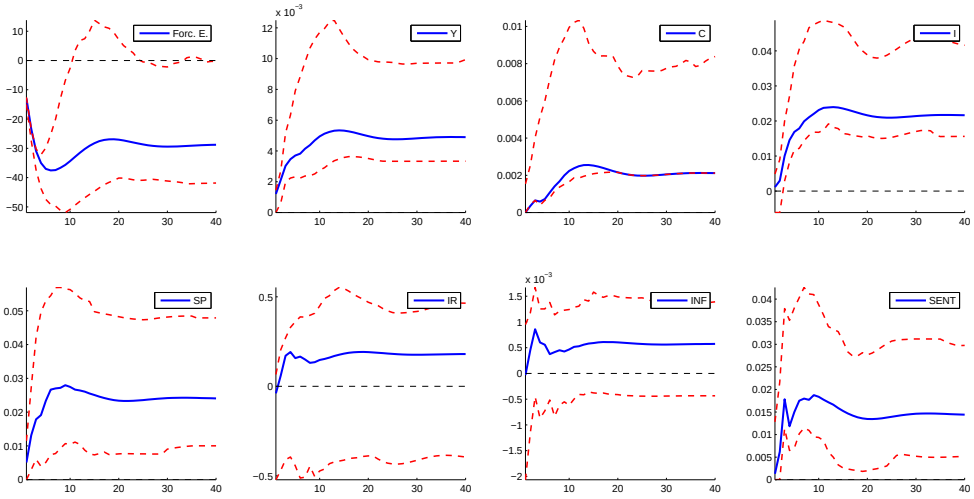

The graph presents the impulse responses to the permanent shock of the estimated forecast error, output and consumption (first row), investment, stock prices and interest rates (second row) and inflation and sentiment (third row).The blue line is the point estimate and the red lines are 90% error bands.

Figure B.24: US data - IRFs to noise shock (extended identification)

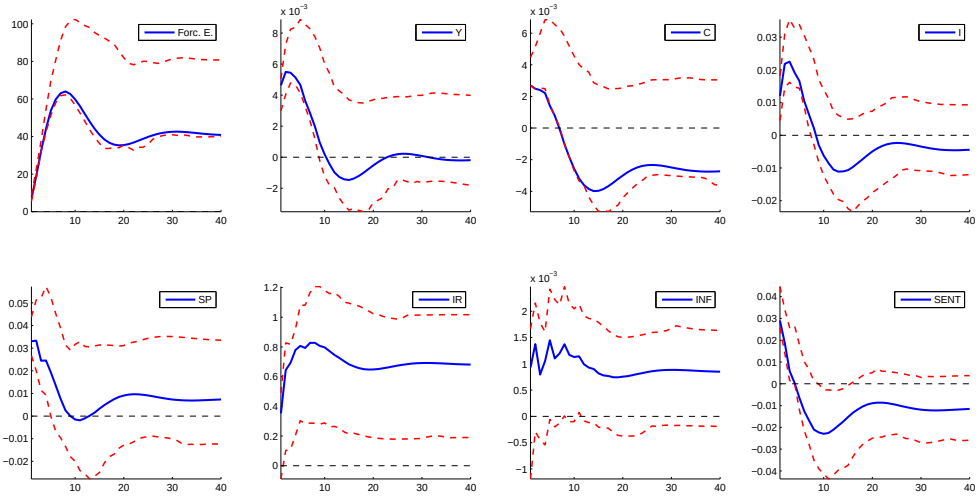

The graph presents the impulse responses to the noise shock of the estimated forecast error, output and consumption (first row), investment, stock prices and interest rates (second row) and inflation and sentiment (third row).The blue line is the point estimate and the red lines are 90% error bands.

Figure B.25: US data - IRFs to 'third' shock (extended identification)

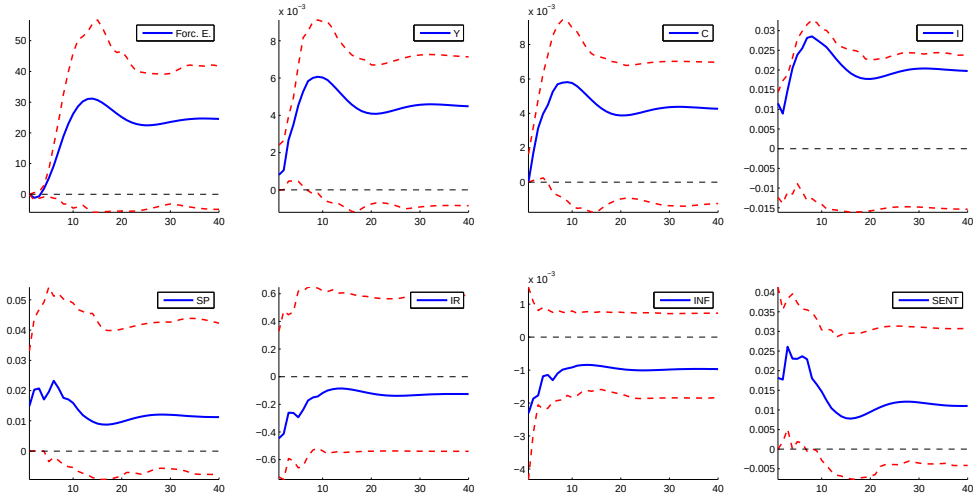

The graph presents the impulse responses to the 'demand' shock of the estimated forecast error, output and consumption (first row), investment, stock prices and interest rates (second row) and inflation and sentiment (third row).The blue line is the point estimate and the red lines are 90% error bands.

Figure B.26: US data - FEVD (extended identification)

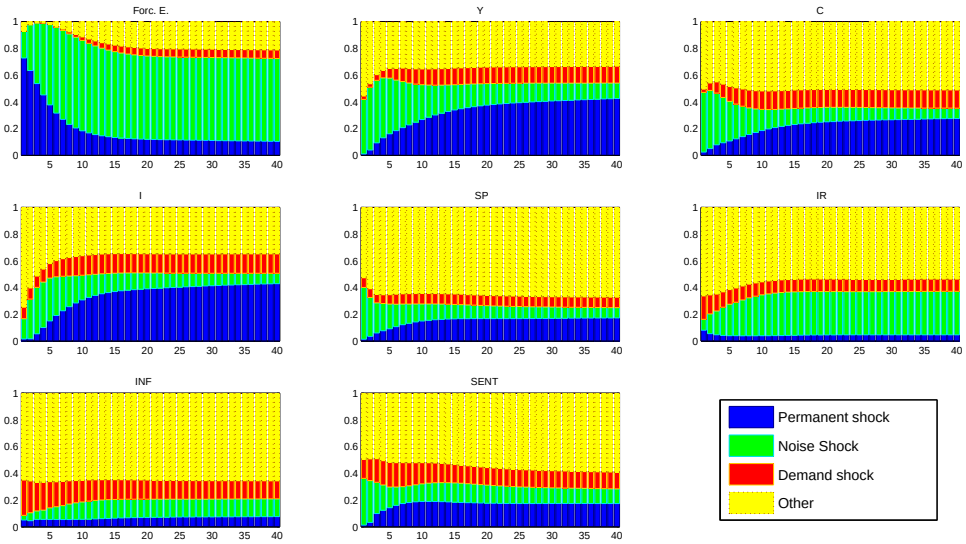

The graph presents the forecast error decomposition of the estimated forecast error, output and consumption (first row), investment, stock prices and interest rates (second row) and inflation and sentiment (third row). The blue area corresponds to the median contribution of permanent shocks, the green area to the median contribution of noise shocks and yellow area to the contribution of all other non-identified shocks.

Figure B.27: US data - IRFs to permanent shock (extended identification)

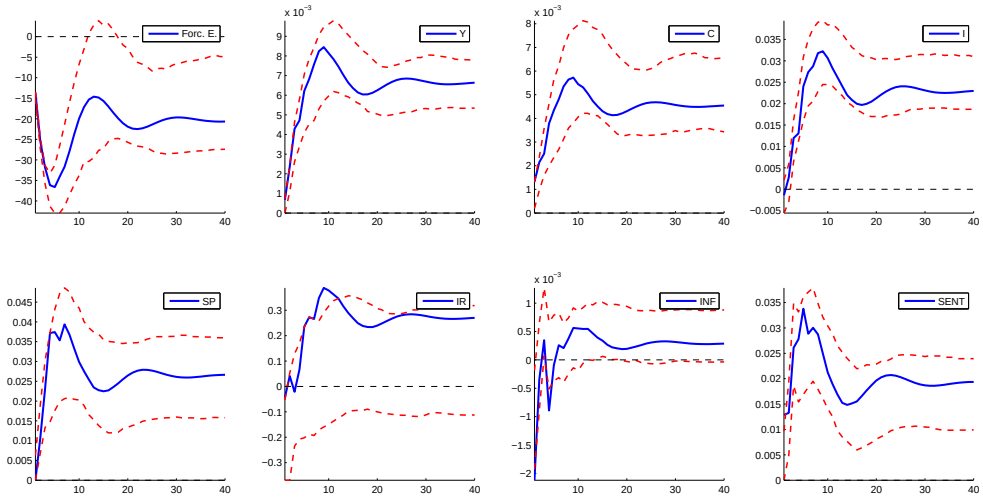

The graph presents the impulse responses to the noise shock of the estimated forecast error, output and consumption (first row), investment, stock prices and interest rates (second row) and inflation and sentiment (third row).The blue line is the point estimate and the red lines are 90% error bands.

Figure B.28: US data - IRFs to noise shock (extended identification)

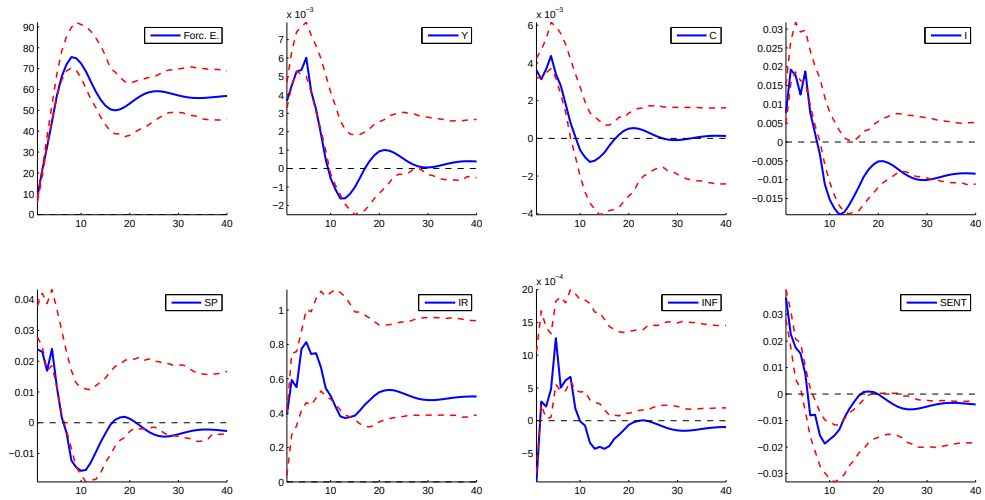

The graph presents the impulse responses to the noise shock of the estimated forecast error, output and consumption (first row), investment, stock prices and interest rates (second row) and inflation and sentiment (third row).The blue line is the point estimate and the red lines are 90% error bands.

Figure B.29: US data - IRFs to 'third' shock (extended identification)

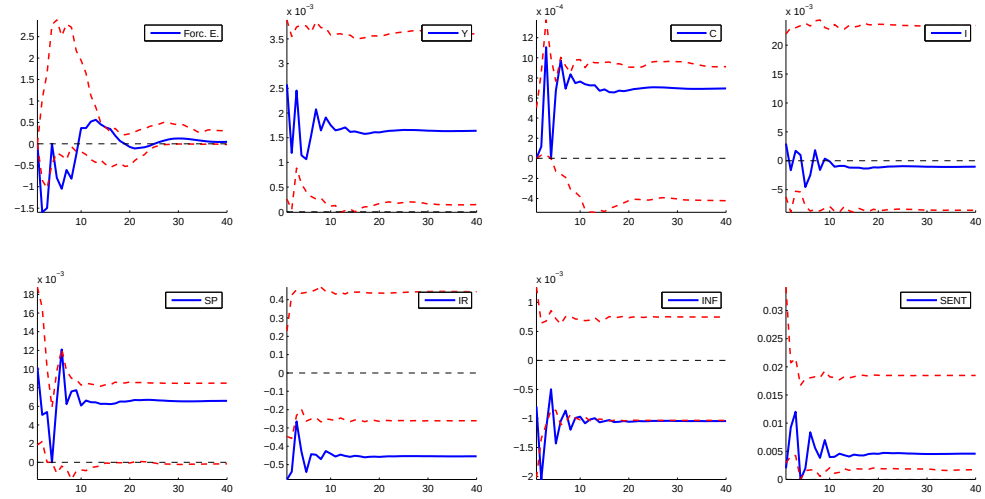

The graph presents the impulse responses to the 'demand' shock of the estimated forecast error, output and consumption (first row), investment, stock prices and interest rates (second row) and inflation and sentiment (third row).The blue line is the point estimate and the red lines are 90% error bands.

Figure B.30: US data - FEVD (extended identification)

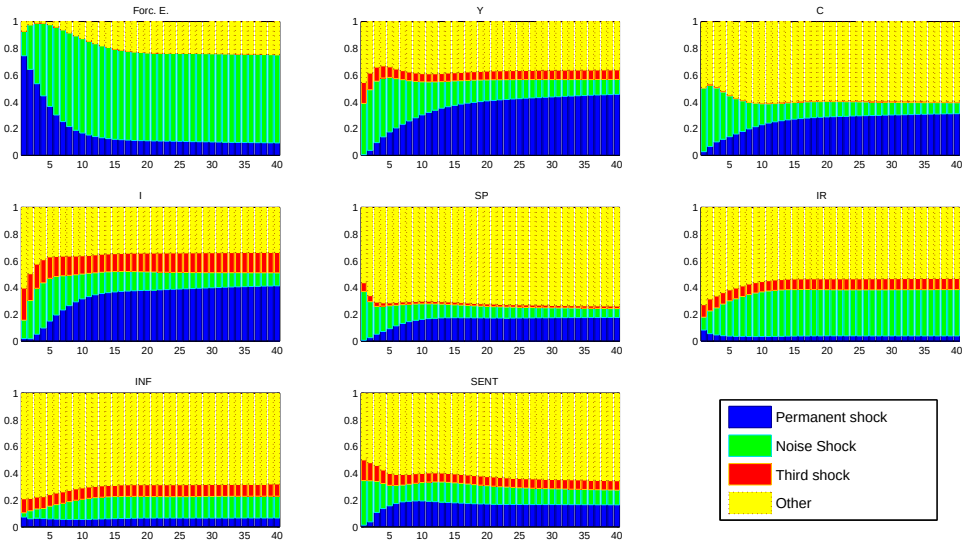

The graph presents the forecast error decomposition of the estimated forecast error, output and consumption (first row), investment, stock prices and interest rates (second row) and inflation and sentiment (third row). The blue area corresponds to the median contribution of permanent shocks, the green area to the median contribution of noise shocks and yellow area to the contribution of all other non-identified shocks.

Figure B.31: US data - IRFs to permanent shock (extended identification)

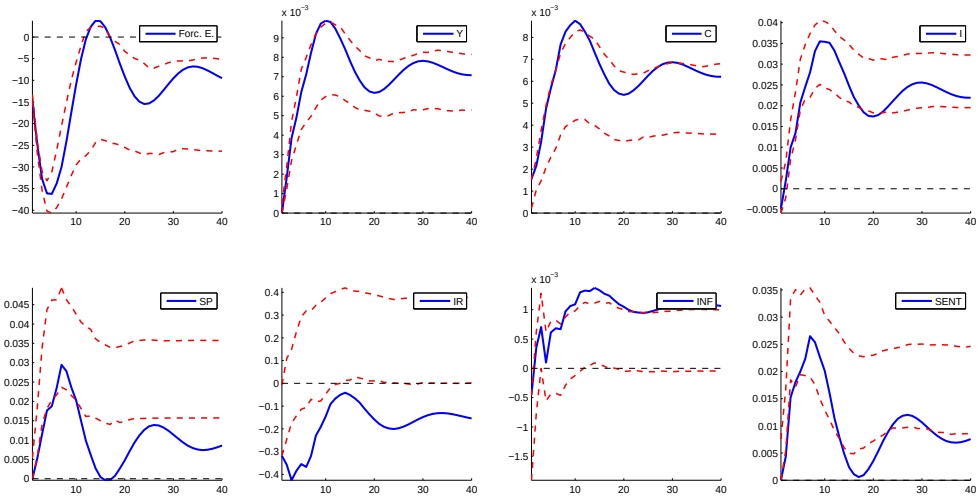

The graph presents the impulse responses to the noise shock of the estimated forecast error, output and consumption (first row), investment, stock prices and interest rates (second row) and inflation and sentiment (third row).The blue line is the point estimate and the red lines are 90% error bands.

Figure B.32: US data - IRFs to noise shock (extended identification)

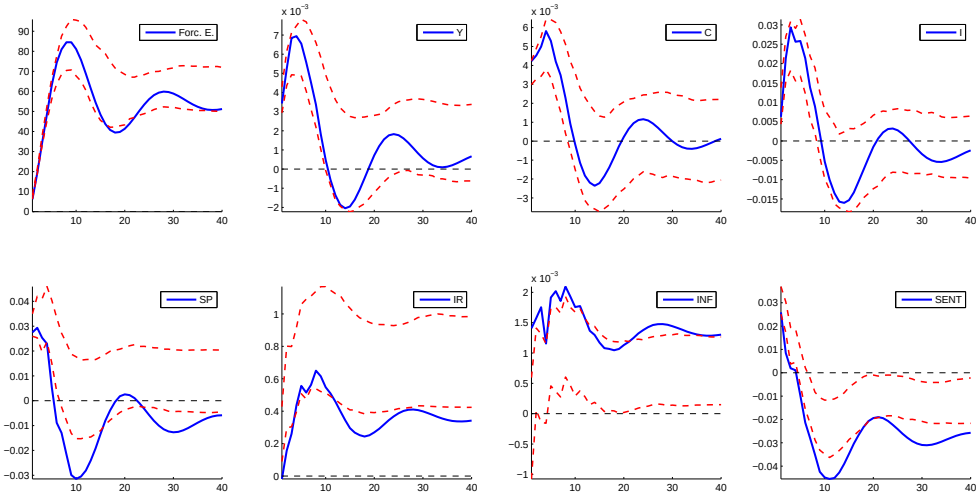

The graph presents the impulse responses to the noise shock of the estimated forecast error, output and consumption (first row), investment, stock prices and interest rates (second row) and inflation and sentiment (third row).The blue line is the point estimate and the red lines are 90% error bands.

Figure B.33: US data - IRFs to 'supply' shock (extended identification)

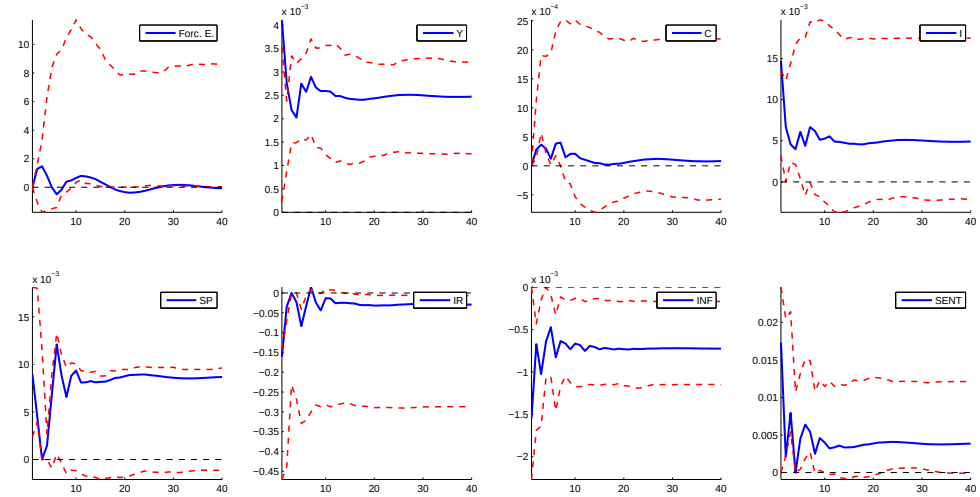

The graph presents the impulse responses to the 'demand' shock of the estimated forecast error, output and consumption (first row), investment, stock prices and interest rates (second row) and inflation and sentiment (third row).The blue line is the point estimate and the red lines are 90% error bands.

Figure B.34: US data - IRFs to 'demand' shock (extended identification)

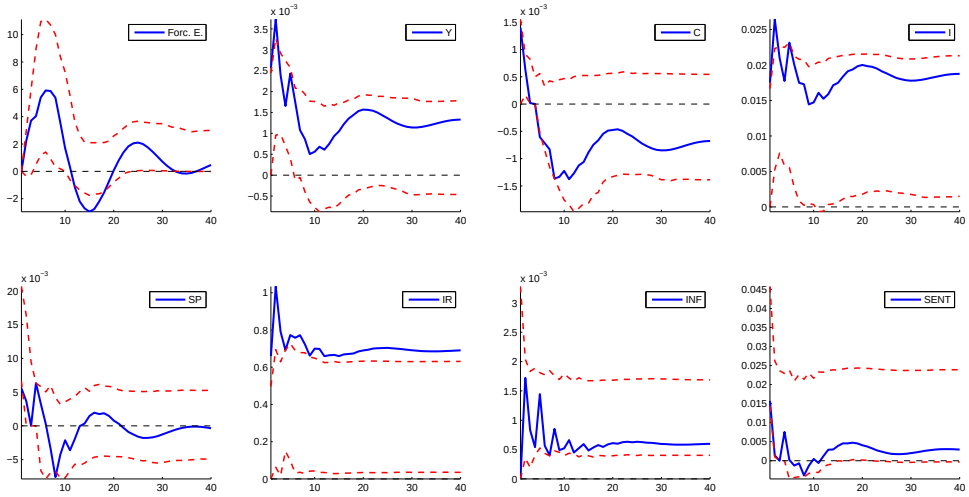

The graph presents the forecast error decomposition of the estimated forecast error, output and consumption (first row), investment, stock prices and interest rates (second row) and inflation and sentiment (third row). The blue area corresponds to the median contribution of permanent shocks, the green area to the median contribution of noise shocks and yellow area to the contribution of all other non-identified shocks.

Figure B.35: US data - FEVD (extended identification)

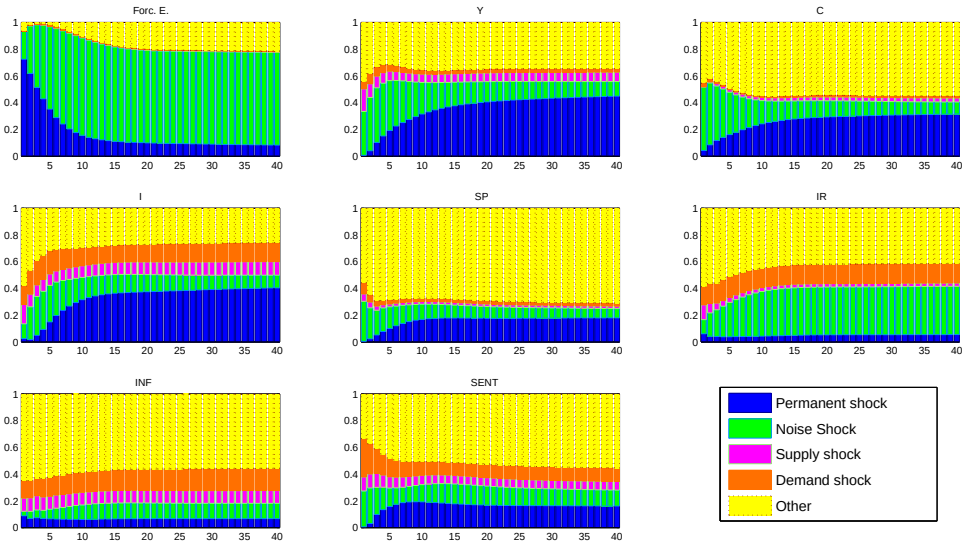

The graph presents the forecast error decomposition of the estimated forecast error, output and consumption (first row), investment, stock prices and interest rates (second row) and inflation and sentiment (third row). The blue area corresponds to the median contribution of permanent shocks, the green area to the median contribution of noise shocks and yellow area to the contribution of all other non-identified shocks.

Chapter 3

Spillovers during Euro Area Sovereign Debt Crisis: a Network Analysis with Absolute Magnitude Restrictions

joint with Roberto De Santis

3.1 Introduction

Spillover effects were central to the propogation of the sovereign debt crisis in the euro area. World leaders and policy makers were confronted with the possibility that spillover effects could endanger countries with otherwise sound economic fundamentals. Such fear was the main driver in justifying the bailout measures. *"This is about nothing less than the future of Europe and the future of Germany in Europe,"* said the German chancellor Angela Merkel when she was defending the 120 billion € bailout package for Greece. In this paper, we measure spillovers, connectedness and contagion across sovereign debt markets in the euro area countries, the United Kingdom (UK) and the United States (US), using a new method to identify country specific disturbances that allow us to single out the sources of spillovers, and investigate how such measures have changed during the euro area sovereign debt crisis.

The literature has studied issues of spillovers and contagion using a variety of econometric approaches, which are summarized in Forbes [2012]. One of the key messages of this literature is that the identification of shocks is the main challenge in estimating the spillover effects and separating the degree of interconnectedness from contagion. With regards to connectedness, Diebold and Yılmaz [2014] suggest a measure based on the importance of a market specific shock for other markets, using the forecast error variance

decomposition (FEVD). The FEVD is typically calculated using the generalized impulse-response functions (GIRFs) of Koop et al. [1996] and Pesaran and Shin [1998]. This method allows for correlation between shocks to different markets, by using the historically observed distribution of the shocks. However, this identification scheme does not provide a causal direction of the spillovers from one market to another. In addition, shocks extracted with this method are not orthogonal.

Given these shortcomings, we propose a method that allows us to pin down the sources of spillover effects, and provides a casual interpretation from one market to another market. The method we suggest relies on the assumption that the magnitude of the instantaneous direct effect of the shock is greater than the magnitude of the instantaneous spillover. Formally, letting ψ_{ij} be the instantaneous response of country i to a shock in country j, our identification scheme requires that $|\psi_{ij}| < |\psi_{jj}| \; \forall \; i \neq j$. In other words, a shock to country j's yield, denoted ε_j, is the shock which has a higher absolute instantanous effect on j's yield than any other country i's yield. In addition, we identify country specific shocks by imposing orthogonality among the shocks. This allows us to provide a causal direction of the spillover from one market to another.

This methodology is closely related to both Kilian and Murphy [2012] and De Graeve and Karas [2014]. Both studies use sign restrictions with elasticity bounds on the impulse responses to identify shocks. This approach allows them to decrease the admissible set of accepted models using external prior restrictions. We employ a similar idea, because we use bounds on the impact matrix to identify shocks, but we do not impose sign restrictions. Our approach is useful when one wants to remain agnostic about the sign of the response functions, and the theory only provides information on the relative size of the responses. The method is particularly suited to study spillovers, or connectedness, in the sovereign debt markets during the financial crisis, when the channels of interconnections were sometimes positive (i.e. flight-to-safety and flight-to liquidity) and sometimes negative (i.e. contagion), and so we do not want to restrict the sign of the effects a-priori.

Our identification method has several advantages over the use of GIRFs. First, it provides a directional measure of spillovers between markets by imposing orthogonality between market specific shocks. Second, it allows for asymmetric responses between countries. Third, in general, our method produces more precise estimates of spillovers and interconnections than alternative identification methods, such as GIRFs or zero restrictions. We show, through Monte Carlo simulations, that the median estimate of spillovers or connectedness obtained with our procedure is close to the true values. Finally, the suggested restrictions can be used together with other a-priori restrictions in order to get more efficient estimates.

Armed with this new methodology, we study the degree of connectedness, spillover and contagion among the euro area, UK and US sovereign debt markets. We use daily data on the yields on 10-year sovereign bonds, over the period January 2005 - August 2014,

controlling for other global shocks using the monetary policy rates. Using the FEVDs based on our identification, we find that total connectedness among sovereign markets declined steadily from October 2009 to the beginning of 2013 because connectedness among euro area countries fell. Using counter-factual experiments, we show that this reduction in connectedness is not due to changes in the size of shocks, but to a fall in cross-market linkages. Cross-market linkages, or contagion à la Forbes and Rigobon [2002], increased from the beginning of the inter-bank credit crisis in August 2007 up to the Lehman bankruptcy in September 2008. They declined steadily in 2009 and fell sharply since the beginning of the euro area sovereign debt crisis in the autumn of 2009. Cross-market linkages reached the lowest point at the beginning of 2013, remained weak in 2013 and rose substantially in 2014. Hence, the results support the hypothesis that during the sovereign debt crisis bond markets were highly fragmented.

We also find that sovereign debt markets are highly interconnected: none of the 12 sovereign yields we consider are insulated from shocks from other markets. Interestingly, over the sample period 2005-2014, the euro area sovereign debt market has been relatively insulated from shocks in the UK and the US. However, in May 2013, when investors perceived a change in US monetary policy, shocks to US sovereign yields became the most important factor influencing European sovereign yields.

Our results show that, in the first phase of the euro area sovereign debt crisis, between 12% and 35% of the variations of Italian, Spanish, Irish and Portuguese bond yields were due to shocks originating in Greece. Instead, in 2011 and 2012, when the sovereign yields in Italy and Spain reached 6-7%, about 10% of the variations of the Spanish yields were due to shocks originating in Italy, while about 5% of the variations of the Italian yields were due to shocks originating in Spain. Furthermore, the spillovers from Italy to Belgium, Germany, the Netherlands, the UK and the US were much larger than those from Spain. Hence, our analysis confirms that shocks originating in Greece and Italy have contributed to developments in sovereign spreads over the last 5 years, and suggest that shocks in Spain have had a smaller impact.

Our results differ from some of the counter-intuitive results obtained with GIRFs. For example, we find that the connectedness of the Greek markets decreased in 2009 and 2010. Conversely, Claeys and Vašíček [2014] find that connectedness increased during the crisis. The discrepancy can be traced to the different specification of the model, as they use common factors from sovereign yield spreads in a Factor Augmented VAR, and in this model a large part of the contemporaneous spillovers between countries will be absorbed by the principal component.[1]

The remaining sections of the paper are structured as follows. Section 3.2 describes the methodology and shows the performance of our method relative to GIRFs using Monte Carlo simulations. Section 3.3 presents the data and the empirical model. Section 3.4

[1]It can be shown that including principal components in a VAR may produce biased results.

describes the results and provides some robustness checks. Section 3.5 concludes.

3.2 Econometric methodology

3.2.1 SVAR setup

A Structural Vector Auto-Regressive model (SVAR) can be written as:

$$A_0 y_t = A_1 y_{t-1} + A_2 y_{t-1} + ... + A_K y_{t-K} + B\varepsilon_t, \tag{3.2.1}$$

where y_t is the $N \times 1$ vector of endogenous variables, K is a finite number of lags, and the structural shocks ε_t are assumed to be white noise, $\mathcal{N}(0, I_N)$. A_0 describes the contemporaneous relations between the variables, while matrices A_k, $k = 1, 2, \ldots, K$ describe the dynamic relationships. The diagonal matrix B contains the standard errors of the structural shocks.

The system (3.2.1) implies a following structural moving average representation, $y_t = B(L)\varepsilon_t$, where $B(L)$ is a polynomial in the lag operator. The system in (3.2.1) cannot be estimated directly, but needs to be estimated in its reduced form:

$$y_t = A_1^* y_{t-1} + A_2^* y_{t-1} + ... + A_P^* y_{t-K} + u_t, \tag{3.2.2}$$

where $u_t = A_0^{-1} B\varepsilon_t$ and $A_k^* = A_0^{-1} A_k$ for $k \in [1, 2, ..., K]$.

The moving average representation of (3.2.2) is $y_t = C(L)u_t$. Therefore, the reduced form response function, $C(L)$, is related to the structural impulse response function by $B(L) = A_0 C(L)$. In other words, to identify the structural shocks and obtain the structural impulse responses, we need to identify A_0.

Defining $S = A_0^{-1} B$, A_0 must be such that $\Sigma_u = SS'$, where Σ_u is the variance-covariance matrix of the reduced form errors. The decomposition $\Sigma_u = SS'$ is not unique. For any H such that $HH' = I$, the matrix SH also satisfies this condition. In this case, $SH(SH)' = SHH'S' = SS' = \Sigma_u$. Therefore, starting from any arbitrary $\tilde{S}$ such that $\Sigma_u = \tilde{S}\tilde{S}'$, such as the Cholesky decomposition of Σ_u, alternative decompositions can be found by post-multiplying by any H satisfying $HH' = I$.

Once such an H matrix is selected and the corresponding shocks are identified, one can compute the h-step ahead forecast error:

$$y_{t+h} - E_t y_{t+h} = \sum_{\tau=0}^{h-1} C_\tau \tilde{S} H \varepsilon_{t+h-\tau}. \tag{3.2.3}$$

Denoting by $\psi_{i,j,h}$ the $(i,j)^{th}$ element of the orthogonalized impulse response coefficient

matrix $C(L)\tilde{S}H$ at horizon h, the h-step ahead forecast error variance of variable i is:

$$\varsigma_i^2(h) = \sum_{\tau=0}^{h-1}(\psi_{i,1,\tau}^2 + \psi_{i,2,\tau}^2 + ... + \psi_{i,K,\tau}^2), \tag{3.2.4}$$

while $(\psi_{i,j,0}^2+\psi_{i,j,1}^2+...+\psi_{i,j,h-1}^2)$ provides the contribution of shock j to the h-step forecast error variance of variable i. Hence, the percentage contribution of shock j to the h-step forecast error variance of variable i is:

$$\omega_{i,j}^2(h) = \frac{(\psi_{i,j,0}^2 + \psi_{i,j,1}^2 + ... + \psi_{i,j,h-1}^2)}{\varsigma_i^2(h)} \tag{3.2.5}$$

3.2.2 Measuring connectedness

Following Diebold and Yılmaz [2014], we measure spillovers and connectedness by means of the FEVD. The FEVD is an adjacency matrix that defines a directed weighted network.[2] The connectedness table, shown in Table 3.1, describes how the adjacency matrix captures connectedness.

Table 3.1: Connectedness Table

	ε_1	ε_2	$\cdots$	ε_N	From Others
y_1	$\omega_{1,1}^2(h)$	$\omega_{1,2}^2(h)$	$\cdots$	$\omega_{1,N}^2(h)$	$\frac{1}{N-1}\sum_{j=1}^{N}\omega_{1,j}^2(h), j \neq 1$
y_2	$\omega_{2,1}^2(h)$	$\omega_{2,2}^2(h)$	$\cdots$	$\omega_{2,N}^2(h)$	$\frac{1}{N-1}\sum_{j=1}^{N}\omega_{2,j}^2(h), j \neq 2$
$\vdots$	$\vdots$	$\vdots$	$\ddots$	$\vdots$	$\vdots$
y_N	$\omega_{N,1}^2(h)$	$\omega_{N,2}^2(h)$	$\cdots$	$\omega_{N,N}^2(h)$	$\frac{1}{N-1}\sum_{j=1}^{N}\omega_{N,j}^2(h), j \neq N$
To Others	$\frac{1}{N-1}\sum_{\substack{i=1\\ i\neq 1}}^{N}\omega_{i,1}^2(h)$	$\frac{1}{N-1}\sum_{\substack{i=1\\ i\neq 2}}^{N}\omega_{i,2}^2(h)$	$\cdots$	$\frac{1}{N-1}\sum_{\substack{i=1\\ i\neq N}}^{N}\omega_{i,N}^2(h)$	$\frac{1}{N}\sum_{i=1}^{N}\sum_{\substack{j=1\\ i\neq j}}^{N}\omega_{i,j}^2(h)$

The upper-left $N\times N$ block contains the FEVD at horizon h. The off-diagonal elements describe pairwise directional connectedness measures from market j to market i, $C_{i\leftarrow j}^H = \omega_{i,j}^2(h)$. The network is weighted, $\omega_{i,j}^2(h) \in [0,1]$, and directed, $C_{i\leftarrow j}^H \neq C_{i\rightarrow j}^H$.[3] The diagonal elements define a market's own connectedness, $C_{j\leftrightarrow j}^H = \omega_{j,j}^2(h)$.

The aggregate connectedness statistics are obtained by taking row and column sums of the off-diagonal elements. Total directional connectedness from market j to other

[2]For more details see Diebold and Yılmaz [2014].

[3]In an unweighted network $\omega_{i,j}$ is either 1 or 0, so that the adjacency matrix only specifies whether a relation exists or not, but does not specify the strength of the relation. In an undirected network relations are symmetric, $C_{i\leftarrow j}^H = C_{i\rightarrow j}^H$.

countries is defined as:

$$C^{H}_{\bullet \leftarrow j} = \frac{1}{N-1} \sum_{\substack{i=1 \\ i \neq j}}^{N} \omega^2_{i,j}(h) \tag{3.2.6}$$

In other words, $C^{H}_{\bullet \leftarrow j}$ is the sum of the j-th column elements of the FEVD except its own share, $\omega^2_{j,j}(h)$. This connectedness 'to others' provides the average share of the h-step forecast-error variance explained by shock j and, therefore, it summarizes the importance of shocks in country j in inducing fluctuations in all other markets.[4]

Similarly, by taking sums over rows, a total directional connectedness to market i from all shocks can be constructed:

$$C^{H}_{i \leftarrow \bullet} = \frac{1}{N-1} \sum_{\substack{j=1 \\ i \neq j}}^{N} \omega^2_{i,j}(h) \tag{3.2.7}$$

$C^{H}_{i \leftarrow \bullet}$ gives the average share of the h-step forecast-error variance of market i coming from shocks originating from all other markets. Finally, total connectedness is:

$$C^{H} = \frac{1}{N} \sum_{i=1}^{N} \sum_{\substack{j=1 \\ i \neq j}}^{N} \omega^2_{i,j}(h) \tag{3.2.8}$$

Similarly, for $\mathcal{S} \subset \{1, \ldots, N\}$,

$$C^{H}_{i,j \in \mathcal{S}} = \frac{1}{N_{\mathcal{S}}} \sum_{i \in \mathcal{S}} \sum_{\substack{j \in \mathcal{S} \\ i \neq j}} \omega^2_{i,j}(h) \tag{3.2.9}$$

measures total connectedness among a subset of markets, for example only euro area countries.

3.2.3 Magnitude restrictions

Having discussed the computation of connectedness, spillovers and contagion measures for a given matrix H, it still remains to identify the structural shocks. In order to obtain partial identification of the system, we impose restrictions on the size of contemporaneous spillovers.

Let $\hat{\psi}_{ij}$ be the instantaneous response of variable i to shock j and $\hat{\psi}_{jj}$ the instantaneous response of variable j to the structural shock j. We identify the orthogonal structural shock in market j, ε_j, by assuming that $|\hat{\psi}_{ij}| < |\hat{\psi}_{jj}| \; \forall \; i \neq j$. Intuitively, this assumption implies that the contemporaneous spillovers to other markets from shock ε_j are smaller

[4] Compared to Diebold and Yılmaz [2014], we prefer to scale 'to others' connectedness by $N-1$, because this statistic is bounded in the interval $[0, 1]$ and it is easier to interpret. We adopt the same scaling for 'from others' connectedness.

than the direct effect of shock ε_j on market j.

It is very easy to implement such restrictions in principle. For a given H we obtain an estimate of A_0, denoted $\hat{A}_0$, which gives us the impact response matrix $\hat{A}_0^{-1}\hat{B}$. With the diagonal elements of $\hat{A}_0$ normalized to 1, the non-diagonal elements can be written as:

$$\hat{a}_{ij} = \frac{\hat{\psi}_{ij}}{\hat{\psi}_{jj}} \tag{3.2.10}$$

Hence our identifying restriction is that $|\hat{a}_{ij}| < 1 \; \forall \; i \neq j$. Thus for each H, we keep the corresponding estimate of the IRFs and FEVD only if the resulting $\hat{A}_0$ satisfies the restrictions on the size of spillover effects.

3.2.4 Estimation algorithm

The estimation procedure consists of three steps. In the first step, the reduced form VAR model is estimated. In the second step, the structural shocks are identified taking into account identification uncertainty. In the third step, estimation uncertainty is taken into account. Formally, the steps are:

1. **Estimate reduced-form VAR:** Given a chosen number of lags, $\widehat{K}$, a $VAR(\widehat{K})$ is estimated by Ordinary Least Squares (OLS) to obtain an estimate of autoregressive coefficients $A^*(L)$ and of the variance-covariance of reduced form errors, $\widehat{\Sigma_u}$.

2. **Identification restrictions:** The reduced form impulse response function, $C(L)$, is related to the structural impulse response function via $B(L) = A_0 C(L)$ and reduced form errors, u_t, are related to structural shocks as $u_t = A_0^{-1} B \varepsilon_t$. The impact matrix, $S = A_0^{-1} B$, must satisfy:

$$\Sigma_u = SS' \tag{3.2.11}$$

   We distinguish the approach used in small systems, with few variables, and larger ones.[5]

   Small systems:

   (a) The initial estimate of $\hat{S}$ is obtained by a Cholesky decomposition of the variance-covariance matrix of reduced form errors, $\hat{\tilde{S}} = chol(\hat{\Sigma}_u)$, giving an initial estimate of the impulse response function is $\hat{\tilde{B}}(L) = \hat{C}(L)\hat{\tilde{S}}$.

   (b) A $q \times q$ matrix P is drawn from standard normal distribution, $\mathcal{N}(0,1)$ and the QR decomposition of P is derived. Note that $P = QR$ and $QQ' = I$.

[5]Different approaches are used only because of computational convenience. While randomly drawing orthonormal matrices using the QR decomposition is faster when only a small number of variables are used, numerical optimization becomes necessary when the number of variables is large because the probability of obtaining a successful draw is decreasing with the size of the system.

(c) The initial estimate of the impulse response function is post-multiplied by Q, to obtain a candidate impulse response function $\hat{B}^*(L) = \hat{C}(L)\hat{\tilde{S}}Q$.

(d) The steps 2b-2c are repeated until the candidate impulse responses, $\hat{B}^*(L)$, satisfies the identifying restrictions.

Large systems:

(a) The problem is initialized as in step 2a above, with $\hat{\tilde{S}} = chol(\hat{\Sigma}_u)$.

(b) A random matrix A_0^{*-1} is drawn satisfying the identifying restrictions. In particular, in the baseline estimation, we construct a matrix with 1s on the diagonal and off-diagonal elements randomly drawn from $[0, 1)$.

(c) Given A_0^{*-1}, the matrix Q^* is defined through the following minimization problem:

$$\begin{aligned} Q^* \;=\; & argmin \quad (\hat{A}_0{}^{-1} - A_0^{*-1})^2 \\ & subject\ to \quad Q^*Q^{*\prime} = I \\ & \hat{S} = \hat{\tilde{S}}Q^* \\ & \hat{A}_0{}^{-1}(i,j) = \hat{S}_{ij}/\hat{S}_{jj}\ \forall\ i,\ j \\ & c(\hat{A}_0{}^{-1}) \geq 0 \end{aligned} \tag{3.2.12}$$

where $c(.) \geq 0$ represents the identifying restrictions. In other words, we look for an orthonormal matrix, Q^*, that implies a decomposition, $\hat{\Sigma}_u = (\hat{\tilde{S}}Q^*)(\hat{\tilde{S}}Q^*)'$, such that the resulting matrix of impact coefficients, $\hat{A}_0{}^{-1}$, is close to A_0^{*-1}, and satisfies the identifying restrictions.[6]

(d) In case the minimization does not converge to a feasible solution, steps 2b and 2c are repeated. Once the minimization converges, the candidate impulse response function is calculated as $\hat{B}^*(L) = \hat{C}(L)\hat{\tilde{S}}Q^*$, and satisfies the restrictions by definition.

3. **Estimation uncertainty:** to account for estimation uncertainty, we repeat steps 1-2 1000 times, each time with a new artificially constructed data sample, Y^*. To construct data samples, we use re-sampling of errors. The new data sample is constructed recursively as $y_t^* = \hat{A}_1^* y_{t-1}^* + ... + \hat{A}_N^* y_{t-N}^* + \widehat{u_t}^*$, starting from initial values $[y_0, ..., y_{N-1}]$. $\hat{A}_n^*$ are the estimated reduced form autoregressive coefficients and $\widehat{u_t}^*$ are drawn randomly, with replacement, from the estimated reduced form errors, $\widehat{u_t}$.

The point estimates and confidence bands are given by the median and relevant percentiles of the distribution of retained impulse response functions.

[6]Note that this minimization could be carried out without the matrix A_0^{*-1}, for example using a constant objective function. However, the role of A_0^{*-1} in our algorithm is to ensure that we search the full space of permissible matrices, satisfying the identifying restrictions, in a more complete way.

3.2.5 Comparison with alternative identification methods

The advantage of using magnitude restrictions over alternative methods can be appreciated with a simple example. Consider a system with two variables, and let:

$$A_0^{-1} = \begin{bmatrix} 1 & b \\ c & 1 \end{bmatrix} \qquad B = \begin{bmatrix} \sigma_1 & 0 \\ 0 & \sigma_2 \end{bmatrix}$$

so that

$$A_0^{-1}B = \begin{bmatrix} \sigma_1 & b\sigma_2 \\ c\sigma_1 & \sigma_2 \end{bmatrix} \qquad \Sigma_u = \begin{bmatrix} \sigma_1^2 + b^2\sigma_2^2 & c\sigma_1^2 + b\sigma_2^2 \\ c\sigma_1^2 + b\sigma_2^2 & c^2\sigma_1^2 + \sigma_2^2 \end{bmatrix}$$

In case of zero restrictions, the estimated impact matrix obtained via Cholesky decomposition of the variance-covariance matrix when the variables are ordered as $[y_1\ y_2]$ is:

$$\widehat{A_0^{-1}B}^{z} = \begin{bmatrix} \sqrt{\sigma_1^2 + b^2\sigma_2^2} & 0 \\ \frac{c\sigma_1^2 + b\sigma_2^2}{\sqrt{c^2\sigma_1^2 + \sigma_2^2}} & \sqrt{c^2\sigma_1^2 + \sigma_2^2 - \frac{(c\sigma_1^2 + b\sigma_2^2)^2}{\sigma_1^2 + b\sigma_2^2}} \end{bmatrix}$$

Clearly $\widehat{A_0^{-1}B}^{z}$ will coincide with the true $A_0^{-1}B$ only when $b = 0$, namely when there is no instantaneous spillover from market 2 to market 1. If the variables are ordered as $[y_2\ y_1]$ it can be similarly shown that the estimated and true impact matrix will coincide when $c = 0$.

The GIRFs for the first period are:

$$\widehat{A_0^{-1}B}^{g} = \begin{bmatrix} \frac{\sigma_1^2 + b^2\sigma_2^2}{\sqrt{\sigma_1^2 + b^2\sigma_2^2}} & \frac{c\sigma_1^2 + b\sigma_2^2}{\sqrt{c^2\sigma_1^2 + \sigma_2^2}} \\ \frac{c\sigma_1^2 + b\sigma_2^2}{\sqrt{\sigma_1^2 + b^2\sigma_2^2}} & \frac{c^2\sigma_1^2 + \sigma_2^2}{\sqrt{c^2\sigma_1^2 + \sigma_2^2}} \end{bmatrix}$$

In this case $\widehat{A_0^{-1}B}^{g}$ will coincide with the true $A_0^{-1}B$ only when $b = 0$ and $c = 0$, namely only when there are no instantaneous spillovers between markets. Since in general the off-diagonal elements of $\widehat{A_0^{-1}B}^{g}$ are non-zero, shocks identified with GIRFs are not orthogonal.

How big are the errors when measuring spillovers via GIRFs? To simplify, assume that $\sigma_1 = x\sigma_2$, where $x > 0$. Then the GIRFs are:

$$\widehat{A_0^{-1}B}^{g} = \begin{bmatrix} \sigma_1\sqrt{1 + c^2x^2} & \sigma_1 b(1 + x^2)\left[\sqrt{b^2 + x^2}\right]^{-1} \\ \sigma_1 c(1 + x^2)\left[\sqrt{1 + c^2x^2}\right]^{-1} & \sigma_1\sqrt{b^2 + x^2} \end{bmatrix} \tag{3.2.13}$$

The true instantaneous impact of y_2 on y_1 is b. The estimated instantaneous impact is $\hat{b}^g = b(1+x^2)\left[b^2 + x^2\right]^{-1}$. Figure C.1 shows the relationship between b and $\hat{b}^g$. The curved area represents the instantaneous impact obtained by using GIRFs, the transparent grey areas represents the bounds implied by the absolute magnitude restrictions, while the red area represents the true b.

Notice that $\hat{b}^g = 0$ when $b = 0$. However, when the standard deviations of the shocks differ substantially, for example when $x = 0.1$ so that the standard deviation of the

shock from y_2 is ten times that from y_1, the estimated instantaneous impact using GIRFs can reach 4, while the true instantaneous impact is close to zero. On the other hand, the absolute magnitude restrictions are designed such that the estimated instantanous impact cannot exceed one in absolute value. Nevertheless, $\hat{b}^g$ is inside the transparent grey areas for certain parameters, meaning that the estimates from the GIRFs satisfy the absolute magnitude restrctions, which implies that the results obtained with the two methodologies in these specific cases may not differ considerably.

Figure C.2 shows the root square error of the estimated instantaneous impact when using GIRFs (red area) and when using absolute magnitude restrictions (blue area). Again, the difference is most pronounced when the standard deviations of shocks differ substantially.

It is useful to anticipate that in the empirical section we find that the spillover from Italian to Greek sovereign yields is more than one when using GIRFs. The numerical example would suggest that this may be due to the standard deviation of shocks to Greek sovereign yields being considerably higher.

3.2.6 Monte Carlo simulations

To extend the results of the simple example shown above, we compare the results of our methodology to those of GIRFs using a Monte Carlo simulation. We use multiple models to simulate a time-varying model.[7] Specifically, data for four markets are simulated using the following SVAR:

$$\begin{aligned} A_0^m y_t^m &= A_1^m y_{t-1}^m + B^m \varepsilon_t^m, \\ y_t^m &= (A_0^m)^{-1} A_1^m y_{t-1}^m + (A_0^m)^{-1} B^m \varepsilon_t^m, \end{aligned} \tag{3.2.14}$$

where $m = 1, 2, ..., M$ denotes the model.

We model a time-varying data generating process by assuming that impact matrices, A_0^m, and the standard errors of the shocks, B^m, are not constant. In the baseline exercise the non-diagonal entries of $(A_0^m)^{-1}$ are randomly selected from the interval $[-0.99, 0.99]$, while diagonal entries equal one.[8] The diagonal entries of matrix B^m, which give the standard errors of structural shocks, are also selected randomly from a uniform distribution $\mathcal{U}[0.05, 0.45]$. We simulate the data across models assuming that A_1^m remains constant,

[7] We simulate a time-varying model because a rolling window estimation is carried out in the empirical section.

[8] In order to better replicate empirical regularities with simulated data, we model the non-diagonal entries of $(A_0^m)^{-1}$ in the following way. Every element $a_{i,j}$ is a sum of three components. The first component serves to replicate the fact that total connectedness is changing over time, therefore we model it as a process ranging from 0 to 0.49. The second component serves to capture the fact that 'to others' connectedness is volatile over time - we model this by adding country specific shocks drawn from the uniform distribution $\mathcal{U}[-0.35, 0.35]$ to every column of matrix $(A_0^m)^{-1}$. The last component is drawn from the uniform distribution $\mathcal{U}[-0.15, 0.15]$ and added to all non-diagonal elements and serves as an idiosyncratic component.

that is $A_1^m = A_1 \; \forall \; m$.

Using this simulated data, we compare the results from our identification scheme with those obtained using GIRFs. The auto-regressive parameters in A_1^m and the variance-covariance matrix, Σ^m, are estimated using OLS and the small sample distribution of parameters is obtained using bootstrap methods.

The performance of the identification schemes can be compared by using the root mean squared error (RMSE) of different statistics. The RMSE of the estimates of the IRFs is:

$$RMSE(irf) = \sqrt{\frac{1}{N^2}\frac{1}{H}\frac{1}{M}\sum_{i=1}^{N}\sum_{j=1}^{N}\sum_{h=1}^{H}\sum_{m=1}^{M}\left(\bar{\hat{\Psi}}_{i,j,h,m} - \Psi_{i,j,h,m}\right)^2} \tag{3.2.15}$$

where $\Psi_{i,j,h,m}$ is the true IRF of variable i to the shock j at horizon h for the model m, and $\bar{\hat{\Psi}}_{i,j,h,m}$ is its median estimated counterpart.[9] The RMSE of estimated 'to others' connectedness is:

$$RMSE(to\ others) = \sqrt{\frac{1}{N}\frac{1}{H}\frac{1}{M}\sum_{j=1}^{N}\sum_{h=1}^{H}\sum_{m=1}^{M}\left(\bar{\hat{C}}_{\bullet\leftarrow j}^{h,m} - C_{\bullet\leftarrow j}^{h,m}\right)^2} \tag{3.2.16}$$

where $C_{\bullet\leftarrow j}^{h,m}$ is 'to others' connectedness for shock j at horizon h obtained from the model m, and $\bar{\hat{C}}_{\bullet\leftarrow j}^{h,m}$ is its median estimated counterpart. Finally, the MSE of estimated grand average connectedness is:

$$RMSE(grand\ average) = \sqrt{\frac{1}{H}\frac{1}{M}\sum_{h=1}^{H}\sum_{m=1}^{M}\left(\bar{\hat{C}}^{h,m} - C^{h,m}\right)^2} \tag{3.2.17}$$

where $C^{h,m}$ is total connectedness at horizon h obtained from the model m, and $\bar{\hat{C}}^{h,m}$ is its median estimated counterpart.

Table 3.2 reports the RMSE of the magnitude restrictions, GIRFs and zero restrictions with random ordering, which were also employed by Diebold and Yılmaz [2014]. In the first 10 periods, on average, the RMSE of the IRF estimates is almost 2 times smaller when using magnitude restrictions relative to GIRFs. Magnitude restrictions are also better than zero restrictions using a random ordering.

Figure C.3 shows directional connectedness 'to others' from all four markets for the first 10 models.[10] Our methodology performs reasonably well, as the true directional connectedness 'to others' is mostly included in the two-standard error bands. The same cannot be said for the estimates obtained using GIRFs, shown in Figure C.4: the true

[9] To calculate RMSE we simulate 1000 different models and each model is estimated from 200 samples.

[10] We show only the first 10 models to simplify the presentation, the figures for other models can be provided on request.

Table 3.2: The relative root mean squared error (RMSE) of the estimates for different identification methodologies

	Magnitude res.		GIRF		Zero res. (random order)	
horizon	*1*	*1-10*	*1*	*1-10*	*1*	*1-10*
IRFs	0.06	0.05	0.11	0.09	0.09	0.07
TO connectedness	0.23	0.12	0.42	0.18	0.39	0.21
Grand Average	0.07	0.09	0.08	0.11	0.08	0.11

directional connectedness 'to others' is mostly outside the two-standard error bands. The RMSE of the estimated directional connectedness 'to others' is around 50 percent smaller when using magnitude restrictions as compared to GIRFs, as shown in Table 3.2.

Estimates of total connectedness differ little across methodologies: as shown in Figures C.5 and C.6, estimates obtained using magnitude restrictions are still closer to the true total connectedness, but the gain in precision in terms of RMSE is now less than 20 percent.

It is also interesting to explore how magnitude restrictions would perform when estimates obtained via GIRFs and the true model coincide. In Section 3.2.5 we showed that, theoretically, they coincide only when there are no contemporaneous spillovers between markets. To see how magnitude restrictions perform when there are no spillovers, we repeat the baseline exercise now setting the non-diagonal entries of $(A_0^m)^{-1}$ to zero, with diagonal entries still equal to one. Table 3.3 reports the RMSE of magnitude restrictions, GIRFs and zero restrictions with random ordering. Clearly, estimates obtained by GIRFs and zero restrictions are more precise since the identification restrictions coincide with the true model, and the errors are only due to small sample estimation errors. Nonetheless, magnitude restrictions perform reasonably well. The RMSE of the IRF estimates, 0.01, and of the estimated directional connectedness 'to others', 0.06, are smaller than in the general case. The estimates of total connectedness obtained with magnitude restrictions are, however, biased when actual total connectedness is zero.[11]

To summarize, if the focus is only on total connectedness, the different identification approaches produce similar results. However, whenever we are interested in less aggregate statistics, such as bilateral relations between countries or the importance of a specific shock, using magnitude restrictions produces more precise estimates.

[11]To understand this result, set $\sigma_1 = \sigma_2 = 1$ in the example from Section 3.2.5. It can be shown that when $b = c = 0$, there are at least two candidate impact matrices that are consistent with the magnitude restrictions. First with $\hat{b} = \hat{c} = 0$, and second with $\hat{b} = -\hat{c}$. In the second case, the estimate of connectedness is not equal to zero, implying it is biased when the true model is such that $b = c = 0$.

Table 3.3: The root mean squared error (RMSE) of the estimates for different identification methodologies - model with no spillovers

	Magnitude res.		GIRF		Zero res. (random order)	
horizon	*1*	*1-10*	*1*	*1-10*	*1*	*1-10*
IRFs	0.02	0.01	0.00	0.00	0.02	0.02
TO connectedness	0.07	0.06	0.00	0.01	0.00	0.04
Grand Average	0.21	0.20	0.01	0.02	0.01	0.02

3.3 Data and specification of the VAR

The measures of spillovers and connectedness depend on the set of variables whose connectedness is to be examined, the predictive horizon H, the VAR model adopted and its dynamics, $A(L)$.

Given the importance of spillovers during the euro area sovereign debt crisis, we apply our method to study the transmission of shocks in the sovereign debt market of ten euro area countries (Austria, Belgium, France, Germany, Greece, Ireland, Italy, the Netherlands, Portugal, Spain), the UK and the US. Monetary policy rates in the three economies are also included in order to control for other domestic and foreign shocks that shape the yield curves.

The sovereign yields we use are the 10-year benchmark rates provided by Reuters. The monetary policy rates are the 3-month Overnight Indexed Swap (OIS) rates provided by Reuters for the euro area and the US, and Thomson DataStream for the UK. An OIS uses an overnight rate index, such as the EONIA for euro-denominated products, the SONIA for sterling-denominated products or the Federal Funds Rate for US dollar-denominated products. The OIS rates, at short maturities, are good indicators of the monetary policy stance. The data is daily, running from January 2005 to August 2014. The policy rates are treated as 'fast moving' variables to absorb common effects on bond markets.

The predictive horizon H is important because spillovers and connectedness measures are time dependent. Following Diebold and Yılmaz [2014] we focus on a medium-run horizon of $H = 12$ days, although in the online appendix we also present results on a short-run horizon of $H = 2$ days.

To provide a sense of the time variation present in the data, we follow Diebold and Yılmaz [2014] and estimate the VAR using a rolling window of 200 days. VAR is estimated in levels with a constant and the lag length of the VAR is selected using the Bayesian Information Criterion (BIC).

3.4 Results

To identify the shock specific to market j, we assume that (i) the instantaneous response of the sovereign yield in country j is larger in absolute value than the instantaneous response of sovereign yields in country i and (ii) monetary policy rates do not react contemporaneously to sovereign yield shocks, while monetary policy shocks contemporaneously affect sovereign yields. In other words, we assume that monetary policy does not respond to yield shocks, but short-term monetary policy rates are one of the driving forces of sovereign yields.

We proceed in two steps. In Section 3.4.1, we show the full-sample (static) connectedness analysis, which sets the stage for Section 3.4.2, where we carry out the rolling-sample (dynamic) analysis. In Section 3.4.3, we use a counter-factual exercise to disentangle the importance of contagion versus the role of shocks in explaining connectedness. Finally, Section 3.4.4 discusses how the results would differ using GIRF analysis.

3.4.1 Full-sample analysis

Table 3.4 shows the connectedness table for the full-sample. The table shows the pairwise directional connectedness between markets obtained using the magnitude restriction method. The numbers in brackets show those obtained using GIRFs.

The diagonal elements, showing 'own connectedness', tend to be the largest individual elements of the table. As expected, 'own connectedness' is particularly large for monetary policy rates. Conversely, 'own connectedness' is relatively smaller for sovereign yield shocks in France (25%), the UK (18%), the Netherlands (30%) and the US (35%). The government yields of these countries are mostly affected by developments in monetary policy rates or sovereign yields in other markets.

Total connectedness of the asset markets amounts to 51%.[12] This means that, on average, 51% of the variance of sovereign yields in the sample can be explained by shocks to foreign sovereign yields and monetary policy rates.

Some blocks of high pairwise directional connectedness exist, especially from German yields to the sovereign yields of Austria (15%), the Netherlands (27%), France (17%), the UK (24%) and the US (17%). Note that Austrian and Dutch sovereign yields do have an important influence on the German Bund (both at 14%). In general, the sovereign markets of Germany, Austria and the Netherlands are highly inter-connected, and the same is true for the markets of Italy and Spain, as well as France and Belgium.

It is useful to point out that UK and US sovereign yields have limited explanatory power in the developments of the euro area sovereign yields. Moreover, the column average of all pairwise connectedness measures corresponding to UK and US sovereign yields

[12]Total connectedness of the asset markets includes the spillovers from monetary policy to sovereign yields, but excludes the spillovers in the other direction.

Table 3.4: Full sample connectedness table at horizon 12 business days

	USm	EAm	UKm	DE	AT	NL	BE	FR	IT	SP	IR	PT	GR	UK	US	FROM
USm	99	0	0	0	0	0	0	0	0	0	0	0	0	0	0	0
	(77)	*(2)*	*(1)*	*(3)*	*(1)*	*(3)*	*(2)*	*(3)*	*(0)*	*(0)*	*(1)*	*(0)*	*(0)*	*(2)*	*(3)*	*(2)*
EAm	5	92	0	1	0	0	0	0	0	0	0	0	0	0	0	1
	(4)	*(69)*	*(3)*	*(7)*	*(3)*	*(4)*	*(1)*	*(3)*	*(0)*	*(0)*	*(0)*	*(0)*	*(0)*	*(4)*	*(1)*	*(2)*
UKm	2	4	91	1	0	0	0	0	0	0	0	0	0	0	0	1
	(2)	*(4)*	*(79)*	*(3)*	*(1)*	*(2)*	*(1)*	*(3)*	*(0)*	*(0)*	*(0)*	*(0)*	*(0)*	*(5)*	*(0)*	*(2)*
DE	5	5	1	45	14	14	2	5	1	1	1	1	0	3	2	5
	(1)	*(1)*	*(0)*	*(21)*	*(14)*	*(18)*	*(8)*	*(14)*	*(0)*	*(1)*	*(0)*	*(0)*	*(0)*	*(12)*	*(8)*	*(6)*
AT	3	4	1	15	42	10	7	8	2	2	1	1	1	2	2	5
	(1)	*(1)*	*(0)*	*(12)*	*(23)*	*(15)*	*(13)*	*(16)*	*(3)*	*(3)*	*(1)*	*(0)*	*(0)*	*(8)*	*(5)*	*(6)*
NL	5	5	1	27	17	30	4	5	1	1	1	1	0	2	2	5
	(1)	*(1)*	*(0)*	*(16)*	*(15)*	*(21)*	*(10)*	*(15)*	*(1)*	*(2)*	*(1)*	*(0)*	*(0)*	*(10)*	*(7)*	*(6)*
BE	4	2	1	6	15	6	41	8	5	3	3	1	2	2	2	5
	(1)	*(0)*	*(0)*	*(7)*	*(14)*	*(10)*	*(25)*	*(16)*	*(8)*	*(7)*	*(3)*	*(1)*	*(0)*	*(4)*	*(3)*	*(5)*
FR	5	4	1	17	20	10	9	25	2	2	1	1	0	1	1	6
	(1)	*(1)*	*(0)*	*(12)*	*(16)*	*(15)*	*(13)*	*(21)*	*(4)*	*(3)*	*(1)*	*(0)*	*(0)*	*(8)*	*(5)*	*(6)*
IT	1	0	0	2	4	4	9	4	43	16	3	3	4	3	2	5
	(0)	*(0)*	*(0)*	*(0)*	*(5)*	*(2)*	*(13)*	*(7)*	*(38)*	*(23)*	*(5)*	*(4)*	*(1)*	*(0)*	*(0)*	*(4)*
SP	1	0	0	2	5	3	4	4	15	44	4	3	6	3	3	5
	(0)	*(0)*	*(0)*	*(1)*	*(6)*	*(3)*	*(9)*	*(7)*	*(21)*	*(40)*	*(7)*	*(4)*	*(2)*	*(1)*	*(1)*	*(4)*
IR	1	0	0	2	3	3	4	2	4	6	53	7	6	4	4	4
	(0)	*(0)*	*(0)*	*(1)*	*(3)*	*(2)*	*(7)*	*(3)*	*(4)*	*(8)*	*(58)*	*(10)*	*(3)*	*(1)*	*(1)*	*(3)*
PT	0	0	0	1	1	1	3	1	4	4	8	61	10	2	2	3
	(0)	*(0)*	*(0)*	*(0)*	*(1)*	*(0)*	*(5)*	*(1)*	*(7)*	*(7)*	*(15)*	*(57)*	*(6)*	*(0)*	*(0)*	*(3)*
GR	0	0	0	0	0	1	1	0	1	1	1	2	91	0	0	1
	(0)	*(0)*	*(0)*	*(1)*	*(0)*	*(0)*	*(3)*	*(0)*	*(7)*	*(4)*	*(5)*	*(5)*	*(74)*	*(0)*	*(0)*	*(2)*
UK	3	3	3	24	8	9	3	4	2	2	2	1	1	28	5	6
	(1)	*(1)*	*(1)*	*(17)*	*(11)*	*(14)*	*(6)*	*(11)*	*(0)*	*(1)*	*(0)*	*(0)*	*(0)*	*(26)*	*(11)*	*(5)*
US	7	1	0	17	6	6	3	4	4	4	3	2	1	7	35	5
	(2)	*(1)*	*(0)*	*(14)*	*(9)*	*(12)*	*(5)*	*(9)*	*(0)*	*(0)*	*(0)*	*(0)*	*(0)*	*(14)*	*(34)*	*(5)*
TO	2	2	0	7	6	4	4	3	3	3	3	2	2	2	2	**51**
	(1)	*(1)*	*(1)*	*(7)*	*(7)*	*(7)*	*(7)*	*(8)*	*(4)*	*(4)*	*(3)*	*(2)*	*(1)*	*(5)*	*(3)*	***(56)***

indicates that total directional connectedness 'to others' is only 2%. The sovereign yield with the largest influence on other markets is the German Bund (7% on average).

3.4.2 Rolling-sample analysis

Moving to the rolling window estimation, we start by presenting, in Figure C.7, the estimated standard deviation of the shocks to sovereign yields for each 200-day rolling-sample windows. The shocks to yields on sovereign bonds issued by Germany, Austria, the Netherlands, Belgium, France, the UK and the US were small and relatively stable over the sample. Conversely, the shocks originating in Greece, Portugal, Ireland, Italy and Spain have been changing over time, and were at times very large.

Overall, the dynamics of the shocks obtained with our method are in line with anecdotal evidence. For example, at their peak, the size of the shock to sovereign yields is largest in Greece, followed by Portugal, Ireland, Italy and Spain. In addition, the dynamics of

the shocks matches the conventional wisdom: there are large shocks in Greece in 2010, resulting in the EU Commission/ECB/IMF program, and 2012, due to the credit event on Greek sovereign debt. There are similarly large shocks in Italy and Spain in 2011 and 2012, due to fears of euro area break-up. However, our method also shows a rising trend for all euro area shocks since the crisis in inter-bank markets in August 2007, which also led to shocks to the UK and US sovereign yields at the end of 2007.

Total connectedness

Total connectedness is plotted in Figures C.8 and C.9. Figure C.8 is constructed using all shocks to sovereign yields and monetary policy rates and, hence, shows the overall degree of connectedness among short-term money market rates and long-term sovereign yields. Figure C.9 is constructed using shocks to sovereign yields only, and therefore measures the degree of connectedness among long-term sovereign yields.

Over the period January 2005 to September 2009, total connectedness among sovereign yields was very volatile and ranged between 60% and 78% according to our results. Total connectedness declined steadily from 77% in October 2009 to 56% at the beginning of 2013. It then increased steadily, returning to pre-crisis levels in 2014.

These dynamics reflect developments in the euro area sovereign debt market. In fact, as Figure C.10 shows, total connectedness among euro area sovereign yields is due to shocks to the euro area sovereign yields only. Total cross-border connectedness among euro area countries declined steadily since October 2009. The negative trend in connectedness was particularly notable from the beginning of 2011 until the summer of 2012, when the fears of the break-up of the euro area exacerbated the financial crisis. At that time, policy makers pointed to financial fragmentation as one of the main causes for the impairment of the transmission mechanism of monetary policy. Connectedness among euro area countries has increased steadily since the beginning of 2013. The degree of connectedness in 2014 is similar to the level recorded before the financial crisis, suggesting that financial fragmentation in the euro area sovereign debt market has seized to be a key issue.

Total directional connectedness

Total directional connectedness among the euro area, the UK and US is plotted in Figures C.11 and Figure C.12. The former combines region specific shocks to sovereign yields and monetary policy rates; the latter focuses on the effects of shocks to sovereign yields only. The plots on the diagonal provide the effects of domestic shocks.[13]

The results are revealing. First of all, during the sample period 2005-2014, the euro

[13]This is why the results from the euro area to itself, reported in Figure C.12, differ from those reported in Figure C.10, where only the cross-border effects are taken into consideration.

area as a whole is relatively insulated from foreign developments, given that about 80% of the variance of the euro area yields can be explained by shocks originated within the euro area. The US had been relatively more important for the euro area before the start of the inter-bank market crisis: in 2006, the first half of 2007 and soon after at the end of 2007, shocks from the US explained about 20 to 25% of variations in euro area sovereign yields. Shocks from the UK can explain 5 to 10% of the variance of the euro area sovereign yields, except in the period just after the bankruptcy of Lehman, when they explain 20% of the variance of euro area sovereign yields. Second, UK and US domestic shocks affected their own economies in a range between 10 and 40% over the entire sample, while sovereign yields of both countries are highly affected by shocks originating in the euro area. Interestingly, Figure C.12 suggests that shocks to euro area sovereign yields, rather than monetary policy shocks, are the driving force of variations in all economies sovereign yields.

Figure C.13 shows the estimated total directional connectedness among countries' sovereign yields due to shocks to sovereign yields stemming from specific countries. Each country's bond yield contributes to the variance of foreign sovereign yields by about 4 to 5% on average. However, there are specific developments in some periods, with larger effects that are in line with conventional wisdom. For example, connectedness from Greece doubled from 5% to 11% in the spring of 2010. Similarly, after the Deauville agreement on Private Sector Involvement on 18 October 2010, when it was agreed that private investors would share the burden of future defaults with the taxpayer, when sovereign yields in the stressed euro area countries started to increase, our results reveal Ireland to be the key source of spillovers, as connectedness from this market rose from 4% on average to 10%. Similarly, when the risk of euro area break-up unfolded in 2011 and 2012, connectedness from Italy rose from 3% in spring 2011 to 7% in the first half of 2012. Connectedness from Italy further increased to 8% in the autumn of 2012 after Mario Draghi's "whatever it takes" speech on 26 July 2012 and the launch, in September 2012, of the Eurosystem's Outright Monetary Transactions (OMTs) in secondary sovereign bond markets. Increased connectedness after such a speech was a desired outcome as sovereign yields started a steady decline. On the other hand, connectedness from Spain has been rather stable, rising only marginally since the beginning of the euro area sovereign debt crisis. This suggests that Italy, and not Spain, is a key source of systemic risk in the sovereign debt markets in the euro area.

Finally, it is useful to note that there was an increase in connectedness from the US in March 2009 and May 2013. In March 2009, the Federal Open Market Committee (FOMC) announced it would purchase 300 billion USD in long-term Treasury Bills, which was subsequently expanded. The average spillover effect from the US rose from 4% in the spring of 2010 to 8% in the summer. Since the FMOC announcement released on 22 May 2013, which financial markets perceived as the beginning of the end of accommodative

monetary policy in the US, connectedness from the US rose sharply from 3% in May 2013 to 10% in March 2014.

Pairwise directional connectedness

Pairwise directional connectedness measures the effect of a specific shock on a specific market. Given that we consider 15 markets, presenting such plots for each of the 210 pairwise directional measures is not feasible. Therefore, we present some relevant case studies, looking at shocks originating in the US, Greece, Italy and Spain.

Figure C.14 shows connectedness from US sovereign yields to the sovereign yields of other countries. Before the bankruptcy of Lehman about 10% of the variance of the US yields is explained by its own shocks; thereafter, this share rose to 17%. As discussed in the previous section, there is an increase in connectedness from the US after March 2009 and May 2013. The sovereign yields most affected are those of the UK and Germany, followed by Austria, the Netherlands, Belgium and France. The stressed countries (Greece, Ireland, Portugal, Italy and Spain) were mildly influenced.

A key case study is Greece. Figure C.15 shows connectedness from the Greek sovereign yields to the sovereign yields of all other markets. Before the sovereign debt crisis, when, recalling Figure C.7), we saw that the shocks were relatively small, a Greek shock affected its own sovereign yield marginally. Thereafter, the shocks become large and explain 40% of the variance of the Greek sovereign yields in 2010 and about 70% in 2013. The sovereign yields most affected by the developments in Greece are, in order of magnitude, Portugal, Ireland, Italy and Spain. Again, this is in line with conventional wisdom. Shocks stemming from Greek sovereign yields in 2010 explain 30% of the variance of Portuguese yields, 25% of the variance of Irish yields, 15% of the variance of Italian yields and 10% of the variance of Spanish yields. Interestingly, the German Bund was also affected: with the intensification of the crisis, international investors became more risk averse, and demanded more liquid and relatively safer assets. After the 2010 peak, Greek shocks did not spillover to the sovereign yields of the other stressed countries, except in March 2012 when Greece declared a credit event. In 2013, sovereign yields in Greece declined sharply. Again, the countries positively affected by these developments were the stressed countries: Portugal (30%), Italy (20%), Spain (15%) and Ireland (15%). There was a period in the first half of 2013, with the peak in March 2013, when the Greek shocks also influenced non-stressed economies, such as the UK (23%) and the US (19%). During that period, the Greek sovereign yields declined from 23% in September 2012 to 10% in March 2013. This large shock contributed to the decline in yields in the stress countries as well as in France, Belgium and Austria and to an increase in yields, by a few basis points, in Germany, the Netherlands, the UK and the US. This could be due to a portfolio reallocation as international investors' risk aversion receded.

Other interesting case studies are Italy and Spain. In 2011 and 2012 the shocks

from Italy, shown in Figure C.16, spilled over to the sovereign yields in other countries, contributing to a rise in Spain (16%) and, again due to a portfolio reallocation, a decline in Belgium (9%), Germany (8%), the Netherlands (7%), the UK (9%) and the US (7%).[14] In 2012, the "whatever-it-takes" speech reversed the dynamics of Italian sovereign yields. They started to decline quickly, contributing to the decline in Spanish sovereign yields, but with the opposite effect on the UK and the US Treasuries. Conversely, the shocks stemming from Spanish sovereign yields have affected its own sovereign market and, only to a limited extent, the developments in Italian sovereign yields, as shown in Figure C.17. All other sovereigns did not record a significant change in the contribution of Spanish sovereign yields shocks.

Spillover effects

The key input for the analysis carried out in the previous sections are the impulse response functions. Given that we consider 15 markets and 46 rolling windows, presenting and discussing 9660 IRFs is impractical. Here, we present a sub-set of IRFs between the sovereign yields of the key countries (Greece, Italy, Germany, UK and US) over the two specific sovereign crisis periods: the October 2009-July 2010 period and the May 2011-April 2012 period.

As shown in Figure C.18, our results suggest that Greece played a key role in 2010, driving up the sovereign yields in stressed countries and down those of non-stressed countries, including the United States. Instead, Italy became a source of volatility in the second phase of the crisis, when financial markets were pricing in the risk of euro area break-up. For example, during the May 2011-April 2012 period, according to our results, a shock amounting to 100 basis points in Italian sovereign yields implied an increase in Spanish sovereign yields equal to 55 basis points, and at peak, after 20 days, an increase in Greek and Portuguese sovereign yields by 300 and 40 basis points respectively.[15] At the same time, flight-to-liquidity and flight-to-safety phenomena drove down the German Bund, the British Guilt and the US Treasury yields by 15 basis points.

It is also interesting to note that US shocks clearly spilled over to Germany in 2010, but not in 2011-2012. In the latter period, the euro area sovereign debt crisis was exacerbated, and so spillovers within the euro area became more important. These results further justify the relevance of the time-varying analysis of such shocks.

3.4.3 What drives changes in connectedness?

Network connectedness, spillover and contagion are sometimes used interchangeably in the literature. In this paper, we have defined them as follows:

[14] All figures refer to peak effects.

[15] Results for Spain and Portugal are not shown but available upon request.

- **Connectedness**:

$$\Omega(h) = f(\Phi(A_1, ..., A_N), A_0^{-1}, B)$$

Connectedness is constructed using the Forecast Error Variance Decomposition (FEVD), which is non-linear function of the dynamic effects of shocks, $\Phi(A_1, ..., A_N)$, the matrix of contemporaneous effects, A_0^{-1}, and the size of the shocks, B.

- **Spillovers**:

$$\Psi(h) = \Phi(A_1, ..., A_N)A_0^{-1}B$$

Spillovers are measured using the IRFs, which are a non-linear function of the dynamic effects, $\Phi(A_1, ..., A_N)$, the matrix of contemporaneous effects, A_0^{-1}, and the size of the shocks, B. While connectedness is always positive, spillovers can be positive or negative.

- **Contagion**:

$$\Upsilon(h) = \Phi(A_1, ..., A_N)A_0^{-1}$$

As in Forbes and Rigobon [2002], contagion is related to the structure of the economy and is captured using the dynamic effects, $\Phi(A_1, ..., A_N)$, and the matrix of contemporaneous effects, A_0^{-1}.

In this subsection, we disentangle connectedness due to contagion from that due to shocks using a counter-factual exercise. Let $\Omega(h)^w$ denote the estimate of total connectedness in sample w. Consider the pre-crisis estimates of (i) dynamic effects, $\Phi(A_1^P, ..., A_N^P)$, (ii) the matrix of contemporaneous effects, A_0^{-1P}, and (iii) the size of the shocks, B^P, where superscript P stands for the estimates from the pre-crisis sample. We can then construct the following three measures of connectedness in a sample w:

- The unconditional effect through both contagion and shocks: $\Omega(h)^w = f(\Upsilon^w, B^w)$
- The effect of contagion given the pre-crisis size of shocks: $\Omega(h)^{w,B^P} = f(\Upsilon^w, B^P)$
- The effect of shocks given the pre-crisis degree of market linkages (i.e. given this degree of contagion): $\Omega(h)^{w,\Upsilon^P} = f(\Upsilon^P, B^w)$

In other words, to construct $\Omega(h)^{w,B^P}$, we fix the distribution of the shocks to that estimated from the pre-crisis period, $B^w = B^P \ \forall \ w$. More specifically, we fix B^w to the estimate obtained in the first sample of the rolling window estimation using data from 3rd January 2005 to 7th October 2005, $B^w = B^1 \ \forall \ w$. The changes in connectedness, as measured by $\Omega(h)^{w,B^P}$, are therefore only due to changes in cross-market linkages or contagion. Similarly to construct $\Omega(h)^{w,\Upsilon^P}$, we fix the degree of contagion to the estimate from the pre-crisis period, $\Upsilon^w = \Upsilon^P \ \forall \ w$. The changes in connectedness in this case are only due to the changes in the distribution of the shocks. Finally, we can compare those

estimates with baseline connectedness measures that takes into account both changes, in contagion and in the distribution of shocks, $\Omega(h)^w$.

Figure C.19 applies the decomposition to total connectedness among sovereign yields due to shocks to sovereign yields. The black line ('Grand Average') is total connectedness as reported in Figure C.9. The green line is the median estimate of total connectedness when contagion is fixed to the pre-crisis level. When keeping the cross-market linkages fixed, total connectedness increases after 2009 due to the size of shocks that have affected the euro area sovereign debt market. The red line is the median estimate of total connectedness when the distribution of shocks is fixed to the pre-crisis level. The drop in total connectedness is due to the decline in cross-market linkages and this is associated to market fragmentation, which has characterized the euro area government debt market between 2009 and 2012 with the intensification of the sovereign debt crisis.

While the shocks originated in the stressed euro area countries, such as Greece, Ireland, Italy, Portugal and Spain, the change in cross-market linkages was a common phenomenon. Financial fragmentation increased across stressed euro area countries, shown in Figure C.20, as well as among core countries, such as Austria, Belgium, France, Germany, the Netherlands, shown in Figure C.21. However, total connectedness within stressed countries and within core countries increased, which shows that market fragmentation was especially severe between the two blocks.

3.4.4 What does traditional identification tell us about sovereign bond markets linkages?

The key issue of using GIRFs is that the resulting shocks are not orthogonal, and might therefore be incorrect. For example, during the October 2009-July 2010 period, the effect of shocks stemming from Italy on Greek sovereign yields turn out to be positive using GIRFs and negative using our method (see Figure C.18). The impact of GIRFs is sometime even larger than unity: during the October 2009-July 2010 period, an Italian shock amounting to 100 basis points identified using GIRFs implies an average increase by 400 basis points in Greek sovereign yields, by 210 basis points in Portuguese sovereign yields and by 150 basis points in Irish sovereign yields. These results are counter-intuitive, given that Greece is believed to be the source of the crisis during this period.

The shocks estimated using GIRFs always overestimate the size of the shocks compared to our method. Moreover, in the period before the start of the crisis in the inter-bank market in August 2007, the size of the shocks identified using GIRFs exhibited a clear declining trend in Germany, Austria, the Netherlands, Belgium, France, Italy and Spain. Similarly, during the periods preceding both the Lehman bankruptcy in September 2008 and the euro area sovereign debt crisis in October 2009, the estimated shocks on the sovereign yields exhibit trends that were steeper than those suggested by our method.

These differences are then reflected in all the relevant measures of connectedness.

The results obtained using absolute magnitude restrictions and GIRFs differ substantially if connectedness is generated by shocks to long-term sovereign yields only, before the beginning of the sovereign debt crisis in October 2009, due to the sizeable influence of monetary policy rates on sovereign yields, which we have been able to disentangle from sovereign yield shocks (see Figure C.9). Since October 2009, the two methods produced very similar results, owing to the relatively marginal impact that the monetary policy rates have had on sovereign yields, given that they have remained stable at very low levels.

The results obtained using absolute magnitude restrictions and GIRFs are generally different when looking at total directional connectedness (see Figure C.13). For example, connectedness estimated using GIRFs from Greece declined in 2009 and 2010, in contrast with conventional wisdom.

3.5 Conclusion

Structural shock identification is a key issue in macroeconomics, and a challenging topic in finance in particular since asset prices move sharply and simultaneously. Diebold and Yılmaz [2014] use the GIRF method to investigate spillovers and connectedness. However, it is a well known fact that shocks identified using GIRFs are not orthogonal, because contemporaneous correlations are not addressed. This is very relevant if one wishes to study the sources and directions of the spillovers.

We propose a new method, which identifies structural shocks in asset prices based on restrictions on the relative size of the contemporaneous impact of the shocks in different markets. The method imposes bounds on the impact matrix, but it remains agnostic about the sign of the responses.

We first show analytically that the GIRF method does not provide identification of structural shocks, and use a Monte Carlo simulation to show that the errors can be important when using GIRFs. Conversely, the absolute magnitude restriction method is, in most cases, much closer to the true value.

Second, we apply the method to the US and European sovereign yield markets. We find that (i) the shocks estimated using GIRFs always overestimate the size of the shocks compared to our method, (ii) the shocks estimated using GIRFs may present different trends than those suggested by our method, (iii) the shocks estimated using GIRFs may present more accelerated trends than those suggested by our method in crisis times.

We find that total cross-border connectedness among euro area countries declined steadily between October 2009 and December 2012, in line with the policy makers' view that financial fragmentation was one of the main causes for the impairment of the transmission mechanism of the monetary policy. Moreover, we find clear evidence that financial

fragmentation has been a common phenomenon among stressed as well as core euro area countries. Connectedness among euro area countries improved in 2013 and in 2014 reached the level recorded before the financial crisis, suggesting that financial fragmentation in the euro area sovereign debt market is no longer a key issue.

We also find that during the period 2005-2014, the euro area as a whole was relatively more insulated from foreign developments, given that about 80% of the variance of the euro area yields can be explained by shocks originated within the euro area. However, the spillovers change over time. For example, in May 2013, when financial markets perceived a potential change in the US monetary policy, the influence of US sovereign yields on the developments in sovereign yields in other countries rose.

One of the key advantages of our method is that it can pin down the source of shocks. For example, we find that in the first half of 2010 shocks stemming from Greek sovereign yields could explain 30% of the variance of Portuguese yields, 25% of the variance of Irish yields, 15% of the variance of Italian yields and 10% of the variance of Spanish yields. Similarly, focusing on the 2011-2012 period, when financial markets were pricing in the risk of a break-up of the euro area, our method suggests that Italy, and not Spain, was a key source of systemic risk in the sovereign debt markets.

Appendix C

Appendix: Spillovers during Euro Area Sovereign Debt Crisis

C.1 Appendix - Absolute magnitude restrictions vs. GIRF

Figure C.1: The estimated and the true spillover

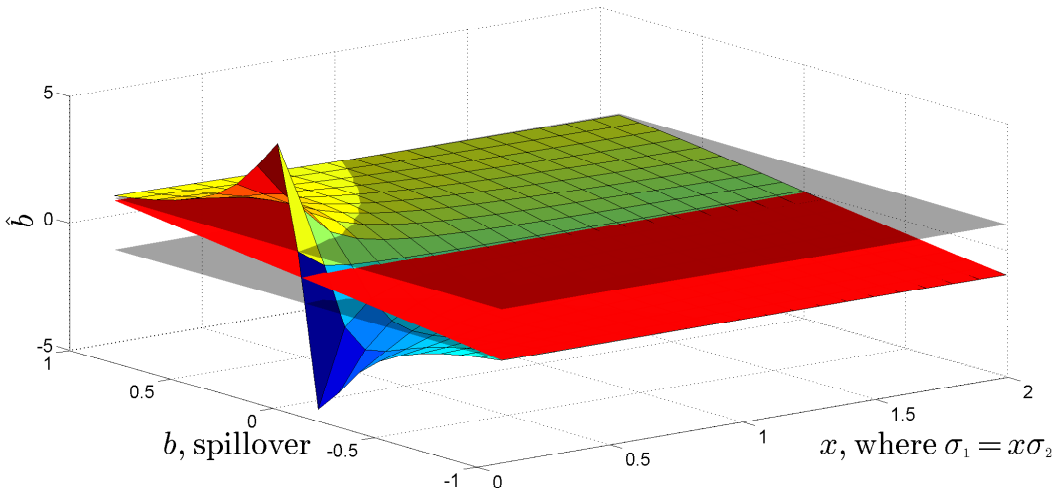

The colored area present the estimated spillover, $\hat{b}$, obtained by GIRF. The red area area is the true spillover coeficient, b. The gray bands represent the absolute magnitude restrictions on the interval $(-1, 1)$.

Figure C.2: The root squared error of estimated spillover by GIRF (red) and magnitude res. (blue)

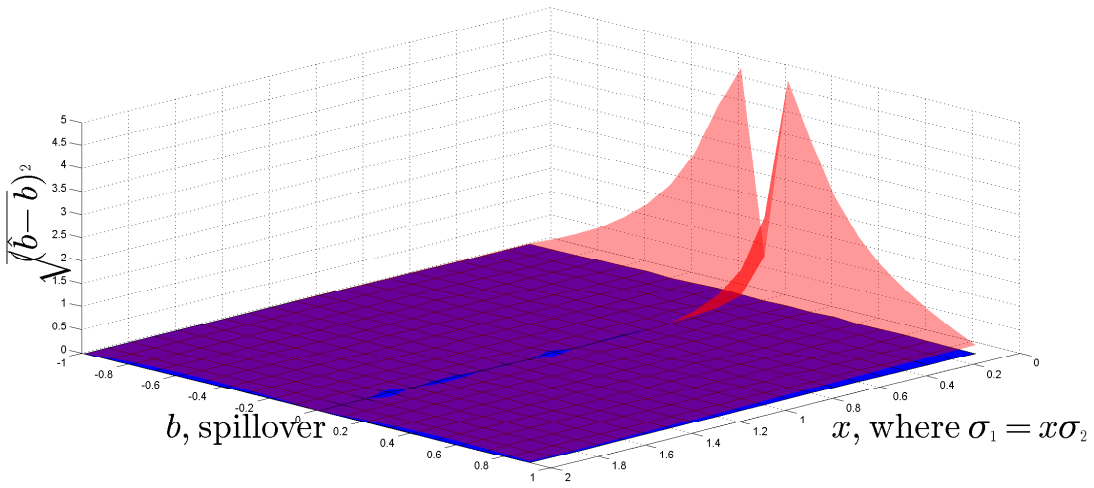

The red area present the graph presents the root squared error of estimated spillover (RSE) by GIRF, while blue area presents the RSE of estimated spillover by absolute magnitude restrictions.

C.2 Monte Carlo results

Figure C.3: Estimated directional connectedness 'to' others by using absolute magnitude restrictions

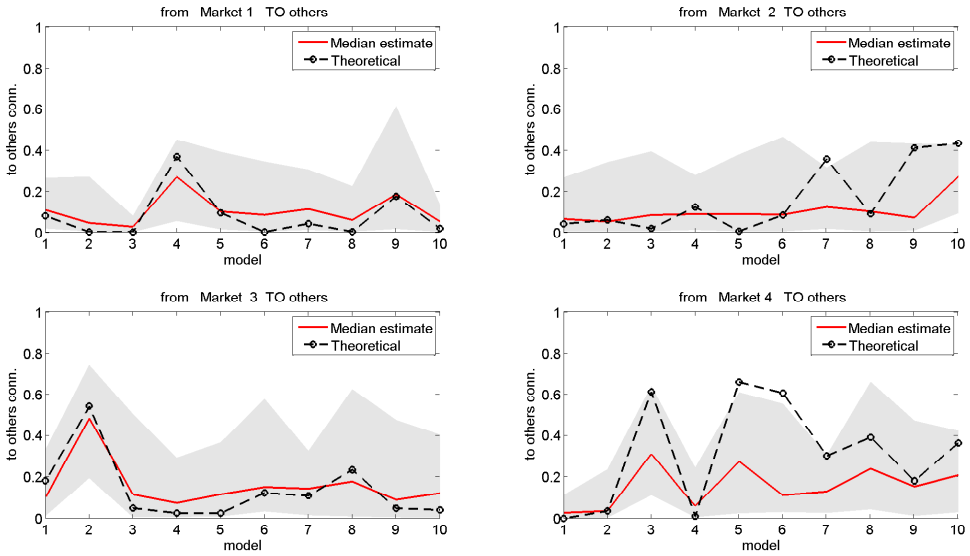

The graph presents the estimated directional connectedness 'to' others for simulated markets. The red line is median estimate and the gray bands are 95% error bands. Black line with circles is the true directional connectedness 'to' others.

Figure C.4: Estimated directional connectedness 'to' others by using generalized IRFs

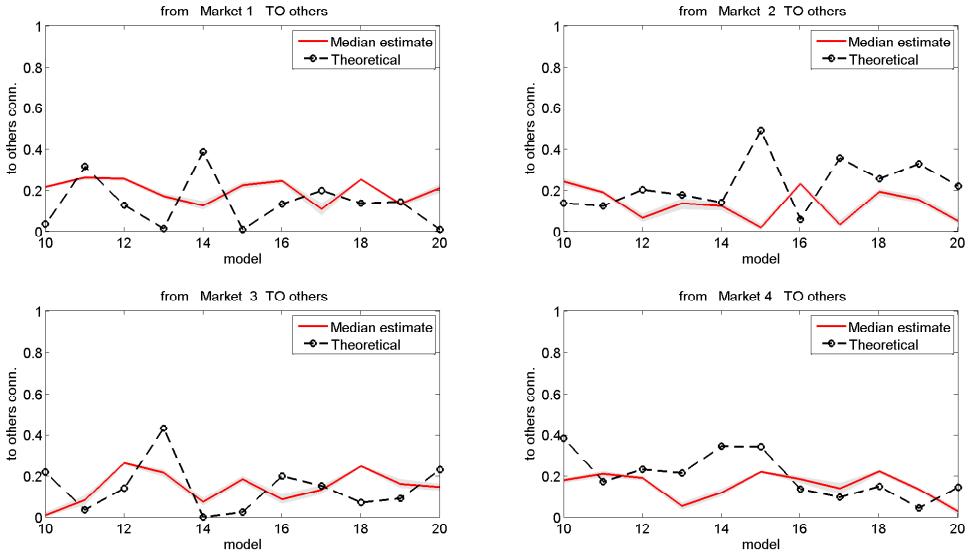

The graph presents the estimated directional connectedness 'to' others for simulated markets. The red line is median estimate and the gray bands are 95% error bands. Black line with circles is the true directional connectedness 'to' others.

Figure C.5: Estimated total connectedness by using absolute magnitude restrictions

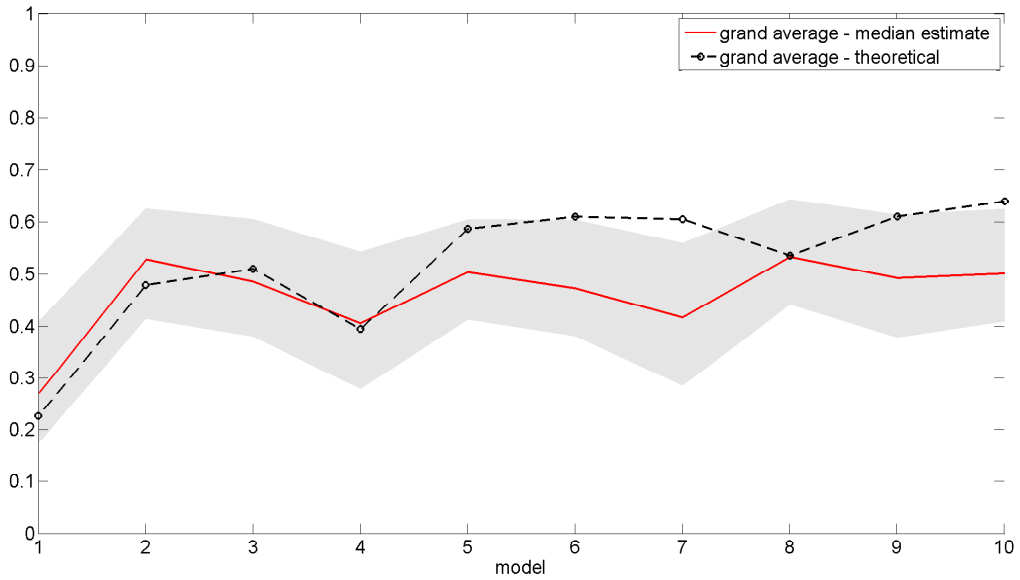

The graph presents the estimated total connectedness for simulated countries. The red line is median estimate and the gray bands are 95% error bands. Black line with circles is the true directional connectedness 'to' others.

Figure C.6: Estimated total connectedness by using generalized IRFs

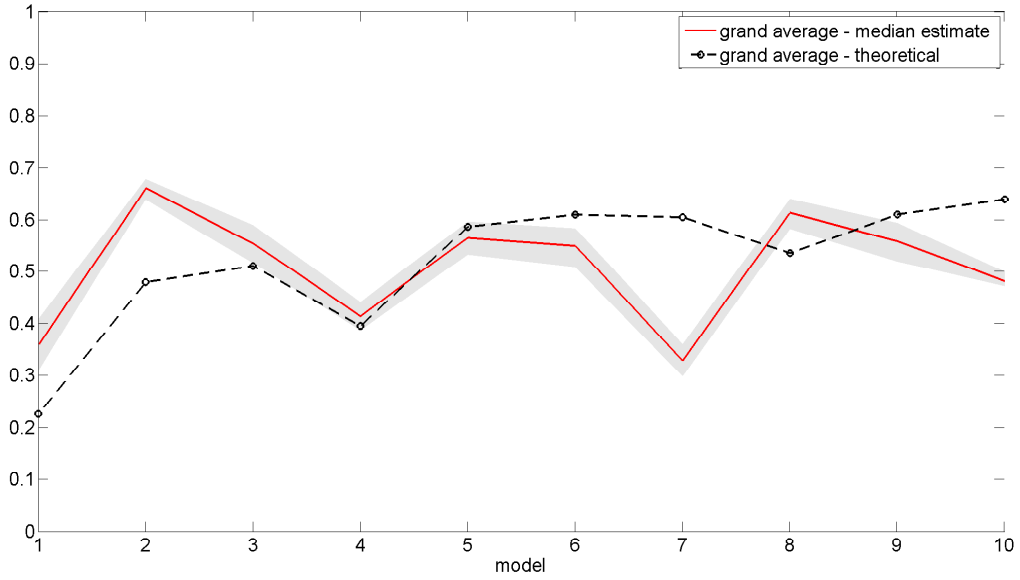

The graph presents the estimated total connectedness for simulated countries. The red line is median estimate and the gray bands are 95% error bands. Black line with circles is the true directional connectedness 'to' others.

C.3 Empirical results

Figure C.7: The estimated standard deviation of the shocks to sovereign yields

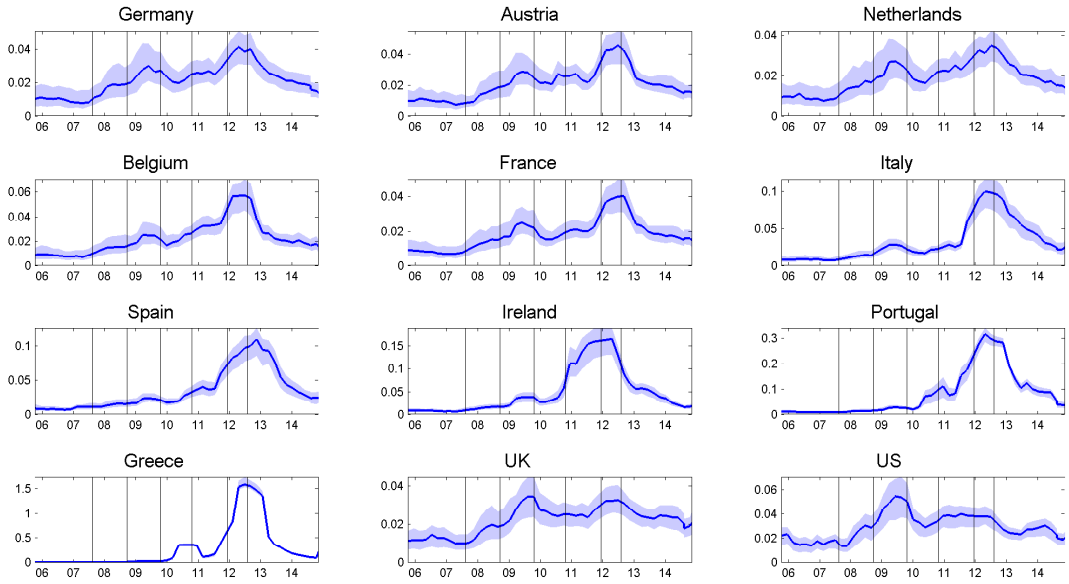

The blue line is median estimate and the shaded area are 68% error bands. The red line is median estimate obtained by GIRF. The vertical axis shows the standard deviation in percentage points. The first vertical bar denotes the beginning of the crisis in the interbank market on 9 August 2007. The second vertical bar denotes Lehmans bankruptcy on 15 September 2008. The third vertical bar denotes the parliamentary speech by the new Greek Prime Minister disclosing the budget situation in Greece on 16 October 2009. The fourth vertical bar denotes the Deauville agreement upon Private Sector Involvement on 18 October 2010. The fifth vertical line denotes the launch of the 3-year LTROs on 8 December 2011. The sixth vertical line denotes the Draghi speech in London on 26 July 2012.

Figure C.8: Estimated total connectedness among sovereign yields and monetary policy rates

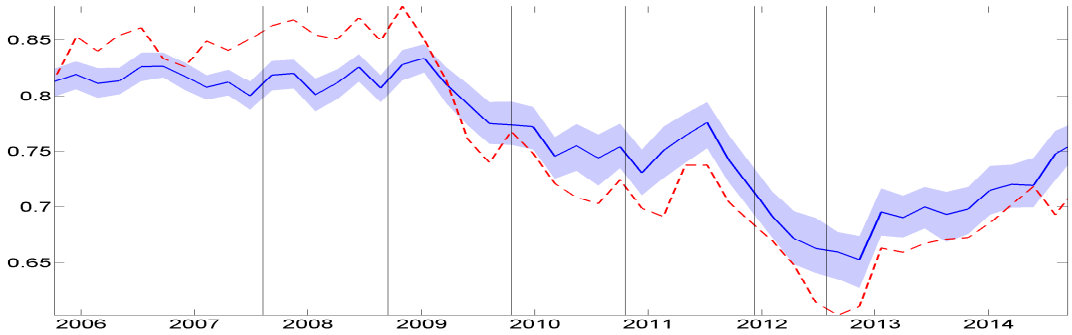

The blue line is median estimate and the shaded area are 68% error bands. The red line is median estimate obtained by GIRF. For the description of dates marked by vertical bars see footnote in Figure C.7.

Figure C.9: Estimated total connectedness among sovereign yields due to shocks to sovereign yields

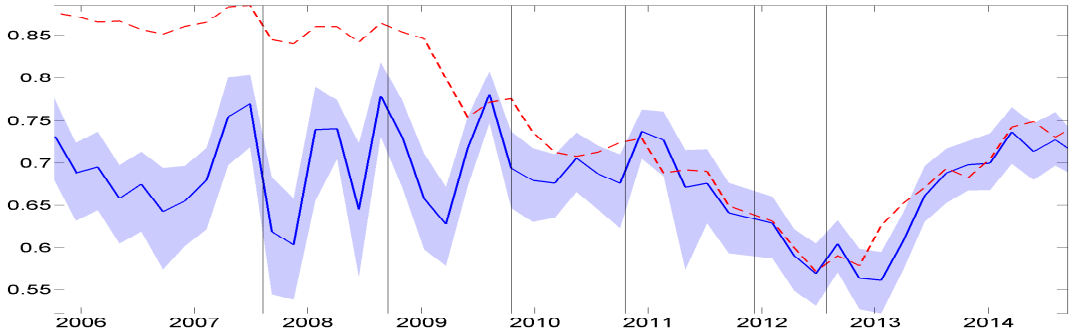

The blue line is median estimate and the shaded area are 68% error bands. The red line is median estimate obtained by GIRF. For the description of dates marked by vertical bars see footnote in Figure C.7.

Figure C.10: Estimated total connectedness among euro area sovereign yields due to shocks to euro area sovereign yields

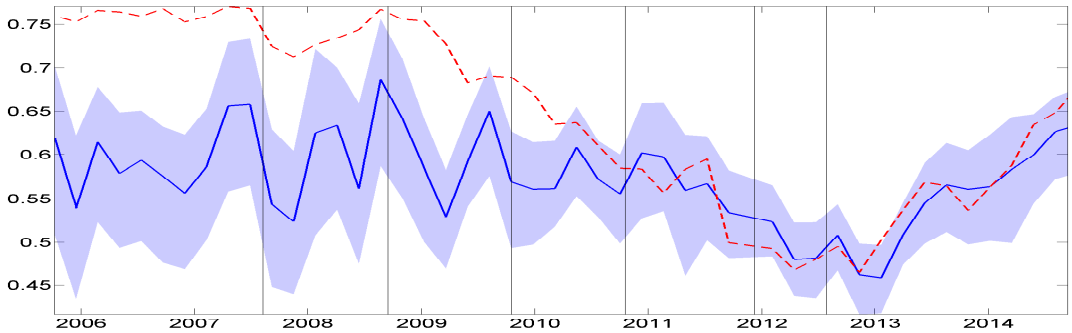

The blue line is median estimate and the shaded area are 68% error bands. The red line is median estimate obtained by GIRF. For the description of dates marked by vertical bars see footnote in Figure C.7.

Figure C.11: Total connectedness among regions sovereign yields due to shocks to sovereign yields and monetary policy rates

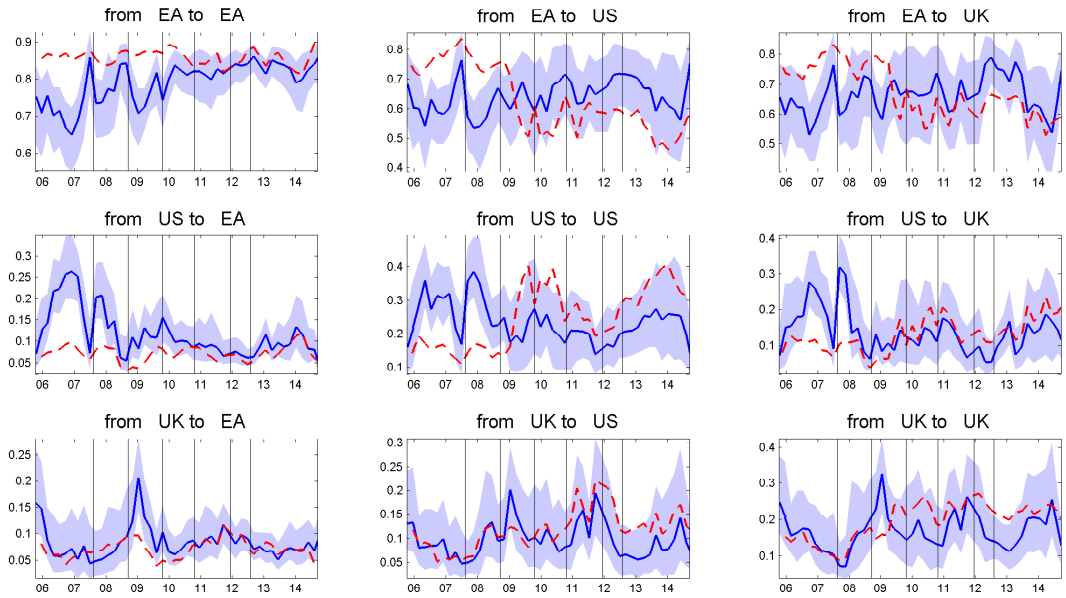

The blue line is median estimate and the shaded area are 68% error bands. The red line is median estimate obtained by GIRF. For the description of dates marked by vertical bars see footnote in Figure C.7.

Figure C.12: Total connectedness among regions sovereign yields due to shocks to sovereign yields

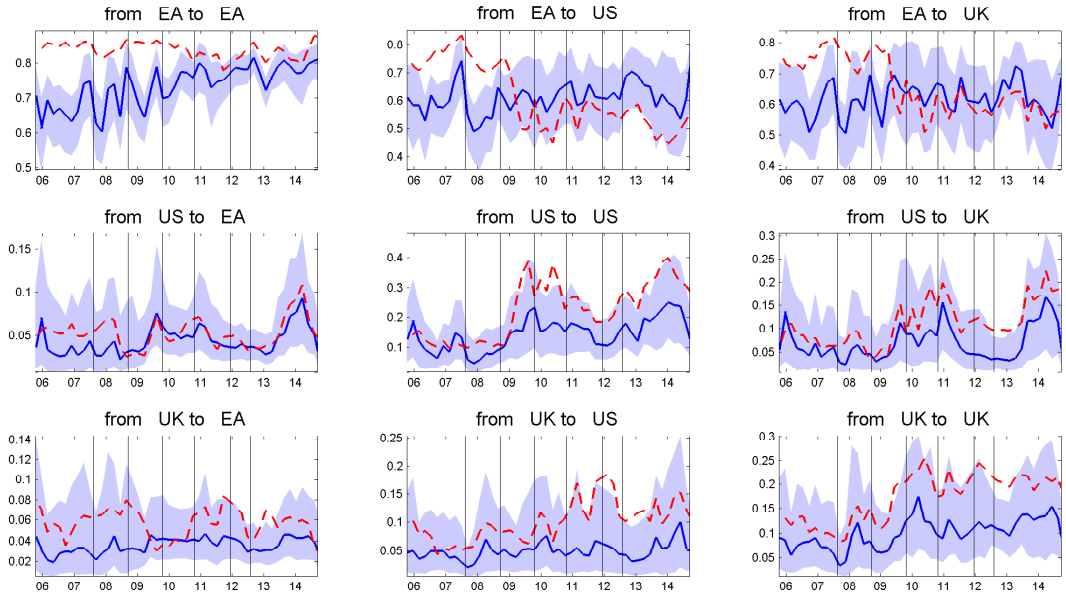

The blue line is median estimate and the shaded area are 68% error bands. The red line is median estimate obtained by GIRF. For the description of dates marked by vertical bars see footnote in Figure C.7.

Figure C.13: Total connectedness among countries sovereign yields due to shocks to sovereign yields

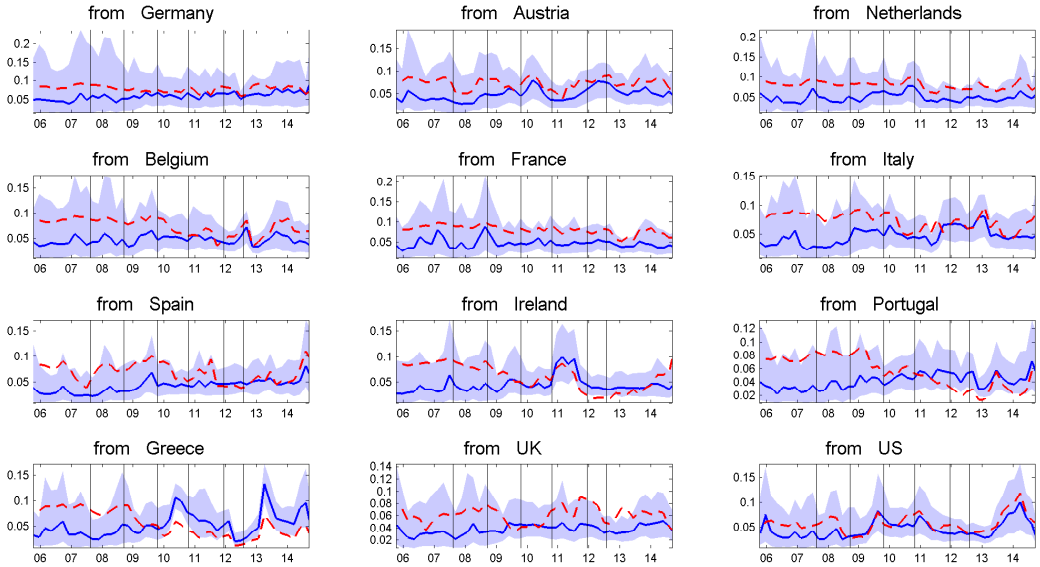

The blue line is median estimate and the shaded area are 68% error bands. The red line is median estimate obtained by GIRF. For the description of dates marked by vertical bars see footnote in Figure C.7.

Figure C.14: Estimated pairwise directional connectedness to countries sovereign yields due to shocks to US sovereign yields

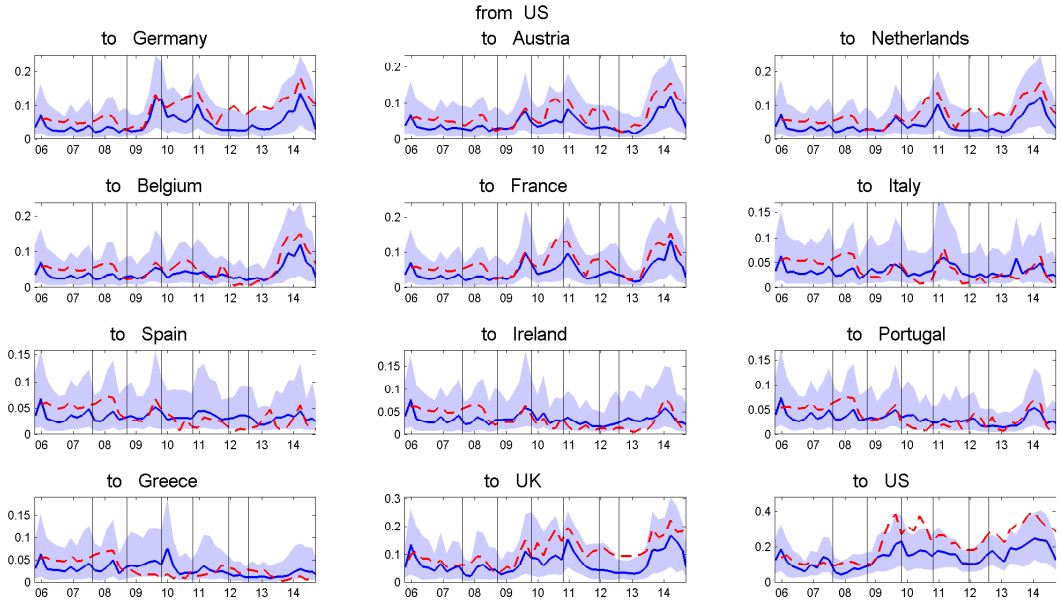

The blue line is median estimate and the shaded area are 68% error bands. The red line is median estimate obtained by GIRF. For the description of dates marked by vertical bars see footnote in Figure C.7.

Figure C.15: Estimated pairwise directional connectedness to countries sovereign yields due to shocks to Greek sovereign yields

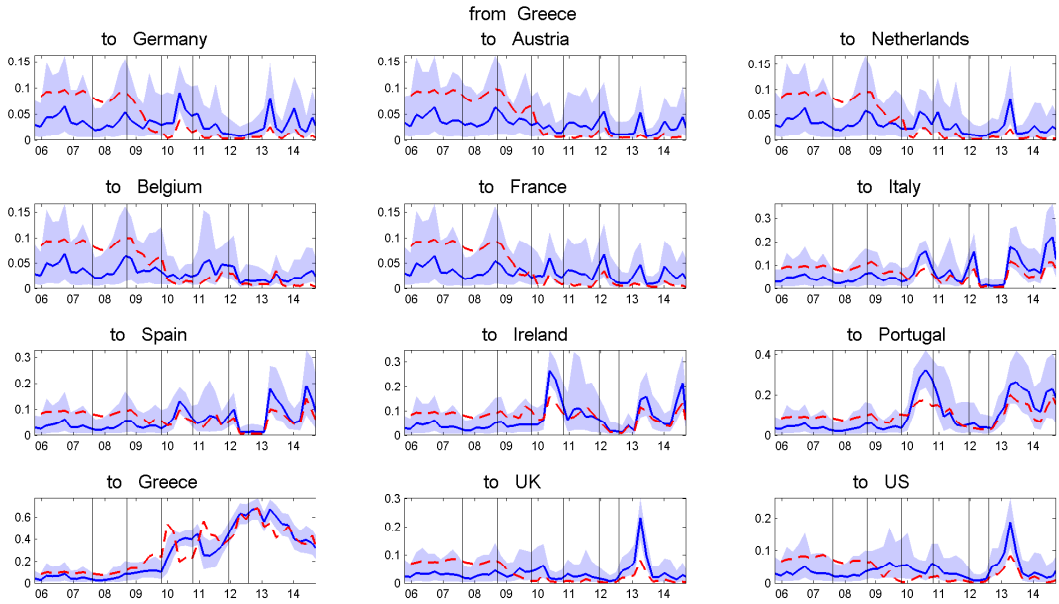

The blue line is median estimate and the shaded area are 68% error bands. The red line is median estimate obtained by GIRF. For the description of dates marked by vertical bars see footnote in Figure C.7.

Figure C.16: Estimated pairwise directional connectedness to countries sovereign yields due to shocks to Italian sovereign yields

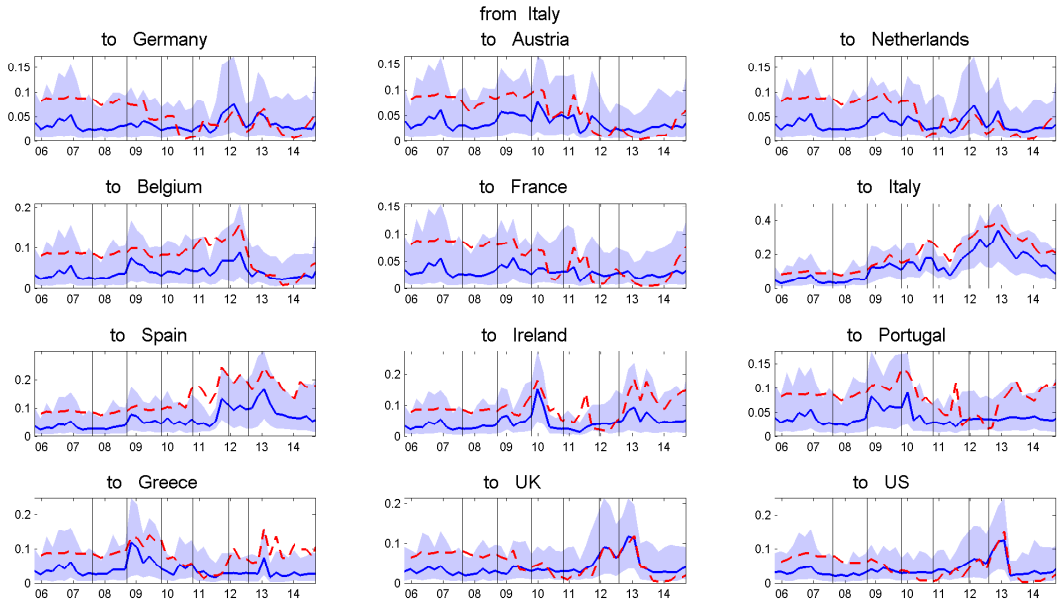

The blue line is median estimate and the shaded area are 68% error bands. The red line is median estimate obtained by GIRF. For the description of dates marked by vertical bars see footnote in Figure C.7.

Figure C.17: Estimated pairwise directional connectedness to countries sovereign yields due to shocks to Spanish sovereign yields

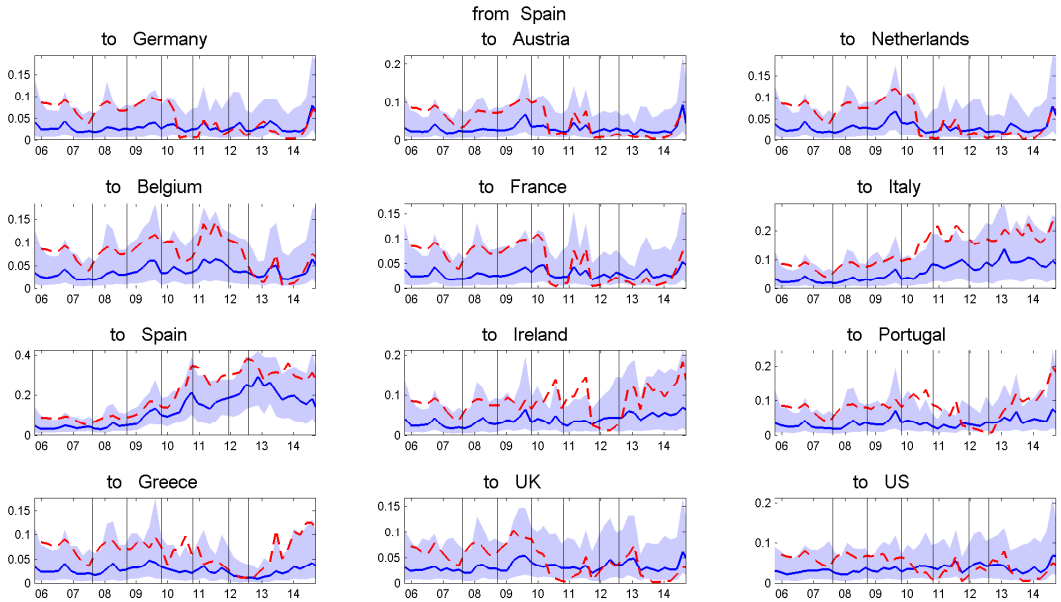

The blue line is median estimate and the shaded area are 68% error bands. The red line is median estimate obtained by GIRF. For the description of dates marked by vertical bars see footnote in Figure C.7.

Figure C.18: Selected impulse response functions for specific periods

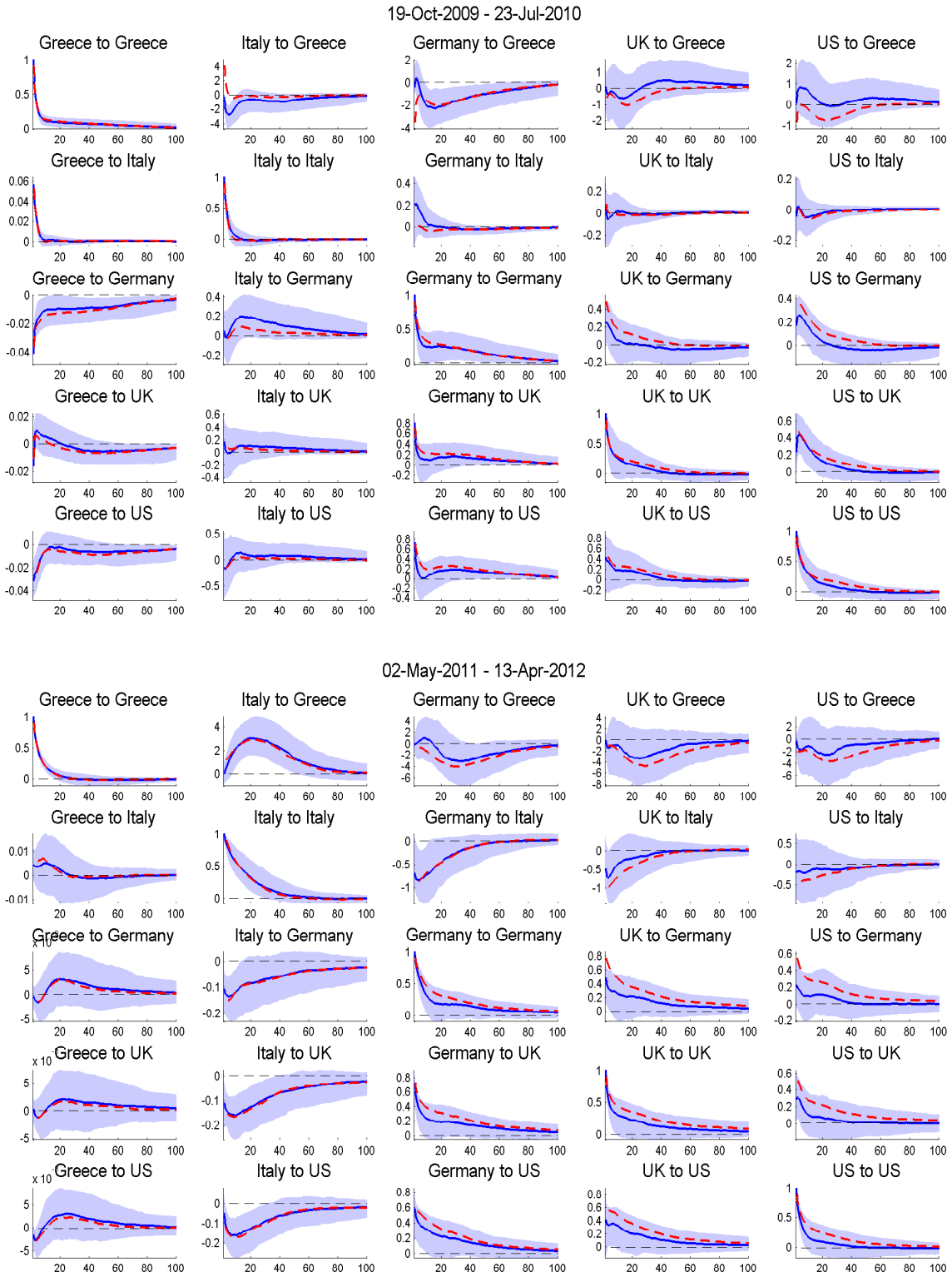

The blue line is median estimate and the shaded area are 68% error bands. The red line is median estimate obtained by GIRF.

C.4 Contagion vs. the size of shocks

Figure C.19: Decomposition of total connectedness among sovereign yields

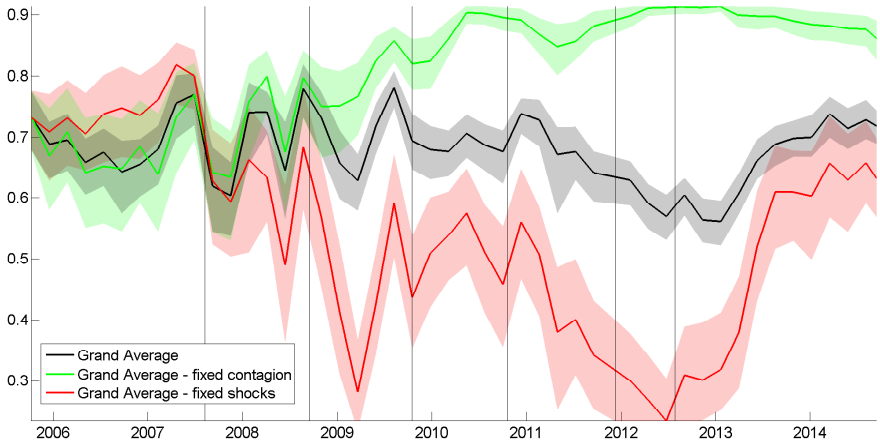

The black line is median estimate of total connectedness (grand average) for Eurozone countries and the shaded area are 68%error bands. The red line is median estimate of total connectedness (grand average) and red shaded area corresponding 68% error bands when the distribution of shocks is fixed to pre-crisis level. The green line is median estimate of total connectedness (grand average) and green shaded area corresponding 68% error bands when the contagion is fixed to pre-crisis level. We fix the distribution of shocks and contagion for all sovereign yields. Grand average is constructed from the pairwise connectedness measures of all 12 countries except monetary rates.

Figure C.20: Decomposition of total connectedness among stressed countries

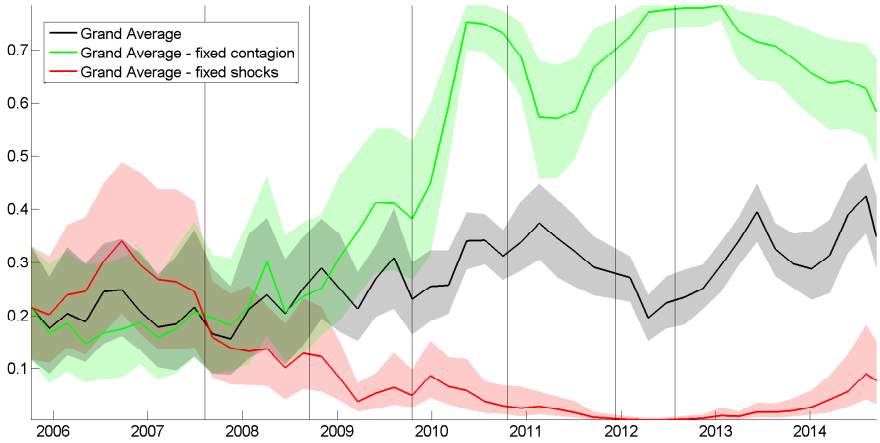

The black line is median estimate of total connectedness (grand average) between stressed Eurozone countries (Italy, Spain, Ireland, Portugal and Greece) and the shaded area are 68%error bands. The red line is median estimate of total connectedness (grand average) and red shaded area corresponding 68% error bands when the distribution of shocks is fixed to pre-crisis level. The green line is median estimate of total connectedness (grand average) and green shaded area corresponding 68% error bands when the contagion is fixed to pre-crisis level. We fix the distribution of the shocks and contagion only for Italy, Spain, Ireland, Portugal and Greece. Grand average is constructed from the pairwise connectedness measures of Italy, Spain, Ireland, Portugal and Greece.

Figure C.21: Decomposition of total connectedness among core countries

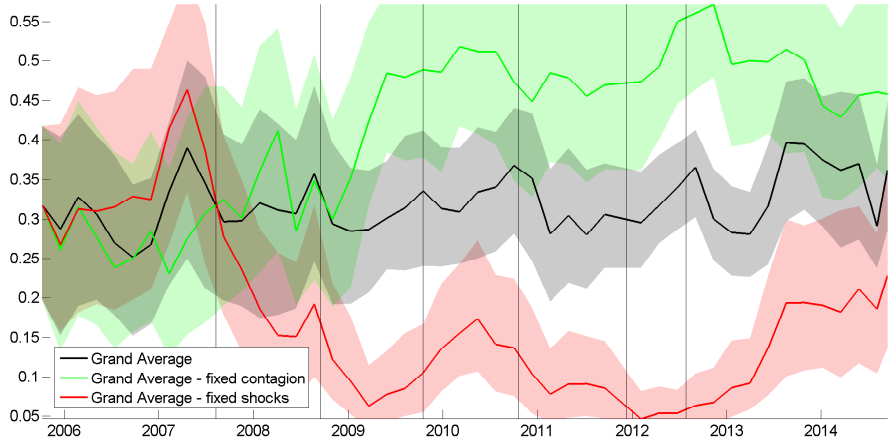

The black line is median estimate of total connectedness (grand average) for core Eurozone countries (Germany, Austria, Netherlands, Belgium and France) and the shaded area are 68%error bands. The red line is median estimate of total connectedness (grand average) and red shaded area corresponding 68% error bands when the distribution of shocks is fixed to pre-crisis level. The green line is median estimate of total connectedness (grand average) and green shaded area corresponding 68% error bands when the contagion is fixed to pre-crisis level. We fix the distribution of the shocks and contagion only for Germany, Austria, Netherlands, Belgium and France. Grand average is constructed from the pairwise connectedness measures of Germany, Austria, Netherlands, Belgium and France.

Bibliography

George-Marios Angeletos, Fabrice Collard, and Harris Dellas. Quantifying Confidence. NBER Working Papers 20807, National Bureau of Economic Research, Inc, December 2014.

Philippe Bacchetta, Cédric Tille, and Eric van Wincoop. Self-fulfilling risk panics. *American Economic Review*, 102(7):3674–3700, December 2012.

J. Bai and S. Ng. Determining the number of factors in approximate factor models. *Econometrica*, 70(1):191–221, 2002.

J. Bai and S. Ng. Determining the number of primitive shocks in factor models. *Journal of Business & Economic Statistics*, 25(1):52–60, 2007.

R.B. Barsky and E.R. Sims. News shocks and business cycles. *Journal of Monetary Economics*, 2011.

Robert B. Barsky and Eric R. Sims. Information, animal spirits, and the meaning of innovations in consumer confidence. *American Economic Review*, 102(4):1343–77, June 2012.

P. Beaudry and B. Lucke. *Letting Different Views about Business Cycles Compete*, pages 413–455. University of Chicago Press, April 2010.

P. Beaudry and F. Portier. Stock prices, news, and economic fluctuations. *The American Economic Review*, 96(4):1293–1307, 2006.

P. Beaudry and F. Portier. When can changes in expectations cause business cycle fluctuations in neo-classical settings? *Journal of Economic Theory*, 135(1):458–477, 2007.

N. Ben Zeev. What can we learn about news shocks from the late 1990s and early 2000s boom-bust period? 2014.

Olivier J. Blanchard, Jean-Paul L'Huillier, and Guido Lorenzoni. News, noise, and fluctuations: An empirical exploration. *American Economic Review*, 103(7):3045–70, December 2013.

F. Canova and G.D. Nicoló. Monetary disturbances matter for business fluctuations in the g-7. *Journal of Monetary Economics*, 49(6):1131–1159, 2002.

Peter Claeys and Bořek Vašíček. Measuring bilateral spillover and testing contagion on sovereign bond markets in Europe. *Journal of Banking & Finance, Elsevier*, 46(C): 151–165, 2014.

Ferre De Graeve and Alexei Karas. Evaluation theories of bank runs with heterogeneity restrictions. *Journal of the European Economic Association*, 12(4):969–996, 2014. ISSN 1542-4774.

Francis X Diebold and Glenn D Rudebusch. Forecasting output with the composite leading index: A real-time analysis. *Journal of the American Statistical Association*, 86(415):603–610, 1991.

Francis X Diebold and Kamil Yılmaz. On the network topology of variance decompositions: Measuring the connectedness of financial firms. *Journal of Econometrics*, 2014.

European Central Bank ECB. Confidence indicators and economic developments. *Monthly Bulletin*, 45(58), January 2013.

Zeno Enders, Michael Kleemann, and Gernot Müller. Growth expectations, undue optimism, and short-run fluctuations. CESifo Working Paper Series 4548, CESifo Group Munich, 2013.

Roger E.A. Farmer. The stock market crash of 2008 caused the great recession: Theory and evidence. *Journal of Economic Dynamics and Control*, 36(5):693–707, 2012.

J. Faust. The robustness of identified var conclusions about money. In *Carnegie-Rochester Conference Series on Public Policy*, volume 49, pages 207–244. Elsevier, 1998.

J. Fernald. A quarterly, utilization-adjusted series on total factor productivity. *Manuscript, Federal Reserve Bank of San Francisco*, 2009.

Kristin Forbes. The 'Big C';: Identifying Contagion. NBER Working Papers 18465, National Bureau of Economic Research, Inc, October 2012.

Kristin J. Forbes and Roberto Rigobon. No Contagion, Only Interdependence: Measuring Stock Market Comovements. *Journal of Finance*, 57(5):2223–2261, October 2002.

M. Forni and L. Gambetti. Macroeconomic shocks and the business cycle: Evidence from a structural factor model. 2010.

M. Forni, L. Gambetti, L. Sala, and Centre for Economic Policy Research (Great Britain). *No news in business cycles*. CEPR, 2011.

Mario Forni, Luca Gambetti, Mario Lippi, and Luca Sala. Noisy news in business cycle. Technical report, mimeo, 2013.

J. Greenwood, Z. Hercowitz, and G.W. Huffman. Investment, capacity utilization, and the real business cycle. *The American Economic Review*, pages 402–417, 1988.

N. Jaimovich and S. Rebelo. News and business cycles in open economies. *Journal of Money, Credit and Banking*, 40(8):1699–1711, December 2008.

N. Jaimovich and S. Rebelo. Can news about the future drive the business cycle? *American Economic Review*, 99(4):1097–1118, September 2009.

John Maynard Keynes. *General theory of employment, interest and money.* Palgrave Macmillian, 1936.

Lutz Kilian. Small-Sample Confidence Intervals For Impulse Response Functions. *The Review of Economics and Statistics*, 80(2):218–230, May 1998.

Lutz Kilian and Daniel P. Murphy. Why Agnostic Sign Restrictions Are Not Enough: Understanding The Dynamics Of Oil Market Var Models. *Journal of the European Economic Association, European Economic Association*, 10(5):1166–1188, October 2012.

R.G. King, C.I. Plosser, and S.T. Rebelo. Production, growth and business cycles:: I. the basic neoclassical model. *Journal of Monetary economics*, 21(2-3):195–232, 1988.

Gary Koop, M. Hashem Pesaran, and Simon M. Potter. Impulse response analysis in nonlinear multivariate models. *Journal of Econometrics, Elsevier*, 74(1):119–147, September 1996.

André Kurmann and Christopher Otrok. News shocks and the slope of the term structure of interest rates. *The American Economic Review*, 103(6):2612–2632, 2013.

L. Ljungqvist and T.J. Sargent. *Recursive macroeconomic theory.* MIT press, 2004.

Guido Lorenzoni. A theory of demand shocks. *American Economic Review*, 99(5):2050–84, December 2009.

A. Onatski. Testing hypotheses about the number of factors in large factor models. *Econometrica*, 77(5):1447–1479, 2009.

H. Hashem Pesaran and Yongcheol Shin. Generalized impulse response analysis in linear multivariate models. *Economics Letters, Elsevier*, 58(1):17–29, January 1998.

A.C. Pigou. *Industrial fluctuations.* MacMillan, London, 1926.

Arthur Cecil Pigou. *Industrial fluctuations.* Macmillan, 1929.

Juan F. Rubio-Ramrez, Daniel F. Waggoner, and Tao Zha. Structural Vector Autoregressions: Theory of Identification and Algorithms for Inference. *Review of Economic Studies*, 77(2):665–696, 2010.

S. Schmitt-Grohe and M. Uribe. What's news in business cycles. *Econometrica*, 80(6): 2733–2764, 2012.

R.J. Shiller. Irrational exuberance. *Irrational exuberance*, 2001.

Dan Simon. *Optimal state estimation: Kalman, H infinity, and nonlinear approaches*. Wiley. com, 2006.

James H. Stock and Mark W. Watson. Forecasting inflation. *Journal of Monetary Economics*, 44(2):293–335, October 1999.

J.H. Stock and M.W. Watson. Implications of dynamic factor models for var analysis. Technical report, National Bureau of Economic Research, 2005.

Harald Uhlig. What are the effects of monetary policy on output? results from an agnostic identification procedure. *Journal of Monetary Economics*, 52(2):381–419, 2005.

D.C. Wheelock, M.E. Wohar, et al. Can the term spread predict output growth and recessions? a survey of the literature. *Federal Reserve Bank of St. Louis Review*, 91(5 Part 1):419–440, 2009.